2017

Small Molecule Biofilm Inhibitors with Antivirulence Properties against Pseudomonas aeruginosa

van Tilburg Bernardes, Erik

UNIVERSITY OF CALGARY

Small Molecule Biofilm Inhibitors with Antivirulence Properties against *Pseudomonas aeruginosa*

by

Erik van Tilburg Bernardes

A THESIS

SUBMITTED TO THE FACULTY OF GRADUATE STUDIES

IN PARTIAL FULFILMENT OF THE REQUIREMENTS FOR THE

DEGREE OF MASTER OF SCIENCE

GRADUATE PROGRAM IN MICROBIOLOGY AND INFECTIOUS DISEASES

CALGARY, ALBERTA

JANUARY, 2017

Abstract

The opportunistic pathogen *Pseudomonas aeruginosa* grows within biofilms in the Cystic Fibrosis airways, leading to chronic, life-threatening infections. Biofilms are dense communities of bacteria surrounded by a protective polymeric extracellular matrix comprised of exopolysaccharides (EPS), proteins and extracellular DNA. The two major EPS molecules produced by *P. aeruginosa* are the Pel and Psl. Considering the essential role of EPS in biofilm formation, antimicrobial resistance and immune evasion, we developed a high-throughput gene expression screen for the identification of small molecules that reduce both *pel* and *psl* gene expression. Testing of the identified *pel/psl* repressors demonstrated their antibiofilm activity against static and flow biofilm models. Moreover, these antibiofilm molecules also reduce PAO1 virulence in a nematode infection model, as well as increase *P. aeruginosa* biofilm susceptibility to antibiotic killing. These small molecules represent a novel anti-infective strategy for the possible adjuvant treatment of chronic *P. aeruginosa* infections.

Acknowledgements

My most sincere gratitude to my supervisor, Dr. Shawn Lewenza, for this unique opportunity and the mentorship that has been essential for the completion of this project. I would also like to thank my co-supervisor, Dr. Rebekah DeVinney, and my supervisory committee members, Dr. Joe Harrison and Dr. Tao Dong, for all the valuable ideas and guidance throughout this graduate program. Without your expertise and continuous direction, this thesis would not be conceivable.

My deepest gratitude for all the amazing people and staff that directly and indirectly supported the completion of this project. To the current and past members of the Lewenza lab, especially Dr. Mike Wilton and Laetitia Charron-Mazenod, it was an honour sharing the lab space with you. Thank you for your friendship and countless advises. Moreover, my deepest gratitude for all the amazing friends I made in the program, specially my *Microbiology chums*, Alya, Kelsey, Rai and Renata, for all the support and companionship since the beginning of this journey.

My most sincere acknowledgements to my whole family, particularly my parents, George and Yara, and brothers, Nicolas and Pieter, for their constant love, support, and for always being there whenever I was feeling homesick or just in need of some comforting words. Also, a special thank you to my partner, Julio Ferreira, your company and worried-way were essential for keeping me sane through the toughest times of this program.

Furthermore, a special thank you for all my friends back in Brazil and in Calgary for the numerous laughs and special moments. Thank you for not letting distance bring us apart. Having you with me through all the challenges and successes have made this journey easier to pursue.

Finally, I would like to acknowledge the Beverley Phillips Rising Star scholarship (Snyder Institute), Cystic Fibrosis Canada studentship and the Natural Sciences and Engineering Research Council (NSERC) Discovery Grant for the funding support that allowed me to follow this dream and made this project feasible.

Dedication

I dedicate this thesis to everyone that directly or indirectly helped me throughout this whole journey. Family, friends and coworkers, this thesis is as mine as it is yours.

Table of Contents

List of Tables

List of Figures

List of Symbols, Abbreviations and Nomenclature

Symbol	Definition
–	Minus, negative
+	Plus, positive
$(NH_4)_2SO_4$	Ammonium sulfate
%	Percentage
% exp	Percentage of expression (relative to control)
°C	Degrees Celsius
< or >	Under or above (a certain value)
~	Approximately
AHL	Acylhomoserine lactone
AIDS	Acquired Immune Deficiency Syndrome
Amp	Ampicillin
AMP	Antimicrobial peptides
B. cenocepacia	*Burkholderia cenocepacia*
BM2	Basal minimum media 2
c-	Negative control
c-di-GMP	Bis-(3′-5′)-cyclic dimeric guanosine monophosphate
C. elegans	*Caenorhabditis elegans*
c+	Positive control
$CaCl_2$	Calcium chloride
CCBN	Canadian Chemical Biology Network
cDNA	Complementary DNA
CF	Cystic Fibrosis
CFTR	Cystic Fibrosis Transmembrane Conductance Regulator
CFU	Colony forming units
Ci	Ciprofloxacin
Cl^-	Ion chloride
cm	Centimeter
$CoCl_2.6H_2O$	Cobalt (II) chloride hexahydrate
Col	Colistin
CPS	Counts per second
CR	Congo red
CV	Crystal violet
DE	Differentially expressed
DGC	Diguanylate cyclase
DMSO	Dimethyl sulfoxide
DNA	Deoxyribonucleic acid
DspB	Dispersin B
E. coli	*Escherichia coli*
ECM	Extracellular matrix
eDNA	Extracellular deoxyribonucleic acid

EPS	Exopolysaccharides
$FeSO_4$	Iron (II) sulphate
Fig	Figure
FUdR	5-fluoro-2'-deoxyuridine
g	Relative centrifugal force
GFP	Green fluorescent protein
GI	Gastrointestinal
Gm	Gentamycin
H_3BO_3	Boric acid
HTS	High-throughput screening
I1-14	Inhibitor compounds (numbers 1 to 14)
K_2HPO_4	Dipotassium phosphate
KH_2PO_4	Monopotassium phosphate
Km	Kanamycin
KNO3	Potassium nitrate
L. monocytogenes	*Listeria monocytogenes*
LB	Lysogeny Broth medium
lux	Luciferase (*luxCDABE*) encoding reporter
MBEC	Minimum biofilm eradication concentration
Mg^{2+}	Ion magnesium
$MgCl_2$	Magnesium chloride
$MgSO_4$	Magnesium sulphate
min	Minutes
ml	Millilitre
mm	Millimeter
mM	Millimolar
$MnSO_4.H_2O$	Manganese (II) sulphate monohydrate
mRNA	Messenger ribonucleic acid
n	Sample size
NaCl	Sodium chloride
ND	Not determined
NGM	Nematode growth medium
nm	Nanometer
NO	Nitric oxide
OD_{490}	Optical density at 490nm
OD_{600}	Optical density at 600nm
P. aeruginosa	*Pseudomonas aeruginosa*
P. chlororaphis	*Pseudomonas chlororaphis*
P.S.	Postscript
PB	Polymyxin B
PBS	Phosphate buffered saline
p_{DLC}	Palmitoyl-$_{DL}$-carnitine
pel	Pellicle formation locus
pmr	Polymyxin resistance operon
psl	Polysaccharide synthesis locus
QS	Quorum sensing

RNA	Ribonucleic acid
RNA-seq	Ribonucleic acid sequencing
ROS	Reactive oxygen species
rpm	Revolutions per minute
rRNA	Ribosomal ribonucleic acid
RSCV	Rugose small colony variants
SK	Slow killing
T3SS	Type three secretion system
T6SS	Type six secretion system
TCS	Two-component system
Tet	Tetracycline
Tm	Tobramycin
Tp	Trimethoprim
U	Units
VCC	Viable cell counts
$ZnCl_2$	Zinc dichloride
β-ME	Beta-mercaptoethanol
Δ	Deletion mutant
μ	Median
μCPS	Median counts per second
μg	Microgram
μM	Micromolar
μm	Micrometer

Epigraph

“The future belongs to those who believe in the beauty of their dreams.”

Eleanor Roosevelt

Chapter One: Literature review and introduction to the project

1.1 Literature review

1.1.1 Pseudomonas aeruginosa *in Cystic Fibrosis (CF) disease*

P. aeruginosa is a ubiquitous Gram-negative bacterium that can be isolated from many moist environments, such as soil and water, but also infects and causes disease in a wide variety of hosts. [1-3] Although *P. aeruginosa* is generally unable to infect healthy hosts, it is a remarkable opportunistic pathogen, causing a variety of acute and chronic infections in immunocompromised patients. [1, 4-6]

Normally, the host innate immune response is sufficient to clear the pathogen and stop infection, although, whenever this immune barrier is defective, *P. aeruginosa* can survive and cause severe illnesses. [1] This bacterium is among the leading causes of hospital-acquired infections, being a major threat for patients in intensive care units. [4] *P. aeruginosa* infections are frequent in patients with burn wounds, undergoing mechanical ventilation or chemotherapy, suffering from acquired immunodeficiency syndrome (AIDS), organ transplantation and especially among those with Cystic Fibrosis (CF) disease. [1, 4, 7]

CF is the most common fatal genetic inherited disease, which affects predominantly the Caucasian population. [8] It is caused by autosomal recessive mutations in the CF transmembrane conductance regulator (CFTR) gene, located on chromosome 7q31.2, which promotes an altered electrolyte transport and associated consequences in different tissues throughout the patient's body. [8, 9]

Defective permeability to the ion chloride (Cl^-) is the best characterized phenomena in CF disease, which severely reduces fluid secretion. [9] Although affecting many organs, its

primary consequences remain in the respiratory and digestive systems. [10, 11] CF patients suffer with decreased paraciliary fluid in their lungs, leading to the production of a thick, dehydrated mucus, which usually culminates in persistent cough, difficulty breathing and chronic lung infections. [1, 9-11] The persistence of bacteria within the CF lungs despite intensive antimicrobial interventions fosters constant inflammation and decrease in lung function, eventually leading to patient's death. [1, 10]

The CF lung environment is inhabited by a diverse set of microorganisms. [12] Throughout disease progression, this CF microbiota tends to lose diversity and become dominated by a more specialized set of pathogenic bacteria, including members of the Pseudomonadaceae and Burkholderiaceae families, which are associated with reduced lung function. [12, 13] *P. aeruginosa* remains one of the leading cause of morbidity and mortality in CF patients, [7, 11] expressing an arsenal of defense and adaptive mechanisms that facilitates its survival within the CF lung. [1, 2, 7] Additionally, *P. aeruginosa* is remarkably resistant to antibiotics, surviving intense antimicrobial treatments and, therefore, promoting chronic infections that are almost impossible to eradicate. [1, 3, 11]

Finally, *P. aeruginosa* is a very adaptable bacterium, which after transitioning from an environmental reservoir or cross-infecting patients [14] can switch gene expression and/or undergo mutations, that selects for its survival within the adverse environmental conditions of the mucous plug, which are both highly oxidative with anaerobic pockets, and hyperosmotic. [1-3, 6] Within its defense arsenal, it is proposed that one of the main reasons for *P. aeruginosa* persistence within CF airways is the ability to develop and grow in biofilms. [3, 11]

1.1.2 The biofilm lifestyle

P. aeruginosa is a notorious biofilm-forming pathogen, that grow in biofilms within CF lungs. [3, 15, 16] Biofilm formation is a universal virulence strategy adopted by both environmental and clinically relevant bacteria to survive within hostile surroundings and cause infections. Biofilms are sessile microbial communities, enmeshed in a hydrated extracellular matrix (ECM) comprised of polymeric substances, which provides bacteria survival advantages over the planktonic mode of growth. [1, 15, 17] At the bacterial level, there is a facilitated metabolic exchange and horizontal gene transfer due to cell-cell proximity, [15] additionally, the polymeric ECM that surrounds these communities also protects the microbes against immune clearance and antimicrobial interventions. [1, 3, 15, 16]

Biofilm formation is a very intricate process that starts with the attachment of free-swimming bacteria to a substratum or one another. The bacteria then start to multiply, leading to an increased community mass, defined as microcolonies, which further mature and form complex three-dimensional mushroom-shaped macrocolonies (Fig 1.1). [1, 3, 18] Eventually, these macrocolonies release new planktonic cells to the environment in a dispersion step occurring naturally or triggered by events such as small molecules or phage-mediated killing, which ultimately re-starts the biofilm cycle. [18, 19]

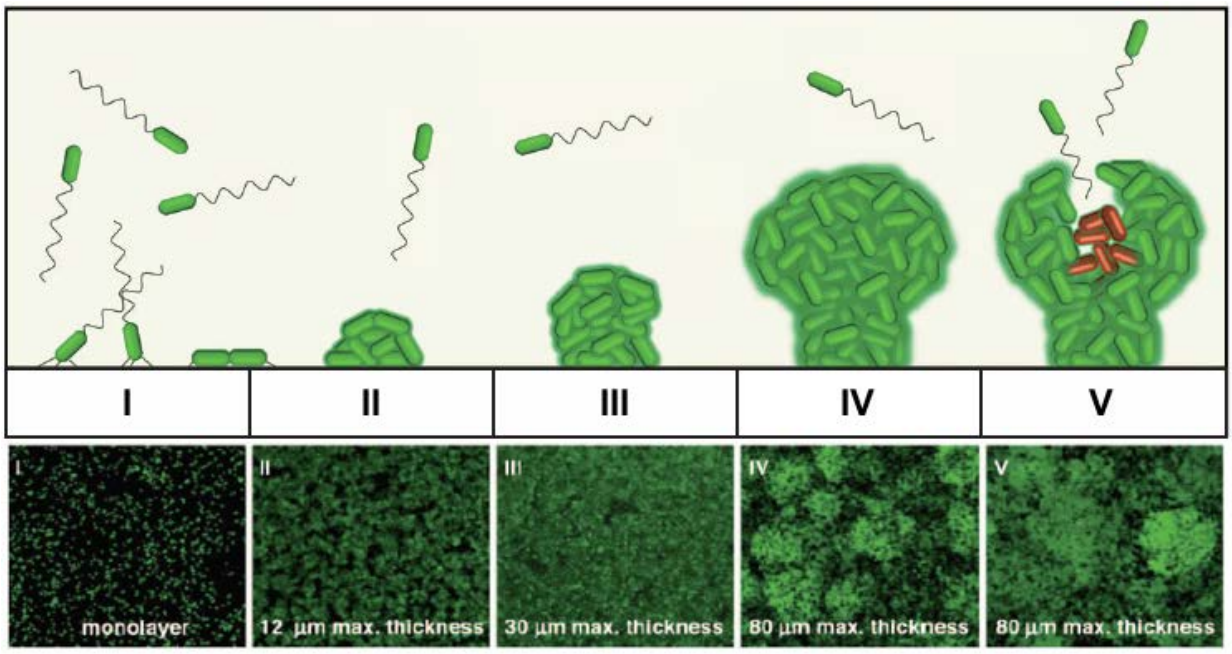

Figure 1.1: The coordinated process of biofilm formation.

Upper panel shows a schematic diagram of the biofilm formation steps, while lower panel shows imaged green fluorescent protein (*gfp*)-labeled bacteria throughout biofilm development. Free-swimming (or planktonic) bacterial initially attach to a surface or one-another (I) and multiply forming microcolonies (II). With the increased microbial mass, bacteria coordinate gene expression and start secreting exopolysaccharides (EPS) molecules that form the biofilm matrix, which enmeshes the growing population, among other alterations (III). Biofilms then develop into mushroom-shaped large colonies (IV) and, eventually, naturally and/or via cell death inside biofilm (represented by red bacterial cells) and polymeric matrix degradation, new planktonic cells are released to the environment (V). Panels adapted from Mikkelsen *et al*. [18] and Wagner and Iglewski [3] with permission.

1.1.3 Biofilm exopolysaccharides (EPS)

EPS are a major component of the biofilm matrix. [16, 17, 20-22] They contribute to initial attachment, biofilm maturation, promote the basis of biofilm scaffolding, have been show to disrupt biofilms of competitor strains (modulating bacterial interactions) and also play an essential part in protecting the community from antibiotics and the immune system. [16, 18, 20, 23, 24] *P. aeruginosa* produces three major EPS: alginate, Pel and Psl, all with individual and/or redundant functions within the development and maintenance of the biofilm. [16, 20]

Alginate is a high molecular weight negatively charged polysaccharide, composed of non-repetitive monomers of D-mannuronic and L-guluronic acids, encoded by a twelve-gene operon. [24, 25] It is secreted to form the ECM, and although it's usually not produced by environmental strains, mucoid strains that overproduce alginate are frequently isolated from CF patients. [24] It is not required for biofilm development, though overproduction of alginate not only changes the biofilm architecture, but also increases *P. aeruginosa* resistance to antimicrobials, phagocytosis and free radical attacks. [25]

Pel is a positively charged glucose-rich polysaccharide, composed partially by N-acetylgalactosamine and N-acetylglucosamine residues, encoded by a seven-gene operon, called pellicle formation locus (*pel*). [16, 24, 26] Pel has a secreted and a cell-associated form, [26] it functions as an adhesin, being critical for initial and later biofilm interactions, and it is essential for pellicle formation in the liquid-air interface. [16, 20, 24] Pel is able to cross-link with eDNA in the biofilm core and is enough for maintaining biofilm structure in its peripheral region. [26] Pel also increases resistance to aminoglycoside antimicrobials. [20] Additionally, Pel is required for biofilm formation in the *Drosophila melanogaster* oral feeding model, limiting bacterial aggregates to the crop and delaying bacteremia and fruit fly death. [27]

Psl is a neutrally charged EPS composed of repeating pentamers of D-manose, L-rhamnose and D-glucose, encoded by the 12-gene polysaccharide synthesis locus (*psl*). [16, 24] Psl can be found as part of the bacterial capsule and secreted to form the biofilm matrix. It arranges in fiber-like structures, important for the initial cell-surface interaction, biofilm development and conservation of the biofilm architecture. [16, 22, 25] In contrast to Pel, Psl needs to be continuously produced for keeping its scaffolding characteristics. [16, 17, 24, 25] Additionally, Psl is critical for antimicrobial resistance in initial stages of biofilm development against polymyxins, aminoglycosides and fluoroquinolone antibiotics [28] and it was also shown to reduce early recognition by the innate immune system, blocking phagocytosis, lowering the release of reactive oxygen species (ROS) and protecting bacteria from cell killing by neutrophils. [29]

It is proposed that this chemical charge diversity of EPS within *P. aeruginosa* matrix may give extra protection to cells in different conditions. [26] Strains of *P. aeruginosa* produce the Pel and Psl EPS in the early colonizing, non-mucoid isolates, as well as mucoid isolates, which overproduce alginate. [30-32] It is suggested that within the CF context, the increased inflammatory infiltrate in the lungs, the high production of ROS by phagocytes, and the reduced oxygen concentrations, selects for biofilm-related phenotypes of *P. aeruginosa*, including mucoid isolates or rugose small colony variants (RSCVs), that overproduce Pel and Psl. [11, 24, 33, 34]

1.1.4 Biofilm regulation

Bacteria in biofilms show very divergent phenotypes and gene expression profiles throughout growth, highlighting the complexity and strict regulation of the biofilm growth cycle.

[35, 36] Not surprisingly, Pel and Psl biosynthesis is regulated by an intricate signalling network, including multiple systems and associated factors, which coordinate *P. aeruginosa* gene expression on both transcriptional and post-transcriptional levels (Fig 1.2). [16, 37]

After individual cells attach to a substrate and start multiplying, it is estimated that quorum sensing (QS) is an initial player in biofilm formation and differentiation processes. [1, 7, 38] *P. aeruginosa* is known to possess at least four sets of connected hierarchical QS systems, [39] which are able to detect the increased microbial mass and other environmental signals and coordinate its gene expression patterns, inducing many virulence genes and promoting the biofilm mode of growth. [1, 38, 39]

Bacteria also respond to environmental changes via activation of two-component systems (TCS), which regulate gene expression and many have been shown to be involved in biofilm formation. The complex regulatory pathway that controls biofilm formation includes numerous TCS in *P. aeruginosa* such as the GacAS and PhoPQ sensor-regulator systems. [2, 17] Another central signalling pathway involved in controlling *pel* and *psl* expression and, consequently, biofilm formation, is the one formed by the second messenger bis-(3′-5′)-cyclic dimeric guanosine monophosphate (c-di-GMP) molecule. [37, 40]

One important pathway is formed by the GacAS two-component system, which regulates mRNA stability by sequestering the post-transcriptional RNA-binding protein, RsmA, allowing free translation of *pel* and *psl* transcripts. [2, 41] When the Gac/Rsm pathway is activated, GacS histidine kinase forms homodimers, which phosphorylates and activates the GacA sensor kinase molecule. The activation of GacA induces the expression of *rsmY* and *rsmZ* small regulatory RNAs (sRNAs), which in turn, sequester free RsmA molecules (Fig 1.2). [2, 25, 42, 43] RsmA is a global regulator that promotes a negative post-transcriptional feedback over many

transcripts, including *pel* and *psl*, reducing biofilm formation (Fig 1.2). [25] RsmA also indirectly affects expression of many genes on a transcription level by inhibiting QS networks. [44, 45]

In addition, the Gac/Rsm pathway is controlled by the RetS and LadS orphan sensors, which indirectly and antagonistically coordinate *pel* and *psl* expression (Fig 1.2). [42, 46] RetS was originally described as a transcriptional repressor of *pel* and *psl* using microarray analysis [42] although the mechanism of RetS transcriptional control of *pel/psl* is not understood, given the lack of a known cognate response regulator. RetS is able to form heterodimers with the GacS sensor kinase, inhibiting GacA activation and reducing Pel and Psl translation. [18] Therefore, mutants in *retS* gene show elevated *pel*/*psl* expression and translation, resulting in a hyperbiofilm phenotype. [25] On the contrary, the LadS sensor kinase positively modulates RsmZ levels, increasing Pel and Psl synthesis and biofilm formation. [25, 46]

The PhoPQ TCS is a cation sensor complex that is activated in conditions with limiting divalent magnesium (Mg^{2+}) cations. [2] Our lab has shown that the PhoPQ system is also induced in acidic pH conditions [47] and in the presence of eDNA rich conditions, including biofilms or exposure to neutrophil extracellular traps. [48, 49] We identified two important properties of eDNA that may be relevant in DNA rich biofilms. DNA is an efficient chelator of Mg^{2+}, and can impose Mg^{2+} limitation in DNA rich conditions, [48] but DNA can also acidify biofilms, and thus activate the PhoPQ pathway in multiple ways. [47]

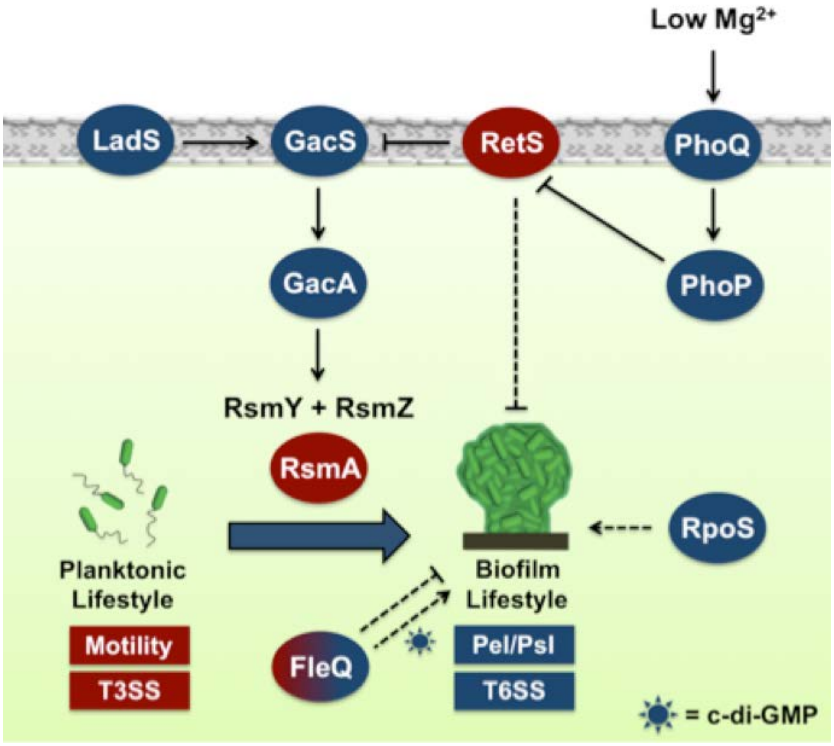

Figure 1.2: The Gac/Rsm regulatory pathway in *P. aeruginosa* is the central pathway that controls the switch to a biofilm lifestyle.

Whether activated by LadS, or repressed by RetS, both additional inner membrane orphan sensors, the Gac/Rsm pathway promotes stability of the *pel* and *psl* transcripts and ultimately EPS production and biofilm formation (solid lines). This pathway inversely controls the Type Three Secretion System (T3SS), largely thought to be an acute virulence factor and not required for chronic infections caused by biofilms. RetS also contributes to the transcriptional repression of *pel* and *psl*, along with the transcriptional activators RpoS and FleQ (dashed lines). FleQ can function as a repressor or activator of the *pel* operon, depending on the presence of cyclic-di-GMP. The Mg^{2+}-sensing PhoPQ TCS directly represses *retS*, which in turn induces biofilm formation. Positive regulators of the biofilm lifestyle are represented in blue, negative regulators in red.

A subsequent observation of our lab is that under limiting Mg^{2+} concentrations (or by DNA-mediated cation chelation), PhoP directly represses *retS* expression and thereby activates the Gac/Rsm pathway (Fig 1.2), promoting biofilm formation. [17] DNA-mediated cation chelation and acidification induces antibiotic resistance mechanisms based on cell surface and lipopolysaccharides (LPS) modifications that limit antimicrobial peptide and aminoglycoside entry. [47, 50] PhoPQ system was additionally shown to be involved in *P. aeruginosa* virulence, with PhoQ mutants showing severe decreased fitness for infection and persistence in diverse infection models, including plant and mammalian hosts. [2, 4]

Both Gac/Rsm and c-di-GMP regulatory pathways are connected (Fig 1.2). Diguanylate cyclase (DGC) enzymes are involved in c-di-GMP synthesis, and high levels of c-di-GMP promote the biofilm lifestyle. [16, 37, 51] Previous reports have shown that mutants in the *wspF* gene, which functions in signal transduction and promotes continuous activation of the WspR DGC, demonstrate increased intracellular levels of c-di-GMP and hyperaggregative phenotype. [40] Additionally, Moscoso *et al.* [51] reported elevated c-di-GMP levels in a *retS* mutant, which were independent of biofilm formation and the presence of active *pel* and *psl* genes.

Several groups have identified the connective link between the Gac/Rsm and c-di-GMP systems. In one report, Baraquete *et al.* [52] identified the transcription regulator FleQ to be an activator of *pel* expression in the presence of c-di-GMP. Interestingly, in the absence of the signalling molecule, FleQ binds the promoter region and represses *pelA* transcription. [52] Also, the DGC SadC promotes biofilm formation in a Pel-dependent matter, [37, 53] which accounts for the hyperbiofilm phenotype in *retS* mutant. [37]

Many other factors are also involved in Gac/Rsm activation, EPS secretion and biofilm formation. One example is the hybrid sensor kinases PA1611, which is able to regulate RsmA

levels by directly interacting with RetS and de-repressing the Gac/Rsm pathway. [54] Also the stationary phase σ-factor RpoS, functions as a transcription regulator that activates *psl* expression in a different cascade than RsmA. [41]

1.1.5 The biofilm inhibition premise

1.1.5.1 Current research approaches to target the biofilm mode of growth

Besides their significant presence in nature and industrial settings, biofilms are remarkably dangerous in the clinical context. [55] There are no antibiotics that specifically target cells growing within biofilms, as conventional antimicrobials were developed against planktonic cultures. High antibiotic tolerance is a hallmark feature of biofilms and much higher concentrations are needed to eradicate the encased cells. [56, 57] Therefore, several efforts have been made to identify new ways of preventing and/or disrupting biofilms. Some of these efforts have already shown some degree of success in promoting human health. [55] Most of the antibiofilm-targeted clinical trials focused on reducing bacteria colonization on abiotic surfaces, therefore inhibiting subsequent bacterial infections in patients. [55, 58] Some of the strategies used to avoid catheter-related infections have been recently reviewed. [55]

We have recently reviewed many research approaches for targeting the biofilm mode of growth. [58] These approaches include the use of antimicrobial peptides (AMP) with effective antibiofilm properties, naturally occurring or engineered bacteriophages that kill the encased bacterial cells, specific enzymes able to degrade matrix components and disperse biofilms, and also small molecules that target the biofilm mode of growth by distinct mechanisms. [58]

1.1.5.2 High-throughput screening (HTS) approaches identify biofilm inhibitors

In order to characterize new molecules effective against biofilms, researchers have assessed the potential of HTS approaches for the identification of antibiofilm molecules. HTS techniques allow an efficient and rapid method to test a huge number of compounds in drug libraries. [58] One of the first HTS reports of antibiofilm compounds in *P. aeruginosa* used a quantitative luminescence-based approach to test 66,095 compounds that reduced the adhered biomass. [59] They reported 30 molecules that efficiently blocked *P. aeruginosa* initial attachment and reduced biofilm formation by 50%, at concentrations < 20 μM, [59] but there has been little follow up of their possible mechanism of action.

In another example, Wenderska *et al.* [60] screened a defined set of molecules in a high-throughput fashion and identified four molecules that reduce *P. aeruginosa* biofilm formation. Palmitoyl-$_{DL}$-carnitine ($p_{DL}c$) was further characterized and shown to inhibit biofilm formation even under biofilm-inducing conditions. [60] Dr. Lori Burrows' group has further tested the same library for detection of active agents against the food-borne pathogen *Listeria monocytogenes*, and in addition to $p_{DL}c$ and sphingosine, identified additional 13 compounds which reduce *L. monocytogenes* biofilm formation by > 50%, showing the broad antibiofilm potential of some of these molecules. [61]

These and diverse other approaches have succeeded in identifying compounds that block biofilm formation and/or detached preformed biofilms in many species of bacteria. [58] However, most of these studies use a generic approach of quantifying biofilm biomass without any insights in the specific bacterial targets. Therefore, even though many antibiofilm compounds have been identified to date, the lack of a characterized mechanism of action and a

proper toxicological/pharmacological assessment of these molecules have delayed their possible use in therapeutics. [62]

1.2 Project rationale and hypothesis

The biofilm mode of growth provides bacteria survival advantages in hostile environments. [1, 3, 15, 16] As biofilms are intimately related to antibiotic tolerance and chronic infections, [1, 20] there is an urgent need for the identification of new approaches that target the biofilm mode of growth for the prevention and/or treatment of chronic bacterial infections.

Given the conservation and importance of Pel and Psl throughout all stages of biofilm formation in *P. aeruginosa*, [25] these EPS are an attractive target for the identification of new antibiofilm compounds. For this project we hypothesized that compounds able to block *pel* and *psl* gene expression could serve as novel antibiofilm compounds by reducing or blocking EPS biosynthesis and biofilm formation in *P. aeruginosa*. Additionally, we hypothesized that reduced EPS production and hypobiofilm phenotype could render bacteria less virulent and, possibly, more susceptible to antimicrobial treatments.

Therefore we developed a high throughput gene expression screen of 31,096 compounds in the Canadian Chemical Biology Network (CCBN) drug library, for the identification of small molecules that repress expression of EPS genes in *P. aeruginosa*, without affecting overall bacterial growth. If our hypothesis proves to be true, this class of compound will represent an example of an anti-virulence strategy for use in preventing or treating biofilm infections. Another advantage to this class of anti-infective compounds is to overcome the development of antibiotic resistance, typical of conventional antibiotics. Compounds that don't reduce bacterial growth

may limit the selective pressure and the development of antibiotic resistance if advanced for use as novel treatments for chronic *P. aeruginosa* infections.

1.3 Objectives

In order to identify new compounds that inhibit biofilm formation as an antivirulence approach for treating chronic *P. aeruginosa* infections, this project was divided in four core objectives:

Objective #1: To implement a HTS for the identification of EPS gene repressors.

Objective #2: To determine the antibiofilm activity of EPS repressors.

Objective #3: To test the antibiofilm molecules for their ability to reduce *P. aeruginosa* virulence and to increase biofilm susceptibility to antimicrobials.

Objective #4: To develop a RNA-seq pipeline to investigate the global changes in gene expression after antibiofilm treatment.

Chapter Two: High-throughput screening for the identification of EPS-gene repressors

2.1 Introduction

One of the major constituents of *P. aeruginosa* biofilms are EPS. [21, 22] The Pel and Psl EPS display important and partially redundant roles for biofilm matrix establishment, scaffolding and protection, [16, 20, 28] and are therefore critical targets for the identification of new antimicrobials that reduce biofilm formation.

Many reviews have outlined the possible use of small molecules that block EPS production for the characterization of new antibiofilm approaches, [58, 63, 64] but few experimental studies have focused on targeting such biofilm matrix polymers. Most of the HTS antibiofilm approaches to date have focused on the identification of molecules that reduce microbial biomass through direct imaging or biofilm quantification, [59, 61, 65-67] without much concern in acknowledging the mechanism of action of the identified hits. Furthermore, other antibiofilm approaches have targeted the QS and c-di-GMP signalling systems, using both *in silico* and targeted-gene screening approaches. [68-71]

Nevertheless, the studies that target the polysaccharide constituents of the matrix for the purpose of blocking biofilms employ EPS degrading enzymes, such as alginate lyase, [72] Pel/Psl specific hydrolases, [73] or dispersin B (DspB). [74, 75] Other studies focused on naturally occurring EPS-degrading phages [76] or engineered strain-specific lytic bacteriophage therapies [77] for their ability to degrade EPS molecules and disperse the biofilm matrix.

In this chapter, I will describe the first aim of this project, which was to implement a high throughput gene expression screen to identify compounds that reduce the expression of EPS biosynthesis genes. We hypothesized that compounds that reduce the EPS gene expression

would reduce biofilm formation. This novel approach is different than simply screening for compounds that reduce biofilm biomass. By screening for compounds that reduce expression of essential genes required to build a biofilm, we are using a more targeted approach that should ultimately help determine their mechanism of action. Our lab has previously reported that *P. aeruginosa* forms robust biofilms and aggregates in liquid culture when grown in limiting magnesium conditions. [17] Therefore, we wanted to screen for repressors of EPS gene expression under biofilm-promoting growth conditions.

2.2 Specific methods

2.2.1 Bacterial strains and growth conditions

The strains and plasmids used throughout this study are listed in Table 2.1. Reporters were grown in Basal Minimal Medium 2 (BM2) at 37^{o}C, containing excess or limiting Mg^{2+} concentrations. BM2 medium was prepare with 100 mM Hepes pH 7.0, 7 mM $(NH_4)_2SO_4$, 1.03 mM K_2HPO_4, 0.57 mM KH_2PO_4, 20 μM–2 mM $MgSO_4$, 10 μM $FeSO_4$ and ion solution, containing 1.6 mM $MnSO_4.H_20$, 14 mM $ZnCl_2$, 4.7 mM H_3BO_3 and 0.7 mM $CoCl_2.6H_20$. The media was supplemented with 20 mM sodium succinate as a carbon source for all assays. Stock solutions of ampicillin (50 mg/ml, AMRESCO), ciprofloxacin (2 mg/ml, BioChemika), colistin (10 mg/ml, Sigma), gentamicin (30 mg/ml, Sigma), kanamycin (100 mg/ml, Sigma), polymyxin B (30 mg/ml, Sigma), and tobramycin (25 mg/ml, Sigma) were made in ultrapure water and stored at -20^{o}C, and used as indicated. Trimethoprim stock (10 mg/ml, Sigma) was prepared in methanol and stored at 4^{o}C.

Table 2.1: Strains and plasmids used in this study.

Name	Description/Characteristics	Reference
***P. aeruginosa* wild type**		
PA14	Wild type *P. aeruginosa* strain PA14	RE Hancock
PAO1	Wild type *P. aeruginosa* strain PAO1	RE Hancock
Green fluorescent protein (*gfp*)-tagged *P. aeruginosa*		
PA14-*gfp*	PA14-Tn*7*::*gfp*. Wild type *P. aeruginosa* constitutively producing GFP. Gm^r	This study
PAO1-*gfp*	PAO1-Tn*7*::*gfp*. Wild type *P. aeruginosa* constitutively producing GFP. Gm^r	[78]
Gene reporters and mutant		
PAO1::*p16Slux*	Wild type *P. aeruginosa* transcriptional *luxCDABE* fusion of 16S rRNA genes	[79]
pelB::lux	*pelB* transposon mutant and transcriptional *lux* reporter (66_B7)	[80]
retS::lux	*retS* transposon mutant and transcriptional *lux* reporter (18_F4)	[80]
PAO1 p*pslA-lux*	*pslA* promoter-*lux* transcriptional reporter in pMS402. Tp^r	[17]
PAO1 p*exoT-lux*	p*exoT-lux* integrated in att site of PAO1	[81]
PAO1 p*cdrA-lux*	*cdrA-lux* transcriptional reporter. Km^r	This study
PAO1 pMS402	*pMS402* plasmid for constructing *lux* transcriptional fusions. Km^r	This study
$pslA_{TL}$*::lacZ*	PAO1 with a translational reporter for *pslA* on miniCTX-lacZ	[41]
Δpsl	*Δpsl* mutant with pMA8 used in PAO1 background	[82]
pel/Δpsl	Double *pel/psl* mutant in PAO1 background	[17]
PD0300	*ΔmucA22.* Mucoid derivate of PAO1.	[83]
Plasmids		
pBT270	Mini-Tn7-*gfp*(mut3). Integration vector for *gfp*. Gm^r, Amp^r	[84]
pTNS2	Helper plasmid for mobilizing mini-Tn7 plasmid in *P. aeruginosa*. Amp^r	[84]
pMS402	Promoterless *lux* reporter construct. Km^r	[85]
pMS402::pcdrA	pMS402 containing the *cdrA* promoter region. Km^r	[86]
OP50	*Escherichia coli* strain OP50. Bacterial food source for nematode maintenance and control of low virulence	[87]

2.2.2 HTS optimization

We initially optimized the growth media and incubation time to suit the HTS approach by selecting the condition in which the *pelB::lux* reporter shows maximum gene expression in 384-well microplate format. An overnight culture of the *pelB::lux* reporter was diluted 100 times in basal minimum media 2 (BM2) containing high (2 mM), low (80 μM) and limiting (20 μM) Mg^{2+} concentrations, to a final concentration of approximately $1x10^7$ CFU/ml. Using a 384-well microplate with 96 replicates for each of the three conditions, growth and gene expression from the *pelB::lux* reporter were monitored in a Wallac Victor luminescence plate reader (Perkin-Elmer). Luminescence (in counts per second, CPS) and bacteria growth (optical density at 600 nm, OD_{600}) were measured every hour throughout 24 hours at 37ºC incubation, in microplates covered with mineral oil to prevent evaporation.

2.2.3 HTS statistics

To determine if our assay was suitable for a HTS approach, we measured gene expression under control induced conditions, and compared to background noise in order to determine the statistical parameters for the assay. The *pelB::lux* reporter strain was incubated for 14 hours in half of two 384-well microplates containing limiting magnesium (induced). Half of each plate also contained negative condition (background control) of sterile media (n=384 measurements for each condition). Gene expression (CPS) was determined in the Victor luminescence plate reader. Using these control data of maximum gene expression and background noise, we determined the Z' and Z scores, as previously described. [88] The Z' score is a quality parameter of the assay itself, used to validate the approach used in the HTS, by means of the controls' median and standard deviation values. [88] Nevertheless, we also determined the Z

score, which is a statistical parameter for the precise qualification of a HTS assay, as it also takes in consideration the signal dynamic range of the tested library. [88]

It is noteworthy to acknowledge that facing the fact that we are using a inhibition type assay approach, looking for repressors of the *pel* gene, the mean and standard deviation control values used for calculation of the Z factor arrived from the negative, sterile control as recommended. [88]

2.2.4 Primary HTS

The primary HTS consisted of testing all 31,096-small molecules within the CCBN library against the *pelB::lux* reporter. The molecules were transferred from the stock 96-well microplates to 384-well assay optical microplates with the assistance of 96-pin plastic transfer devices (Phoenix Research Products). Assay plates contained 100x dilution of the *pelB::lux* overnight culture in BM2 20 μM Mg^{2+} (~$1x10^7$ CFU/ml). Compounds were tested at a final concentration of approximately 10 μM, estimated by the volume transferred by the pin device. All compounds were tested once with no replicates in the primary screen. Microplates containing the *pelB::lux* reporter and small molecule combinations were covered with an air-permeable membrane and incubated at 37ºC for 14 hours. At the end of the incubation time, luminescence in CPS was determined in Victor luminescence plate reader. The percentage of expression (% exp) for each treatment was calculated in reference to the mean CPS value (μCPS) of each microplate, according to the following formula:

$$\% \text{ exp} = 100 * \frac{\text{CPS for a drug}}{\mu\text{CPS of the plate}}$$

2.2.5 Secondary HTS

For the confirmation of *pelB::lux* repression and investigation of *pslA-lux* inhibition, we ran a secondary gene expression experiment for every compound that showed at least 50% repression of *pelB::lux* reporter. The 163 small molecules were retested in duplicate, in the same 384-well microplate format. Compounds were transferred with the 96-pin plastic transfer devices to plates containing 100x dilution of an overnight culture of the *pelB::lux* or *pslA-lux* reporters in BM2 20 μM Mg^{2+} (~1x10^7 CFU/mL), to a concentration of approximately 10 μM. Wells were covered with mineral oil and reporter's expression (CPS) and growth (OD_{600}) were monitored throughout 18 hours of incubation at 37^{o}C, in a Victor luminescence plate reader.

2.2.6 Reordering of identified compounds and confirmation of **pel** *and* **psl** *repression*

From the 14 compounds that reproducibly repressed *pelB::lux* and *pslA-lux* expression, 13 were reordered for further testing, while one was not commercially available. Upon arrival, 1 mM stocks were prepared for each compound in dimethyl sulfoxide (DMSO), which were stored at -20^{o}C and thawed on ice when needed for an assay. For confirmation of *pel/psl* repression, we retested all 13 reordered compounds for their ability to reduce expression on both *pelB::lux* and *pslA-lux* gene reporters on 96-well micropate format. The 13 small molecules were tested in triplicate at a final concentration of 10 μM, under biofilm inducing condition of BM2 20 μM Mg^{2+}, in gene expression experiments as described above.

2.2.7 Investigation of non-specific **lux** *repression and normalized* **pel/psl** *expression*

We wanted to rule out the possibility that *pel* repressors may be repressing luciferase enzymes from the *luxCDABE*-encoding reporters. Gene expression was monitored from other *lux*

reporter strains, including a high expression *16Slux* reporter, and a low expression pMS402 plasmid *lux* reporter. Basal gene expression from pMS402 was due to leaky expression from the plasmid, despite the absence of any promoter to drive expression of the luxCDABE enzymes. [85] Any effects on either of these reporter strains were considered to be a result of non-specific *lux* activation or repression. Gene expression alterations were obtained as previously stated, the 13 *pel* repressor compounds were tested against the *16Slux* and promoterless pMS402 reporter at a final concentration of 10 μM, in BM2 20 μM Mg^{2+}. CPS and OD_{600} were measured throughout 18 hours of incubation, at 37°C, in Victor luminescence plate reader.

2.2.8 Statistical analysis

In this chapter, Z and Z'-factors were used to determine the robustness of the HTS approach, considered ideal if > 0.5. Additionally, statistical significance between populations was determined by paired two-tailed Student's t-test. Data considered significant at level of $p<0.05$.

2.3 Results

2.3.1 HTS optimization and statistics

In agreement with a previous report from our lab, the *pel* EPS biosynthesis genes are induced under Mg^{2+}-limiting conditions (Fig 2.1). [17] The time point for maximum *pelB::lux* expression occurs around 14 hours of incubation at 37°C, as represented by the red arrow in Fig 2.1. We selected the 14-hour time point for performing the HTS, as *pel* expression is maximal.

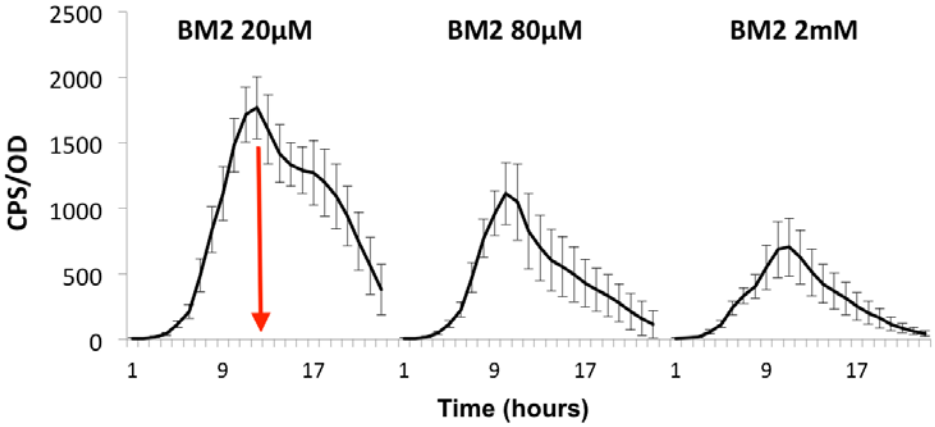

Figure 2.1: Influence of magnesium concentration on *pelB::lux* expression in 384-well format.

Gene expression profiles of the *pelB::lux* reporter expression in BM2 medium containing different Mg^{2+} concentrations. Red arrow indicates point of maximum gene expression (~14 hours). Curves built with average values and the standard deviations from n=96 replicates.

Table 2.2: Summary of the HTS approach and screening statistics.

Parameter	**Value**
Primary HTS	
Number of compounds screened	31,096
Number of hits	163
Secondary HTS	
Number of *pelB::lux* repressors identified	14
Number of antimicrobials identified	26
Assay statistics	
Z'-factor value	0.527
Z-factor value	0.511

Moreover, we also determined some assay screening statistics, which both indicate that the approach we used for running our screening was excellent (Z and Z' $\geq$ 0.5), showing large separation bands and liability to appoint useful data. The validation parameter for the HTS approach and the statistical values for the assay are summarized in Table 2.2.

2.3.2 HTS identified **pel/psl-***gene repressors*

In the primary HTS, we tested the 31,096-small molecules within the CCBN, and identified 163 hits that reduced *pelB::lux* expression by at least 50% (highlighted in red in Fig 2.2.A). We also selected six 'inducers' that increased *pelB::lux* expression over 300%, for further testing in the secondary screen (highlighted in green in Fig 2.2.A).

In total, we retested these 169 compounds (163 repressors + 6 inducers) for their ability to reproducibly affect the *pel* operon. In addition, we tested the ability of these hit compounds to repress expression of the other major EPS gene cluster, the *psl* genes. [30] Pel and Psl are the main EPS produced by non-mucoid strains, and are co-regulated by a common regulatory pathway (see Chapter 1). Due to their co-regulation, we hypothesized that compounds targeting the common regulatory pathway would have the beneficial feature of repressing both major EPS species. Of the 163 initial repressors, 14 compounds consistently repressed expression of *pelB::lux* reporter and most of them also showed effect in repressing *pelA-lux* expression (Table 2.3). It is important to note that none of these *pel/psl* repressors had any effect on bacterial growth, even in concentrations as high as 100 μM, which is ~ 10 times the concentration used in our screening experiments. Additionally, none of the 6 selected inducers demonstrated a reproducible effect over *pelB::lux* expression in the secondary screen.

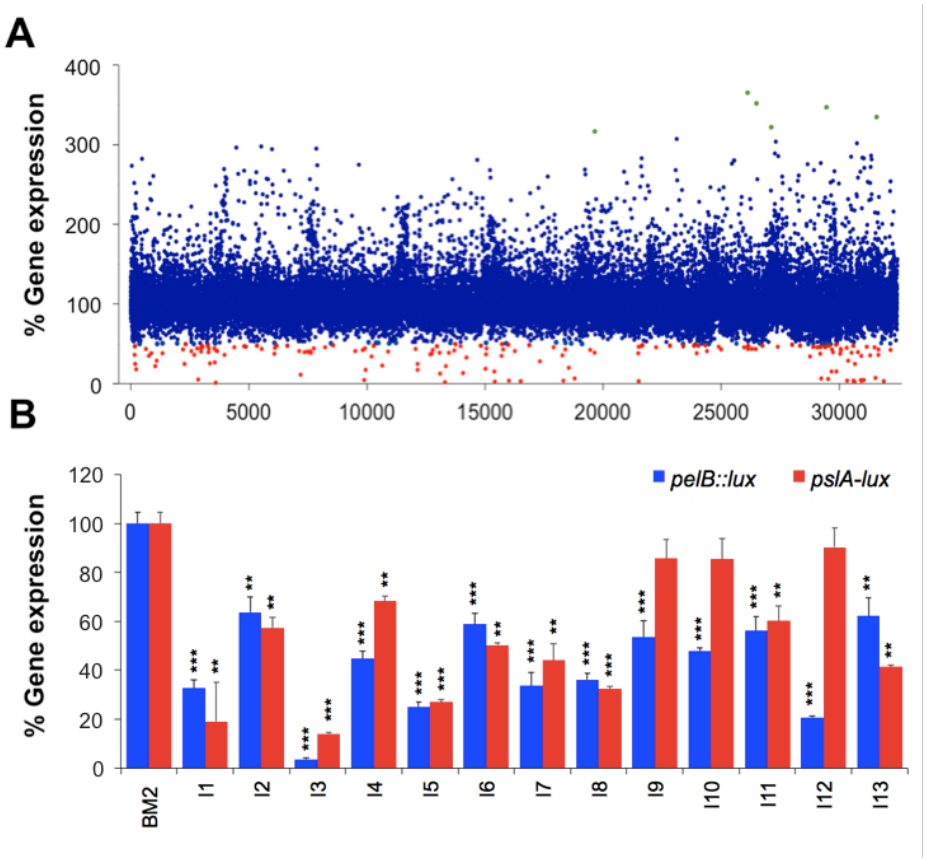

Figure 2.2: HTS identifies small molecules that reduce EPS gene expression.

(A) Summary of HTS showing individual effects of all 31,096 compounds over *pelB::lux* expression. In red are highlighted the 163 treatments that repressed gene expression by ≤ 50%, and in green the 6 that promoted *pelB::lux* expression ≥ 300%. **(B)** Reordered lead compounds were retested for their ability to repress expression of *pelB::lux* and *pslA-lux* transcriptional reporters. Total gene expression after treatment was compared to untreated controls (100%). Values shown are the average area under the curve for triplicate samples and the standard deviation, n=4. Statistical significance between populations was determined by paired two-tailed Student's t-test and significant repression in reporter's expression is indicated: * ($p<0.05$), ** ($p<0.01$) and *** ($p<0.001$).

The molecular structures and nomenclature of the identified *pel/psl* repressor molecules are represented in Figure 2.3 and Table 2.3, respectively. From these 14 compounds identified, 13 could be ordered for further testing. For confirmation of their *pel/psl* repression properties, the reordered compounds at 10 μM were now tested for their ability to repress both gene reporters in a 96-well microplate format. From the 13 gene repressors, all of them reproducibly reduced *pelB::lux* reporter expression in the new format, with repression ranging from 30-90% (Fig 2.2.B), in comparison to reporter grown in biofilm inducing condition alone (100%). Additionally, most of these compounds were also able to reduce *pslA-lux* expression (10/13), with repression ranging from 10-85% (Fig 2.2.B), showing their effect on both EPS-encoding gene clusters.

2.3.3 Confirmation of **pel/psl** *repression after normalization for non-specific effects*

The lead compounds have no effect on bacterial viability, based on growth curves from microplate assays. To test for nonspecific inhibition of the *lux* enzymes, we selected the *16Slux* reporter that uses the promoter from the 16S ribosomal RNA (rRNA) genes. [79] This gene is highly expressed and as it is essential for prokaryotic ribosomal synthesis, and its expression should not be affected by treatments that don't limit bacterial growth. Similarly, the promoterless pMS402 plasmid was used as a second control for low level expression genes, due it's low basal luminescence from the *luxCDABE* cassette [85] that is likely due to leaky expression from the vector.

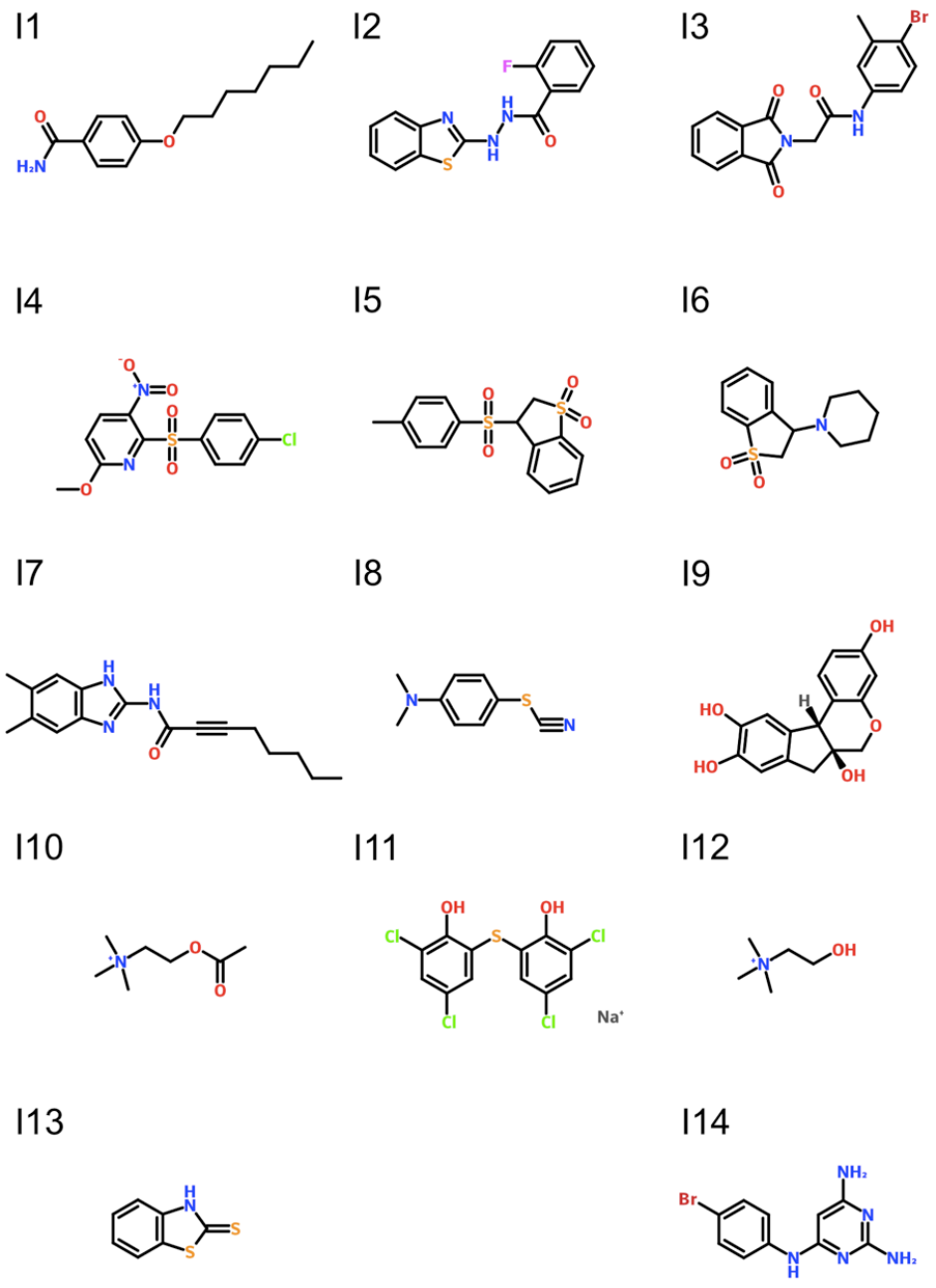

Figure 2.3. Molecular structures of the *pel/psl*-gene repressors identified in the HTS.

For more details and the molecular nomenclature, see Table 2.3.

Table 2.3: Molecular nomenclature of the *pel/psl* gene repressors identified in the HTS.

Code	Vendor	Vendor ID	Chemical name	PubChem CID
I1	ChemBridge	5307707	4-heptyloxybenzamide	1712173
I2	ChemBridge	5636083	N'-(1,3-benzothiazol-2-yl)-2-fluorobenzohydrazide	872872
I3	ChemBridge	6622147	N-(4-bromo-3-methylphenyl)-2-(1,3-dioxoisoindol-2-yl)acetamide	1346797
I4	Maybridge	BTB09154	2-(4-chlorophenyl)sulfonyl-6-methoxy-3-nitropyridine	2801235
I5	Maybridge	KM08157	3R-3-(4-methylphenyl)sulfonyl-2,3-dihydro-1-benzothiophene-1,1-dioxide	6934138
I6	Maybridge	KM08195	3-piperidin-1-yl-2,3-dihydro-1-benzothiophene-1,1-dioxide	281092
I7	Maybridge	RJC01132	N-(5,6-dimethyl-1H-benzimidazol-2-yl)oct-2-ynamide	2728870
I8	Maybridge	TL00118	p-thiocyanodimethylaniline	23540
I9	MicroSource	200012	Brazilin	73384
I10	MicroSource	1500104	Acetylcholine	187
I11	MicroSource	1500148	Bithionate sodium	60148380
I12	MicroSource	1503428	Choline	305
I13	MicroSource	1504225	Captax (2-Mercaptobenzothiazole)	697993
I14	Maybridge	BTB14023	N4-(4-bromophenyl)pyrimidine-2,4,6-triamine	238013

To investigate non-specific effects on luminescence, the *16Slux* and pMS402 reporters were incubated in 96-well microplate format with 10 μM of the reordered repressor compounds. Gene expression throughout growth was determined in Victor luminescence plate reader and the total gene expression from the 18-hour growth period was determined and represented as the area under the curve. Gene expression from the untreated reporter growing in BM2 20 μM Mg^{2+} was set to 100%. While there was no effect on growth (OD_{600}) and minimal effects on expression of the *16Slux* and pMS402 reporters for many of the molecules (such as I4, I6, I7, I10 and I11), compound I3 was a strong *lux* repressor for both reporters (Fig 2.4.A). Interestingly, compound I2 was a *lux* activator of both reporter strains (Fig 2.4.A).

Having identified that some of the compounds were indeed promoting a non-specific repression of the *luxCDABE* reporter, we normalized the expression of the *pelB::lux* and *pslA-lux* reporters to the expression effects on the pMS402 construct for all treatments. We decided to select the pMS402 as the control normalization reporter because it shows a similar, low level of expression to the EPS-gene reporters, and normalization to *16Slux* might distort any non-specific effects. The normalized gene repression is shown as the NET-fold repression and despite some modest effects on the neutral reporters, we concluded that *pelB* and *pslA* expression were truly repressed and repression was not the consequence of any non-specific effect (Fig 2.4.B).

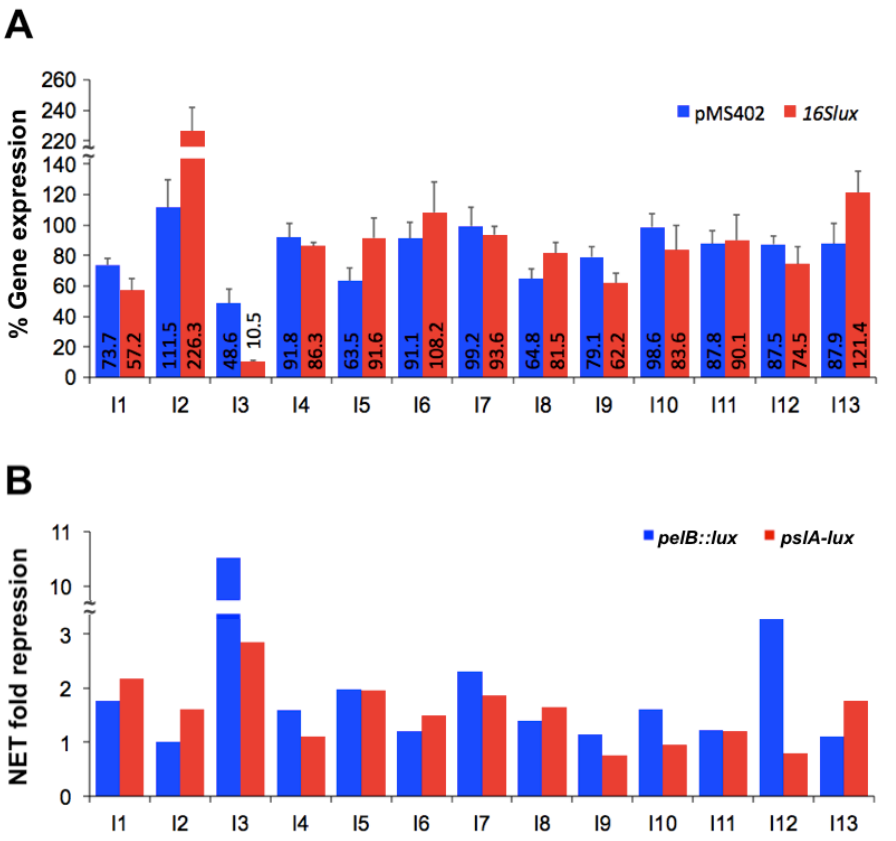

Figure 2.4: Investigation of non-specific *lux* repressors.

(A) Investigation of non-specific effects on expression from the *pMS402* and *16Slux* reporters. Total gene expression after treatment was compared to untreated controls (100%). Values shown are the average area under the curve for triplicate samples and the standard deviation, n=4. **(B)** Expression from the *pelB::lux* and *pslA-lux* reporters was normalized to control for the modest effects on the neutral pMS402 reporter. Bars represent the average net fold repression on triplicate samples relative to the untreated condition, n=2.

2.3.4 Identification of growth repressors

It is noteworthy to acknowledge that although none of the 13 reordered *pel/psl* repressor compounds have any negative effect over bacterial growth, even at concentrations as high as 100 μM, we were able to identify a separate group of compounds that repressed *pel* expression as a result of inhibiting the growth of the reporter. Thus, there were an additional 26 compounds that acted as *pelB::lux* repressors but that also had bactericidal or bacteriostatic properties (Table 2.4).

Consistent with this observation, many of these compounds were known antibiotics (mostly fluoroquinolones) or were previously reported to have some antimicrobial activity. According to our literature review, we separated these antimicrobial compounds into three different groups: small molecules with known antibiotic/disinfectant properties (group A), characterized non-antimicrobial molecules (group B) and uncharacterized molecules (group C) (Table 2.4). Compounds in group C were the most interesting in terms of new antibiotic discovery, and will be the subject of future research projects. The discovery of growth inhibitors highlighted the dual nature of our gene expression screen to find both *pel* repressors and conventional antibiotics. Interestingly, among the uncharacterized molecules (group C), two compounds (SPB07211 and KM07965) were recently identified in a whole-cell based HTS for small molecules that inhibit *Burkholderia cenocepacia* growth [89] and one small molecule (KM06346) was identified in a screen for non-specific repressors of DNA repair enzymes (AddAB helicase nuclease) in *Escherichia coli.* [90] Nevertheless, all these growth inhibitor compounds were removed from this study.

Table 2.4: Antimicrobial compounds identified in the HTS for EPS repressors.

Group*	Vendor	Vendor ID	Chemical name	Function	PubChem CID
A	MicroSource	1504260	Levofloxacin	Quinolone antibiotic	149096
A	MicroSource	1504272	Gatifloxacin	Quinolone antibiotic	5379
A	MicroSource	1505314	Sarafloxacin	Quinolone antibiotic	56208
A	MicroSource	1503614	Ciprofloxacin	Quinolone antibiotic	2764
A	MicroSource	1504303	Moxifloxacin	Quinolone antibiotic	152946
A	MicroSource	1505802	Gemifloxacin	Quinolone antibiotic	9571107
A	MicroSource	1505305	Pefloxacin	Quinolone antibiotic	51081
A	MicroSource	1500545	Sulfacetamide	Sulphonamide antibiotic	5320
A	BIOMOL	GR-317	Coumermycin	Aminocoumarin antibiotic	54675768
A	BIOMOL	GR-311	Mitomycin C	Antineoplasic antibiotic produced by *Streptomyces caespitosus*	5746
A	BIOMOL	NP-223	Patulin	Mycotoxin antibiotoc produced by species of Aspergillus and Penicillium	4696
A	ChemBridge	5153890	A22	Antibiotic (modulator of MreB activity)	348494
A	MicroSource	1500260	Pyrithione Zinc	Fungistatic and bacteriostatic (aspergillic acid derivate)	3005837
A	MicroSource	1500637	Merbromin	Antiseptic (organomercury compound)	441373
A	MicroSource	1500644	Phenylmercury	Antiseptic (organomercury compound)	567
A	MicroSource	1500572	Thimerosal	Antiseptic and antifungal agent (organomercury compound)	16684434
B	MicroSource	211468	Dantron	Stimulant laxative, antioxidant with antifungal properties Toxic and possibly carcinogenic (anthraquinone derivate)	2950
B	MicroSource	1505315	6-Aminonicotinamide	Antineoplastic, apoptosis inducer. NAD-analog	9500
B	MicroSource	1505317	Carmofur	Antineoplasic agent (pyrimidine analog)	2577

Table 2.4 (cont.): Antimicrobial compounds identified in the HTS for EPS repressors.

Group*	Vendor	Vendor ID	Chemical name	Function	PubChem CID
C	Maybridge	SPB07211	2-methylsulfanyl-5-[(5-nitro-1,3-thiazol-2-yl)sulfanyl]-1,3,4-thiadiazole	*Burkholderia cenocepacia* growth inhibitor. Possible thiadiazole derivate antimicrobial agent.	2746762
C	Maybridge	KM07965	2-[(4-chlorophenyl) sulfanylmethyl]-1-azabicyclo[2.2.2]octan-3-one	*Burkholderia cenocepacia* growth inhibitor. Possible chlorobenzyl derivate antimicrobial agent.	2822094
C	Maybridge	KM06346	3-(2-Thienylsulfonyl)-2-pyrazinecarbonitrile	AddAB helicase nuclease repressor. Possible cyanopyridine derivate antimicrobial agent.	2821421
C	Maybridge	HTS06235	N-(4-phenylmethoxyphenyl)-4-(pyridin-4-ylmethyl)piperazine-1-carboxamide	No antimicrobial properties reported. Possible piperazine derivate antimicrobial agent.	2812932
C	Maybridge	BTB08617	2-[5-(trifluoromethyl)pyridin-2-yl]sulfonylethyl benzoate	No antimicrobial properties reported. Possible benzoate derivate antimicrobial agent.	2800996
C	Maybridge	SEW00805	3,5-bis(methylsulfonyl)-1,2-thiazole-4-carboxamide	No antimicrobial properties reported. Possible thiazole derivate antimicrobial agent.	2739198
C	Maybridge	S04233	N-(4-fluorophenyl)-4,5-dihydro-1H-imidazol-2-amine	No antimicrobial properties reported. Possible nitroimidazol derivate antibiotic agent.	2731293

* Antimicrobial compounds were separated into three different groups: small molecules with known antibiotic/disinfectant properties (A), characterized non-antimicrobial molecules (B) and uncharacterized molecules (C).

2.4 Discussion

Currently, most antimicrobials are inefficient in targeting cells growing within biofilms, and much higher concentrations are required to eliminate these sessile communities. [56, 67] Directed by this immediate need for new approaches that target the biofilm mode of growth, several groups have used HTS approaches in an attempt to identify small molecules within large chemical libraries that show effective antibiofilm properties. [58]

HTS assays are needed to screen large number of compounds rapidly and with high efficiency. Therefore, such approaches rely on the ability to identify "hits" with a proper confidence rate, demanding statistical parameters that regard the screening precision and sensitivity to validate the approach used. [88] We performed our screening without calculating such statistical parameters, relying just on initial optimization and determination of the condition of maximum gene expression for the *pelB::lux* reporter in 384-well microplate format. Nevertheless, retrospective calculation of these validation factors from our screening assay indicates it is a satisfactory tool for the identification of *pel* gene repressors. Both Z' (0.527) and Z (0.511) scores reinforce the robustness of the approach used and the HTS assay, respectively, validating the ability of such screening to detect significant hits among the large number of compounds tested.

Ultimately, we were able to select 163 compounds that were retested in a secondary screen, and 14 reproducibly repressed *pelB::lux* expression (Table 2.3). Besides these 14 compounds, there were additionally 26 small molecules that showed antimicrobial characteristics in the concentration tested (Table 2.4). These growth inhibitors could not be distinguishable in the primary screen, due to lack of OD_{600} measurements, therefore being misinterpreted as gene repressors. Within this list of growth inhibitors (Table 2.4), the majority (16/26) consisted of

compounds that have been previously show to have antibiotic/disinfectant properties (group A), via different mechanism of actions. Interestingly, among the uncharacterized molecules (group C), three molecules have been previously identified in screens searching for new antibacterial agents.

It is noteworthy to acknowledge that some of these identified gene-repressing molecules share common structural features, such as benzothiazole rings in compounds I2 and I13 and benzothiophene rings in I5 and I6. Moreover, I10 (acetylcholine) is derived from I12 (choline). A search of these molecules in the PubChem BioAssay database (https://pubchem.ncbi.nlm.nih.gov) demonstrated that among these 14 compounds, many have been previously classified although very few have clear biological properties. In support of our observations that suggest these compounds have antibiofilm activity, acetylcholine and other choline derivatives were recently reported to have antibiofilm and antivirulence activity against *Candida albicans and P. aeruginosa.* [91, 92] The remaining *pel* repressors represent potentially novel compounds with biofilm repressing potential.

2.5 Conclusions from Chapter 2

i. In this chapter was completed the first aim of this study, in which we optimized and performed a high-throughput gene expression screen for the identification of small molecules able to repress EPS-gene expression.

ii. The validation statistics indicates the 384-well approach used was a good screening tool, able to potentially find actual hits among the huge number of compounds tested.

iii. Both the primary and secondary screenings culminated in the identification of 14 small molecule *pelB::lux* repressors, from which 13 were reordered for further testing.

iv. Some of the reordered compounds showed minor, non-specific effects on *lux* expression, but normalized *pel/psl* expression to the pMS402 vector control confirmed their repression activity.

Chapter Three: *Pel/psl* repressors reduce EPS secretion and biofilm formation

3.1 Introduction

The role of EPS in biofilm formation is well characterized. Although variable among different strains, both Pel and Psl molecules show essential roles for biofilm development and maintenance. [16] In this chapter we will focus on the ability of the *pel/psl* repressor compounds to affect the secretion of the EPS matrix and to reduce biofilm formation in different models. Biofilm assays were performed in non-mucoid PA14, PAO1 and a *retS::lux* strains, which differ in their ability to produce Pel and Psl as their main matrix EPS for biofilm formation. PA14 produces only the Pel EPS, PAO1 produces both Pel and Psl, while the *retS::lux* mutant overproduces both EPS molecules. We also tested our antibiofilm compounds against a mucoid variant of PAO1, a *ΔmucA22* mutant, which has increased production of alginate.

3.2 Specific methods

3.2.1 Bacterial strains and growth conditions

The bacteria strains used in this chapter are listed in Table 2.1 (please, refer to Chapter 2). Strains and reporters were grown in BM2 media containing 20 μM or 2 mM Mg^{2+}. BM2 medium was supplemented with KNO_3 (1%) to support anaerobic biofilm growth. PA14-*gfp* strain was prepared for this study as previously described, [84] by the transformation of the pBT270 *gfp*-encoding plasmid into PA14 wild type, with the help of a pTNS2 plasmid (Table 2.1). Colonies expressing *gfp* were selected for with gentamycin (Gm) resistance (50 μg/ml) and confirmed fluorescent phenotype with microscopy.

3.2.2 EPS quantification

As a first step to assess the antibiofilm activity of the compounds identified in our HTS, we wanted to determine their potential in reducing EPS secretion. We used the quantitative congo red (CR) binding assay, as previously described, [93] for estimation of the small molecules effects on EPS production via ECM formation. PA14 and PAO1 cultures were grown in 5 mL glass tubes holding 2 mL of BM2 20 μM Mg^{2+} containing 10 μM of antibiofilm compounds. Tubes were incubated at 37ºC, with shaking (150 rpm), for 24 hours. For EPS quantification, CR was added at a final concentration of 40 μg/ml to the 2 ml 24-hour cultures and bound-dye was indirectly calculated by determination of remaining unbound dye still in solution after 2 hours of incubation. [93]

The amount of unbound dye was determined by measuring the OD_{490} after centrifuging cells, and absorbance at 490 nm values were compared to sterile blank tubes (100% CR) containing BM2 medium + 1% DMSO. Bound CR was then normalized to the bacteria growth (OD_{600}) and determined through the following equation:

$$CR_{bound} = \frac{OD_{490blank} - OD_{490test}}{OD_{600test}}$$

It is noteworthy to acknowledge that a special set of blank tubes was prepared for compound I9, as this compound has pink color in solution and could affect OD_{490} values and interfere with CR measurements. Sterile I9 blank tubes were prepared with BM2 medium + 10 μM I9 in DMSO.

3.2.3 Biofilm cultivation and quantification

3.2.3.1 Microtiter plate biofilm assay

As a second step to assess the antibiofilm activity of the compounds identified in the HTS, we wanted to determine their potential in repressing biofilm formation in wild type (PA14 and PAO1) and hyperbiofilm forming (PAO1 *retS::lux*) strains of *P. aeruginosa.* We selected these three strains as they differ in their ability to form biofilms because of their varying levels of EPS production. Biofilms were cultivated in biofilm inducing conditions of BM2 20 μM Mg^{2+} for the wild type strains, but also in Mg^{2+}-rich conditions for the PAO1 *retS::lux,* which overproduces both EPS molecules and possess hyperbiofilm phenotype even under biofilm repressing conditions. [42] Biofilms were grown in the presence of 10 μM of the repressor compounds in 96-well polystyrene microplates for 18 hours at 37^{o}C with shaking (100 rpm). For each assay, untreated controls of biofilms formed under biofilm inducing and non-inducing conditions were added for comparison of treatment effects.

In addition to testing individual compounds, we also tested select mixtures of 2 or 3 molecules, at a total concentration of 10 μM, that showed greater effects in repressing *pelB::lux* expression, for the observation of possible additive effects in reducing biofilm formation in the same three non-mucoid strains.

We additionally wanted to determine our repressor compounds ability to reduce biofilm formation in a mucoid variant of PAO1. Biofilms of strain PDO300, a *ΔmucA22* variant of PAO1, [83] were cultivated in 96-well microplate with BM2 2mM Mg^{2+} in the presence of 10 μM of the repressor compounds.

Total biofilm formed on the wells of 96-well microplates was determined by crystal violet (CV) staining, as previously described. [17, 94] Before the staining protocol, wells had

their OD_{600} values determined for later normalization. All wells were emptied, CV solution was added at a final concentration of 0.1% (in distilled water), and plates were incubated for 10 min at room temperature for biomass staining. Excess CV was removed by rinsing wells with warm tap water, the plates were dried, and the CV bound to biofilms was ultimately eluted with 95% ethanol. Eluted CV was determined by measuring OD_{600} of wells and total biomass was normalized to cultures OD_{600} reads for accounting of differences in bacteria growth.

3.2.3.2 Flow chamber biofilm assay

We then aimed to investigate the antibiofilm activity against biofilms formed in flow chamber conditions. The BioFlux device is specifically designed to cultivate and image 24 biofilms under flow in custom 48-well plates. [95] *Gfp*-tagged PA14 and PAO1 biofilms were cultivated in 48-well microplates, equipped with input and output channels to allow media flow through. Channels were initially inoculated with the *gfp*-tagged strains and then growth media containing 10 μM of the selected repressor compounds was continuously fed to the system. Due to space limitations we had to select 12 conditions to be tested (in triplicate for both PAO1 and PA14), which included 9 single treatments and 3 compound mixtures that showed good antibiofilm activity in microplate biofilm assays. The biofilms were allowed to grow for 18 hours at 37^{o}C. Positive (BM2 20 μM Mg^{2+}) and negative (BM2 2mM Mg^{2+}) untreated controls of biofilm formation were included within each plate layout. The biofilms formed under flow system were imaged with a Nikon Eclipse Ti inverted epifluorescence microscope in green fluorescence and phase contrast. Images were analyzed using ImageJ Processing and Analysis in Java (software version 1.48).

Biofilm depth was directly measured in the phase contrast images using ImageJ, relative to the 70 μm channel diameter, in at least 6 different areas from each image. For the determination of total biofilm coverage, the total green fluorescence of adhered biofilms formed on the top and bottom of the chamber was compared to the whole channel area.

3.2.4 Anaerobic biofilm cultivation

To determine our repressors ability to reduce biofilm formation under anaerobic conditions, we also cultivated PA14, PAO1 and *retS::lux* biofilms, in 96-well microplate format with 10 μM of repressor molecules, inside an anaerobic chamber (GasPack System, BD) for 48 hours. Biofilms were cultivated in BM2 20 μM Mg^{2+} supplemented with 1% KNO_3. Biofilm inhibition was determined by CV staining as previously described. [17, 94]

3.2.5 Statistical analysis

In this chapter, statistical significance between populations was determined by paired two-tailed Student's t-test. Data considered significant at level of $p<0.05$.

3.3 Results

3.3.1 Pel/psl *repressors reduce ECM formation*

The different strains of *P. aeruginosa* used in this study were selected for their ability to differentially secrete EPS molecules as the main constituent of the ECM. The PA14 strain, due to a 3-gene deletion in the *psl* operon, in only able to produce and secrete Pel, [28] thus, having Pel and the major EPS molecule present in the biofilm matrix. On the other hand, PAO1 is able to produce and secrete both Pel and Psl EPS molecules, although, it depends mainly on Psl for

biofilm development. [16] Nevertheless, we also tested their antibiofilm activity against the *retS::lux* strains, which has an insertion mutation in the *retS* gene, which encodes for the RetS repressor of the Gac/Rsm regulatory pathway, leading to overproduction of both Pel and Psl EPS and hyperbiofilm formation. [42]

EPS production in wild type PA14 and PAO1 strains was estimated by the standard CR binding assay. [93] As predicted, we could see a reduction in the amount of bound CR dye for almost all conditions. In PA14, 7 treatments promoted a significant repression in EPS secretion, while in PAO1 9 showed a significant effect (Fig 3.1). This indicates that the identified molecules, that reduce *pel and psl* transcription, are able to significantly reduce EPS secretion.

3.3.2 Antibiofilm activity against microplate and flow biofilms

Given that the small molecules efficiently reduce EPS secretion, we next wanted to investigate the compounds ability to reduce biofilm formation. Initially, biofilms were grown in 96-well microplates in the absence and presence of each of the top *pel/psl*-repressor compounds and quantitated using the CV staining protocol. [17, 94] PA14 and PAO1 have biofilm formation promoted in limiting Mg^{2+} concentration (Fig 3.2.A), in agreement with previous reports that show increased Pel and Psl secretion in PhoPQ-activating conditions. [17] Additionally, the *retS::lux* mutant strain, which overproduces both EPS molecules, showed increased biofilm formation relative to PAO1 wild type, in non-inducing conditions (Fig 3.2.A).

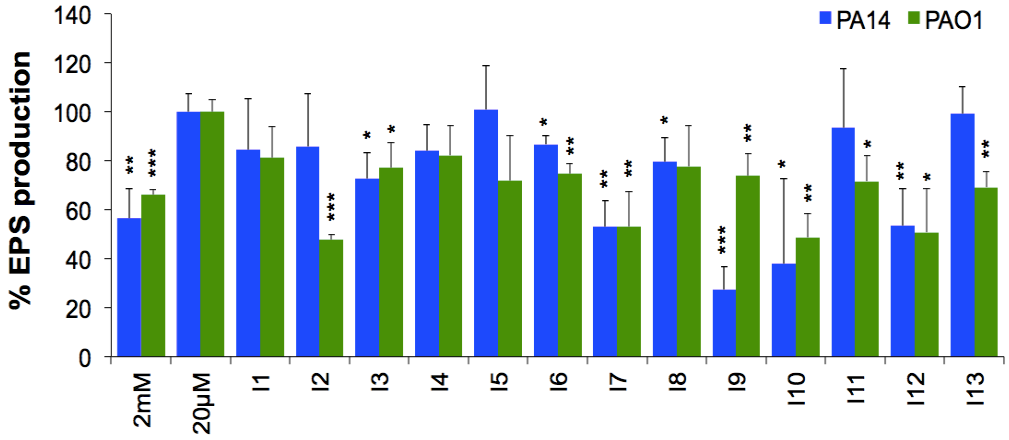

Figure 3.1. *Pel/psl*-repressor compounds reduce ECM formation.

Quantification of bound CR dye in PA14 (blue) and PAO1 (green) biofilms show reduced ECM formation. Cultures were cultivated with the 13 reordered repressor compounds. Bars of compound treated biofilms were compared to strains grown in biofilm inducing conditions (20 µM Mg^{2+}). Values shown are the mean of triplicate samples and the standard deviation, n=3. Statistical significance between populations was determined by paired two-tailed Student's t-test and significant repression in ECM formation is indicated: * ($p<0.05$), ** ($p<0.01$) and *** ($P<0.001$).

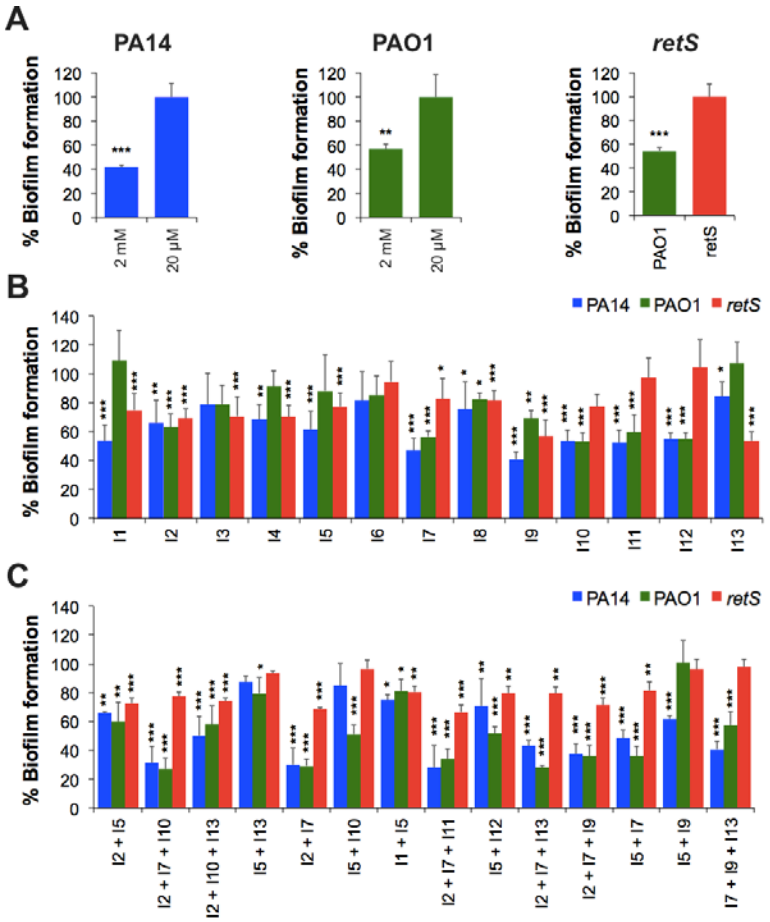

Figure 3.2: Crystal violet (CV) biofilms are reduced by *pel* repressors.

(A) Controls of biofilm formation showing a strong biofilm phenotype for PA14 and PAO1 in biofilm inducing conditions of limiting Mg^{2+}, and the hyperbiofilm phenotype of *retS::lux* compared to PAO1 wild type in high Mg^{2+}. **(B)** CV staining of biofilms formed in microplates after compound treatment of PA14 (blue), PAO1 (green) and *retS::lux* (red) strains. **(C)** Additive effects of compound mixtures in reducing biofilm formation. Treated biofilms were normalized to positive controls and % biofilm values shown are the mean of 6 replicates and the standard deviation, n=3. Statistical significance between populations was determined by paired two-tailed Student's t-test and significant repression in biofilm formation is indicated: * ($p<0.05$), ** ($p<0.01$) and *** ($P<0.001$).

When we tested the repressor compounds against these common laboratory strains of *P. aeruginosa*, consistent with our hypothesis, the *pel/psl* repressors caused significant reduction in microplate biofilm formation. The majority of *pel/psl* repressors (11/13) promoted a significant reduction in biofilm formation in PA14 (Fig 3.2.B), compared to untreated biofilms (100%). Furthermore, the majority were also effective (7/13) in reducing total biofilm biomass produced by PA01 strain (Fig 3.2.B). We also tested their antibiofilm activity against the hyperbiofilm-producing *retS::lux* transposon mutant. Interestingly, 10/13 compounds were also effective in reducing biofilm formation in the *retS::lux* strain (Fig 3.2.B).

To assess the possible additive effects of mixing these compounds, we tested the combination of 2 or 3 repressor molecules, at a total concentration of 10 μM. We initially tested 95 different combinations that included all 78 possible 2-compound mixtures and 17 random 3-compound mixtures, and selected some of the best combinations as additive repressors of *pelB::lux* expression (Fig S1, Appendix A). Many of these select mixtures containing 2 or 3 repressor compounds were additive and resulted in greater degrees of biofilm inhibition than individual compounds (Fig 3.2.C).

It is noteworthy to say that we were using the normalization step of dividing the CV values by the OD_{600} in PA14 and PAO1 microplates to account for differences in growth, especially within the controls of inducing and non-inducing conditions, as strains grow better in the media supplemented with Mg^{2+}. On the other hand, this step was not used for the *retS::lux* biofilms, as the hyperaggregative phenotype produces large aggregates in planktonic culture, and consequently very low OD_{600} values, which impacts any attempt to normalize for growth.

Likewise, to test their ability to reduce biofilm formation in continuous flow systems, we cultivated and quantitated *gfp*-tagged PA14 and PAO1 biofilms in the BioFlux biofilm device.

We selected 9 individual antibiofilm compounds and 3 mixtures for their effect on reducing the coverage and depth of biofilms grown in flow conditions. The biofilm coverage within the channels was determined by calculation of % area covered by the dense fluorescent biomass adhered to the channels walls, in comparison with the total area of the channels (Fig 3.3.A). Biofilm depths, on the other hand, were determined by measuring the biofilm's thickness along the chamber edge, using as a reference the channels diameter (70 μm) (Fig 3.3.A).

Untreated biofilms from wild type strains were actively covering around 30% of the area of limiting Mg^{2+}-control channels, and had ~5 μm of depth. The majority of individual compounds and the combination treatments significantly reduced biofilm formation against PAO1-*gfp* and PA14-*gfp*, reducing both the depth and total coverage of biofilms grown in the BioFlux channel walls (Fig 3.3.B). Treatments that significantly repressed biofilm formation were able to reduce coverage to 5 to 20% of the chamber area, some of them almost comparable to the amount of biofilm formed in non-inducing conditions. As in the CV biofilm assays (Fig 3.2.C), all compound mixtures tested had greater effects on reducing biofilms than individual compounds alone (Fig 3.3.B).

It is noteworthy to acknowledge that two compounds (I2 and I5) caused channel blockage in all replicate wells for PA14-*gfp*, therefore we were unable to determine their effects over flow biofilms formed in this strain.

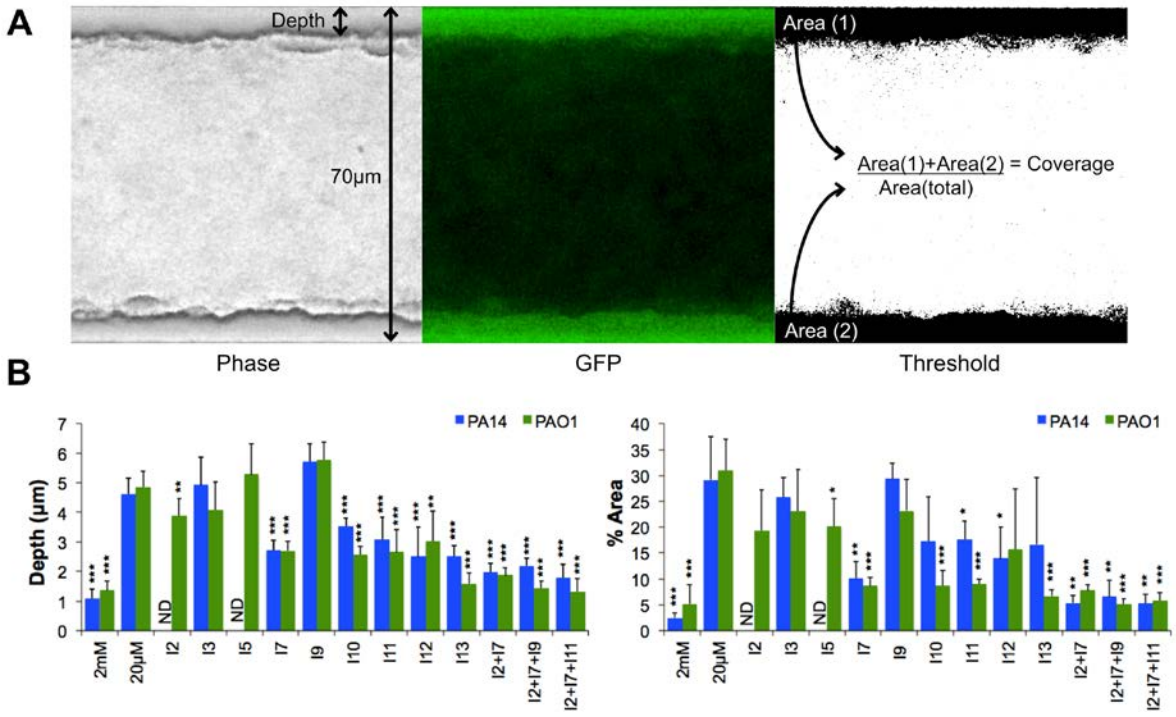

Figure 3.3: EPS repressors reduce biofilms formed under flow conditions.

(A) Schematic visualization of biofilms adhered to channels of the BioFlux flow chamber device. Images shown are phase contrast (left), GFP (middle) and GFP image that was threshold adjusted to isolate the biofilm adhered to the channel walls (right). **(B)** Compound treatments reduce both depth and coverage (% area) of biofilms formed in the BioFlux device. Bars of compound-treated PA14 and PAO1 biofilms were compared to strains grown in biofilm inducing conditions (20 µM Mg^{2+}). ND, not determined. All values shown are the mean of triplicate samples and the standard deviation, n=2. Statistical significance between populations was determined by paired two-tailed Student's t-test and significant repression in biofilm depth/coverage is indicated: * ($p<0.05$), ** ($p<0.01$) and *** ($P<0.001$).

3.3.3 Pel repressors have modest antibiofilm effects on mucoid biofilms

It is known that the stressful CF environment selects for alginate-overproducing *P. aeruginosa* strains, which show mucoid phenotypes. [1, 96, 97] Given the abundance of mucoid isolates in the CF lung, and the necessity of both intact *pel* and *psl* gene operons for biofilm formation and fitness of mucoid strains [98] we wanted to determine if our *pel/psl*-repressor antibiofilm compounds could also reduce biofilm formation in a mucoid variant on *P. aeruginosa*. Biofilms of strain PDO300, a *ΔmucA22* variant of PAO1, [83] were cultivated in *pel/psl* non-inducing conditions (BM2 2mM Mg^{2+}) to minimize the contribution of oversecreted Psl and Pel in this experiment. Biofilms were grown in 96-well microplates and total biomass formed was determined via CV staining. [17, 94] Although antibiofilm effects were not as obvious as for non-mucoid strains, six antibiofilm compounds present at 10 μM promoted a modest but significant reduction in biofilm formation for the mucoid strain (Fig 3.4.A). Interestingly, two of the antibiofilm compounds had a biofilm promoting effect on the mucoid variant of PAO1 (Fig 3.4.A).

3.3.4 Pel repressors reduce anaerobic biofilm formation

Other reports have shown that the CF environment consists of both aerobic and anaerobic microenvironments, [34] therefore, we also aimed to determine our repressors' ability to reduce biofilm formation under anaerobic conditions. Thus, PA14, PAO1 and *retS::lux* biofilms were cultivated in 96-well microplates inside an anaerobic GasPack system (BD), which is able to convert the atmosphere to an anaerobic microenvironment. The antibiofilm compound treatments (10/13) were able to promote a significant reduction in biofilm formation in the PA14 strain under anaerobic conditions, while 6/13 compounds were effective against the PAO1 strain (Fig

3.4.B). Importantly, 10/13 compounds also reduced biofilm formation in the hyperbiofilm forming *retS::lux* strain under anaerobic conditions (Fig 3.4.B). Although most of the compounds showed a similar trend in biofilm repression for both aerobic and anaerobic conditions, compound I6 showed antibiofilm properties only under anaerobic growth. Importantly, we were unable to determine biofilm repression by compound I11, as it was inhibiting bacterial growth under anaerobic conditions for the three strains tested.

3.4 Discussion

The different strains of *P. aeruginosa* used in this study, PA14 ($Pel^{+}Psl^{-}$), PAO1 ($Pel^{+}Psl^{+}$) and the *retS::lux* ($Pel^{++}Psl^{++}$), were selected for their ability to differentially secrete EPS molecules as the main constituent of their biofilm ECM. Additionally, as the stressful conditions in the mucous-clogged CF airways select for mutations that lead to the mucoid phenotype, [1, 96, 97] we also tested the PDO300 strain, which has a mutation in the *mucA22* gene, and has increased alginate secretion. [83]

To investigate the effect of our *pel/psl*-repressor molecules on EPS secretion and biofilm formation in these different strains, we made use of the CR and CV dyes, respectively. CV is a basic dye broadly used for the staining and quantification of bacterial biofilms, which allows the quantification of total bacterial biomass. [94] As the CV dye generally binds to negatively charged molecules, including molecules on the cell surface and in the ECM, [99] we also used the CR staining protocol which has been show to more specifically bind to extracellular components of biofilm matrix, [30] as a better indicator of effects on EPS secretion.

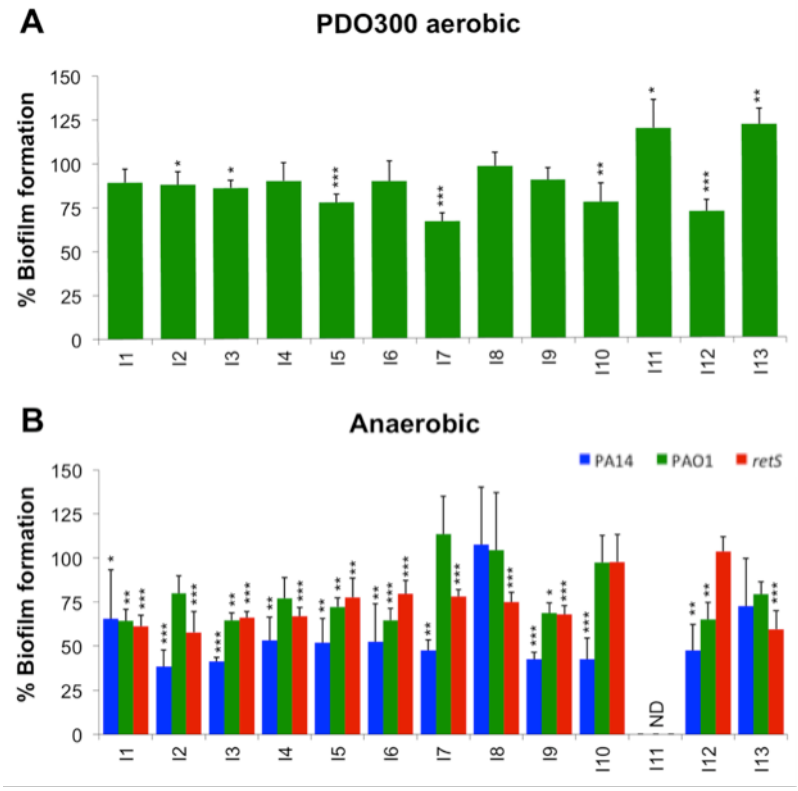

Figure 3.4: Small-molecule EPS repressors reduce mucoid and anaerobic biofilms.

(A) CV staining of mucoid PDO300 (*ΔmucA22*) biofilms in aerobic conditions. Bars of compound treated biofilms were compared to mucoid biofilm grown in Pel/Psl-repressing condition (100%). **(B)** CV staining of biofilms of non-mucoid strains under anaerobic conditions. Bars of treated PA14 (blue), PAO1 (green) and *retS::lux* (red) biofilms were compared to untreated controls (100%). ND, not determined. All values shown are the mean of 6 replicates and the standard deviation, n=3. Statistical significance between populations was determined by paired two-tailed Student's t-test and significant difference in biofilm formation is indicated: * ($p<0.05$), ** ($p<0.01$) and *** ($P<0.001$).

We have shown that our repressors reduce transcription of the *pel* and *psl* genes, which leads to lower secretion of EPS molecules (Fig 3.1). Herein we decided to investigate their effect on biofilm formation under different settings. Initially we determined their antibiofilm properties in the standard microplate format, using CV staining, as previously described, [17, 94] and showed the *pel/psl*-repressor compounds were significantly repressing microtiter biofilm formation for PA14, PAO1 and *retS::lux* strains in both aerobic (Fig 3.2) and anaerobic conditions (Fig 3.4.B), indicating that inhibition of EPS secretion is effectively repressing biofilm formation in wild type strains under biofilm promoting conditions and hyperbiofilm forming strain. Both aerobic and anaerobic environmental conditions were also tested, considering previous reports that show these are both found in the CF lung [34] and *P. aeruginosa* shows greater attachment and biofilm formation under anaerobic conditions, [100] despite slower growth rates. [101]

It is noteworthy to acknowledge that the antibiofilm effects of our most significant candidates are comparable to biofilms grown in non-inducing conditions (Fig 2.3.A), where there is little EPS secretion. [17] Similarly, *pel*-repressor compounds also reduce biofilm formation to levels of a *pel* mutant, and given the role of multiple EPS molecules and adhesins (e.g. flagellum, pili, etc) in bacteria aggregation, [1, 94] more targets other than EPS would potentially need to be affected for a greater phenotype.

As mucoid strains promote long-term survival in the CF lung, by promoting aggregate formation, antibiotic resistance and increased tolerance towards host immune responses, such as oxidative stress, [1, 96, 97] we also investigated our compounds antibiofilm properties in mucoid variant of PAO1. [83] A previous report has shown the necessity of both intact *pel* and *psl* gene operons for biofilm formation and fitness of mucoid strains, [98] hence, treatments

(6/13) promoted a modest but significant effect in inhibiting biofilm formation of the mucoid strain, but unexpectedly, two molecules had a biofilm promoting effect (Fig 3.4.A). There is one common gene (*algC*) for the synthesis of a sugar precursor of all EPS, and competition for precursors of the various EPS polymers. [102] Therefore, a possible explanation for this observed effect could be due to an EPS shift and increased alginate production when both Pel and Psl are repressed.

Lastly, since flow systems tend to better mimic natural biofilms due to hydrodynamic influences, [95, 103] we also determined our compounds antibiofilm properties in the BioFlux device, which consists of microfluidic channels that allow the formation and imaging of multiple biofilms within a controlled flow environment. [95] As for the microtiter plate assays (Fig 3.2), treatment with our *psl/psl* repressors promoted a significant reduction in biofilm formation in the BioFlux device (Fig 3.3). Furthermore, compound mixtures demonstrated additive effects promoting even greater inhibition of biofilms cultivated under flow condition (Fig 3.3).

There are still other experiments that would be interesting to confirm the EPS repression effects. We have demonstrated the EPS-repressing properties of our compounds in CR staining assays, although it would be interesting to replicate these results using Pel and Psl specific fluorescent-labeled lectins [73] and/or antibodies. [16, 20, 104] Additionally, further attempts to determine the antibiofilm compound effects on colony morphology and pellicle formation are of interest, as EPS secretion is essential for pellicle formation in the air-liquid interface and wrinkled colony phenotype in solid agar. [20, 30]

3.5 Conclusions from Chapter 3

i. We demonstrated that EPS-gene repressors significantly reduced ECM secretion in both PA14 and PAO1 strains of *P. aeruginosa.*

ii. EPS inhibition led to reduced biofilm formation in different strains of *P. aeruginosa* under different settings, including aerobic, anaerobic and flow conditions.

iii. Antibiofilm effects on the mucoid PDO300 (*ΔmucA22*) strain were modest compared to the non-mucoid strains

Chapter Four: *Pel/psl* repressors show antivirulence properties *in vivo* and also promote biofilm killing in combination with antibiotics

4.1 Introduction

Although well characterized for their importance in biofilm formation, the role of Pel and Psl EPS in virulence is not very well understood. It is known that *P. aeruginosa* is able to infect *Caenorhabditis elegans* and colonize its intestinal lumen, causing severe morphological alterations. [105] Moreover, it has been observed that *P. aeruginosa* forms clumps in the nematode gut, surrounded by an uncharacterized ECM. [105] Suspecting that these matrix-coated clumps are indeed biofilms being formed in the nematode gastrointestinal (GI) tract, and considering the essential role of both Pel and Psl in biofilm formation, in this chapter we aimed to investigate the ability of reduced *pel* and *psl* secretion to decrease *P. aeruginosa* virulence in the feeding preference and slow killing nematode infection models. [87]

Additionally, since the presence of Pel and Psl EPS molecules in the ECM promotes the biofilm structure and increases resistance to several different classes of antibiotics, [20, 28] we additionally aimed to investigate the role of our EPS-repressor antibiofilm compounds, to act together with antibiotics and promote biofilm killing.

4.2 Specific methods

4.2.1 Bacterial strains, nematode and growth conditions

The bacterial strains used in this chapter are listed in Table 2.1 (please refer to Chapter 2). *C. elegans* Bristol strain N2 (provided by Dr. Kunyan Zhang) were cultivated on nematode growth medium (NGM) plates containing a lawn of *E. coli* strain OP50 as a food source. The assigned number of L4 stage hermaphrodite nematodes was transferred to slow killing (SK)

plates for each assay. NGM medium was prepared with 0.25% Bacto-Peptone, 0.3% NaCl, 2% Bacto-Agar, 5 μg/ml cholesterol, 1 mM $MgSO_4$, 25 mM KH_2PO_4 and 1 mM $CaCl_2$ in distilled water. SK media was supplemented with 0.10% Bacto-Peptone for a total of 0.35%.

4.2.2 Investigation of Pel and Psl roles in PAO1 virulence

To investigate the role of EPS molecules for PAO1 virulence *in vivo* we used both feeding preference and slow killing nematode assays, testing strains unable to produce each or both of the EPS molecules, and additionally an Pel/Psl overproducing *retS::lux* strain.

4.2.2.1 Feeding preference assay

The feeding preference assay was performed as previously described. [87] Briefly, 20 L4 stage hermaphrodite nematodes were transferred from an NGM-OP50 plate to two different spots in opposite sides of a 10 cm-diameter SK assay plate containing a pre-grown grid of 48 colonies. The 6x8 grid contained 45 wild type colonies and 3 internal spots of mutant strains to be tested. The plates were incubated at 25^{o}C and observed twice a day until the disappearance of the initial colonies. In this assay we tested the ability of the *pelB::lux, Δpsl,* or the double mutant *pel/Δpsl* to be preferentially eaten over PAO1 wild type, while the *E. coli* OP50 was used as a positive control for a preferred food source for the nematode. [87]

4.2.2.2 Slow killing assay

The slow killing assay was performed as previously described. [87, 106] Briefly, 30 L4 stage nematodes were transferred from an NGM-OP50 plate to a 5 cm-diameter SK plate containing an individual pre-grown lawn of bacteria to be tested. 25 μg/ml of 5-fluoro-2'-

deoxyuridine (FUdR), a DNA synthesis inhibitor, was added to SK plates on the slow killing assay for the prevention of offspring development. Plates were incubated at 25ºC and nematode survival was determined throughout 10 days by direct observation and counting under a dissecting microscope. In total 90 nematodes were counted for as dead, alive or missing for each assay.

We tested the three EPS deficient strains, *pelB::lux*, *Δpsl* and *pel/Δpsl,* in comparison with the PAO1 wild type and the hyperbiofilm producing *retS::lux* mutant. *E. coli* strain OP50 was used as a positive control of reduced virulence for the nematodes, which shows limited killing of *C. elegans.* [87]

4.2.3 Determination of pel/psl*-repressors antivirulence properties*

To determine the properties of our antibiofilm compounds to reduce *P. aeruginosa* PAO1 virulence *in vivo*, we performed the slow killing assays, as previously described, [87, 106] with small modifications. Antibiofilm compounds were added to SK agar plates at a final concentration of 10 μM, to ensure bacteria treatment throughout the assay. Then, 30 L4 stage hermaphrodite nematodes were transferred from an NGM-OP50 plate to an SK-antibiofilm compound plate containing a pre-grown lawn of PAO1 wild type. SK plates containing 1% DMSO were used as a positive control of normal PAO1 virulence, while *E. coli* strain OP50 was still used as a control of low virulence.

4.2.4 Biofilm killing studies in PA14 and PAO1

To assess our compounds' ability to increase biofilm susceptibility to antimicrobials, we performed susceptibility testing in antibiofilm-treated biofilms from PA14 and PAO1 strains.

Biofilm susceptibility testing was performed as previously described, [107] with minor modifications. Briefly, biofilms were grown for 24 hours on polystyrene pegs (NUNC-TSP) submerged in BM2 20 μM Mg^{2+} containing zero, 5, 10 and 20 μM of select antibiofilm compounds. The cultivated biofilms were rinsed twice in 0.9% saline (NaCl), for removal of non-adherent cells, and transferred to a microplate containing sub-eradication concentrations of antimicrobials in 10% BM2 diluted in 0.9% saline. Biofilms were challenged for 24 hours and after were rinsed in 0.9% saline, for removal of vestiges of the media containing the antibiotics, and submerged in recovery rich medium of Lysogeny Broth (LB) and DNase I (25 μg/ml, Sigma). LB broth was supplemented with 10 mM $CaCl_2$ and 10 mM $MgCl_2$ for better DNase stability/function. [108] Peg-adhered cells were treated with DNase I for 30 minutes and then sonicated for 10 minutes to detach. Cell viability was determined immediately after sonication by serial dilution and direct counting as previously described. [107, 109] Serial dilutions were followed at a 10-fold ratio, in 0.9% saline, and bacterial spots were placed over LB agar plates. Plates were incubated overnight at 25ºC and, if needed, transferred to a 37ºC incubator until colonies reached an ideal size for counting. Increased antimicrobial effects were determined via calculation of viable cell counts (VCC) within the treated biofilms.

4.2.5 Statistical analysis

In this chapter, we used Log-rank test (Graph Pad Prism) for determination of significant differences in *C. elegans* survival. Also, paired two-tailed Student's t-test was used to determine significance between VCC in antibiofilm conditions compared to untreated challenged controls. Data considered significant at level of $p<0.05$.

4.3 Results

4.3.1 Pel and Psl are required for PAO1 full virulence in C. elegans *infection models*

To determine the possible role of Pel and Psl EPS molecules in PAO1 virulence, we initially assessed the ability of *pelB::lux, Δpsl* and *pel/Δpsl* to be preferentially eaten over a choice of PAO1 wild type in the feeding preference infection model. Feeding preference was determined via disappearance of the three mutant spots within a grid of 48 colonies. [87] While single knockouts in either the *pel* or *psl* genes did not promote a significant change in the nematode feeding behaviour, the double *pel/Δpsl* mutant was preferentially eaten by *C. elegans*, when given the choice of between *pel/Δpsl* and PAO1 (Fig 4.1.A).

As a control experiment, the usual laboratory food source *E. coli* OP50 also served as a preferential food source to PAO1 (Fig 4.1.A). It is noteworthy to acknowledge that none of the mutant strains tested in the feeding preference assay showed growth defects in SK media that might also explain faster colony disappearance. In this experiment, the nematodes are active in sampling all colonies on the plate and determining those food sources that are the least pathogenic, and therefore the most edible. [87] This result suggests a virulence role for Pel and Psl *in vivo*.

To confirm a virulence role for EPS molecules in the *C. elegans* infection model, we next tested these EPS deficient strains for their direct toxicity in the slow killing infection model. [87, 106] In the slow killing assays, in addition to the single and double *pel/Δpsl* mutant strains, we also tested *retS::lux*, as this mutant is known to hyperproduce both Pel and Psl and have a hyperbiofilm phenotype. [42]

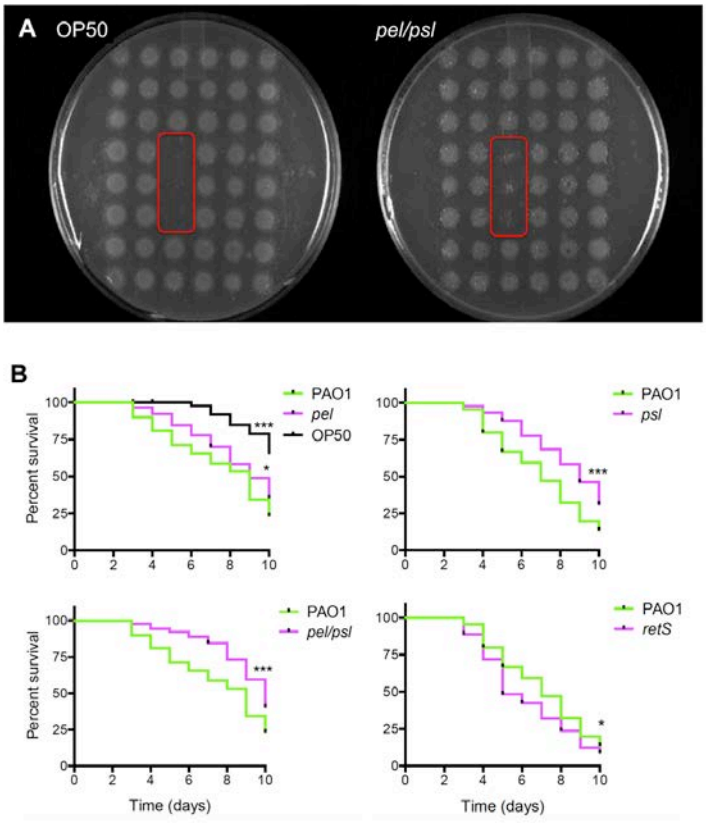

Figure 4.1. Pel and Psl EPS dictate nematode feeding preference and are required for full PAO1 virulence in the *C. elegans* infection model.

(A) The feeding preference assay indicates that *pel/Δpsl* double mutant is a preferred food source over PAO1 wild type. Control spots of *E. coli* OP50 were eaten to completion before PAO1. Triplicate spots of test strains are indicated in a red box, n=3. **(B)** The slow killing infection model show increased nematode survival when fed *pelB::lux*, *Δpsl* and *pel/Δpsl* mutants, while *retS::lux* promoted faster killing relative to nematodes fed PAO1 wild type. Kaplan-Meyer curves with % survival represent three independent experiments (n=30) where the total number of worms equals 90. Statistical significance was determined with Log-rank test (Graph Pad Prism) and significant difference in nematode survival is indicated: * ($p<0.05$) and *** ($p<0.001$).

Both single *pelB::lux* and *Δpsl* mutants, as well as the double *pel/Δpsl* were less virulent and promoted an extended nematode survival throughout 10 days (Fig 4.1.B), in comparison to nematodes fed PAO1 wild type. The killing kinetics of nematodes fed these mutants leaned towards that of nematodes fed a non-pathogenic *E. coli* OP50 food source (Fig 4.1.B). Interestingly, the *retS::lux* mutant revealed increased virulence, promoting faster nematode killing in the *C. elegans* slow killing assay (Fig 4.1.B). Although this effect in the *retS::lux* mutant can be a result of other pleiotropic effects of mutation in this regulatory protein, [42] taken together, these observations indicate that both the Pel and Psl are required for full virulence fitness of *P. aeruginosa* in causing infection and killing *C. elegans.*

4.3.2 *Biofilm inhibitors reduce PAO1 virulence* in vivo

After demonstrating a role of Pel and Psl for *P. aeruginosa* virulence *in vivo*, we predicted that our antibiofilm molecules, which block EPS synthesis, would reduce PAO1 virulence in the slow killing infectious model. Although no significant differences in nematode killing were observed for the majority of antibiofilm compounds tested (Fig S2, Appendix A), treatments I7, I9, I10 and I11 caused a significant reduction in PAO1 virulence, represented by an increased survival of nematodes fed compound-treated bacteria (Fig 4.2). As a control experiment, in absence of infection where nematodes are fed *E. coli* OP50 in slow killing experiments, along with 10 μM of compounds I7, I9, I10 and I11, there were no positive or negative effects on nematode survival (Fig S3, Appendix A). Therefore, the antibiofilm effects appeared to be specific to *P. aeruginosa* and their EPS-repressing characteristics. This increase in nematode survival was comparable to the effects of inactivating the genes in the *pel* and *psl*

operons (Fig 4.1.B), indicating that these small molecules demonstrate antivirulence activity for *P. aeruginosa.*

4.3.3 Small molecule **pel/psl-***repressors promote biofilm killing in PA14 and PAO1*

As both Pel and Psl EPS molecules make biofilms more tolerant to antimicrobial interventions, [20, 28] we hypothesized that our biofilm inhibitor compounds may work in combination with antibiotics to promote biofilm cell killing. *P. aeruginosa*-treated biofilms were challenged against a panel of 5 different antimicrobials, which target *P. aeruginosa* growth by different mechanisms of action. Polymyxins (colistin, Col and polymyxin B, PB) disrupt membrane integrity, aminoglycosides (tobramycin, Tm and gentamicin, Gm) inhibit protein synthesis and fluoroquinolones (ciprofloxacin, Ci) block DNA replication. It is noteworthy to acknowledge that Col and Tm are two clinically important antimicrobial therapies used to treat *P. aeruginosa* infections in CF patients. [110, 111]

PAO1 biofilms treated with our panel of 4 antibiofilm/antivirulence molecules received all 5 treatments, while PA14, which is only Pel efficient, were only challenged with aminoglycoside (Tm and Gm) antibiotics. We limited the antimicrobial testing of PA14 to antibiotics previously shown to be affected by the production of the Pel EPS. [20] As a first approach, we initially tried to determine the MBEC values of these antibiotics, when biofilms were formed in the presence of antibiofilm compounds. Since the MBEC values did not decrease by more than to 2 to 4-fold, and the intrinsic variance of the assay made it hard to take solid conclusions on biofilms susceptibility to the tested antimicrobials, we used an alternative approach to measure antibiofilm effects on antibiotic killing.

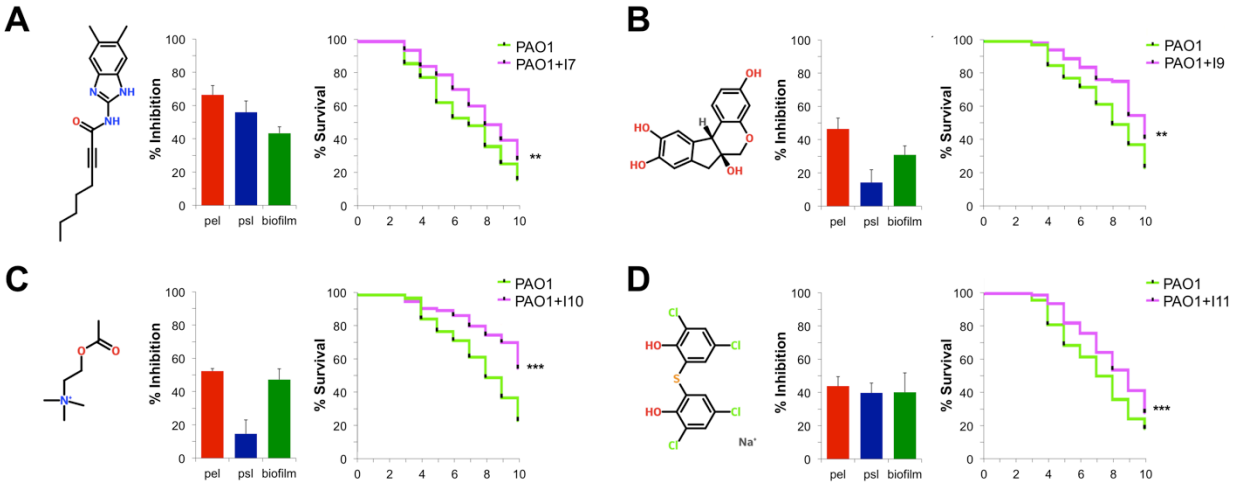

Figure 4.2. Antibiofilm compounds have antivirulence activity in the *C. elegans* slow killing infection model.

Molecular structures for **(A)** N-(5,6-dimethyl-1H-benzimidazol-2-yl)oct-2-ynamide (I7), **(B)** Brazilin (I9), **(C)** Acetylcholine (I10) and **(D)** Bithionate Sodium (I11) are shown beside their inhibitory effects over *pelB::lux* and *pslA-lux* expression and biofilm formation by PAO1 in microplates. Nematodes were fed antibiofilm compound-treated PAO1 and monitored for increased survival. Kaplan-Meyer curves with % survival represent three independent experiments (n=30) where the total number of worms equals 90. Statistical significance was determined with Log-rank test (Graph Pad Prism) and significant difference in nematode survival is indicated: ** ($p<0.01$) and *** ($p<0.001$).

In the second approach, biofilms were treated with antibiotics at sub-eradication concentrations, so that colony forming unit (CFU) counts could be determined from individual peg-adhered biofilms. Combination testing of antibiotics was limited to the 4 lead antibiofilm compounds that also had antivirulence activity (Fig 4.2). The inhibitor-treated biofilms showed minimum reduction in CFU counts compared to untreated (1% DMSO) controls (Fig 4.3.A). But when used in combination with antibiotics, the antibiofilm compounds I7, I10 and I11 increased the PAO1 biofilm susceptibility to all tested antimicrobials by reducing the viable cell counts between 1 and 5 logs (Fig 4.3.B). However, compound I9 only increased biofilm susceptibility to Ci and PB (Fig 4.3.B). We tested a concentration range of antibiofilm compounds, and compound I11 caused a consistent, dose-dependent effect on increasing biofilm killing as the concentration of antibiofilm compound increased from 5 to 20 μM (Fig 4.3.B).

As previously discussed, PA14 and PAO1 strains differ in their ability to secrete EPS molecules. [28] We additionally investigated the sensitivity profile to aminoglycosides in PA14, which is unable to produce Psl. In PA14, all compounds increased biofilms susceptibility to Gm, while only I10 and I11 caused a significant effect for Tm. Interestingly, all treatments mainly caused a dose-dependent effect, showing lowest counts of recovered cells at 20 μM (Fig 4.4). It is noteworthy to acknowledge that we noticed the lack of a second protective EPS promoted biofilm killing in PA14, reducing the number of recovered cells when biofilms were challenged at the same concentrations tested for PAO1. Hence, we reduced the concentrations of antimicrobials tested to observe larger differences in biofilm killing. Thus, in addition to their antibiofilm and antivirulence properties, these small molecules also promote antimicrobial killing of bacteria cells grown within biofilms.

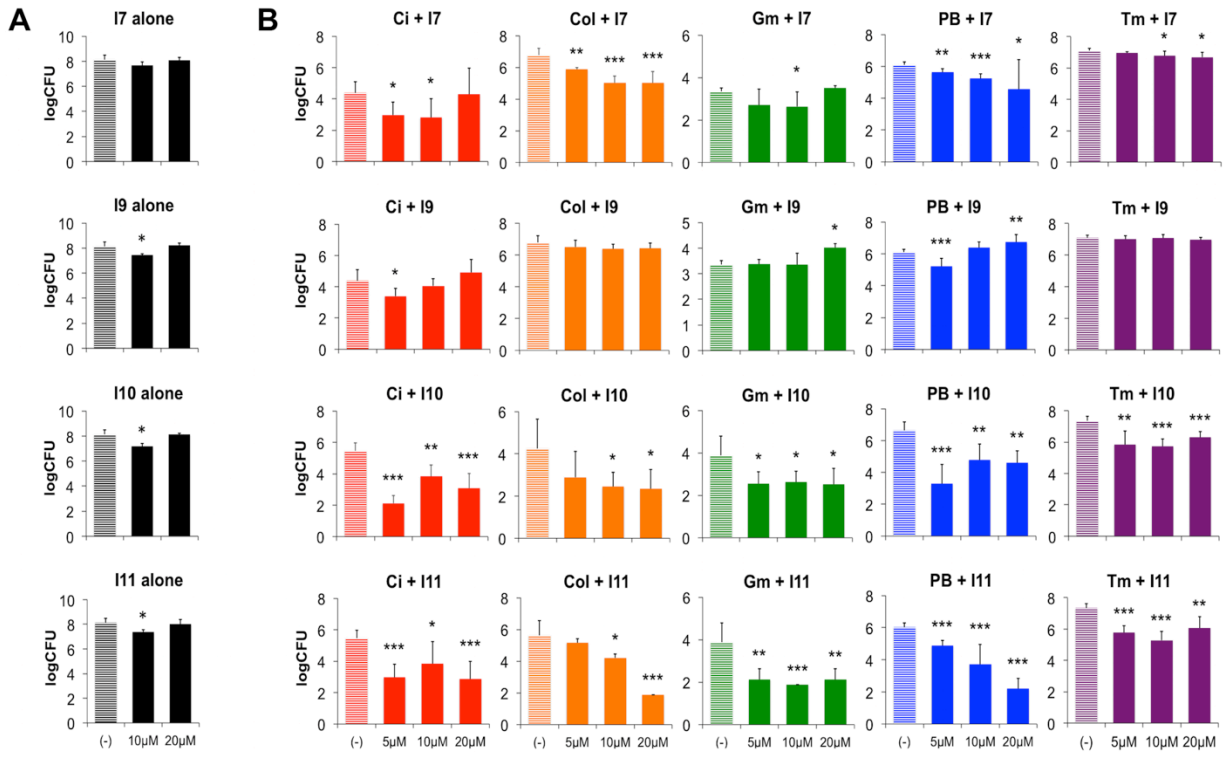

Figure 4.3. Antibiofilm compounds increase killing in PAO1 biofilms when used in combination with antibiotics.

(A) The effect on bacterial counts of treating microplate biofilm with antibiofilm compounds I7, I9, I10 and I11. **(B)** Biofilms grown in the presence of the selected antibiofilm/antivirulence compounds were challenged with sub-eradication concentrations of ciprofloxacin (Ci, 2.5 μg/ml), colistin (Col, 25 μg/ml), gentamicin (Gm, 6.5 μg/ml), polymyxin B (PB, 25 μg/ml) or tobramycin (Tm, 1 μg/ml) antibiotics. VCC were determined by CFU/peg over detached cells on treated biofilms. Values shown are the mean of triplicate samples and the standard deviation, n=2. Statistical significance between populations was determined by paired two-tailed Student's t-test and significant differences in VCC from untreated (-) controls are indicated: * ($p<0.05$), ** ($p<0.01$) and *** ($p<0.001$).

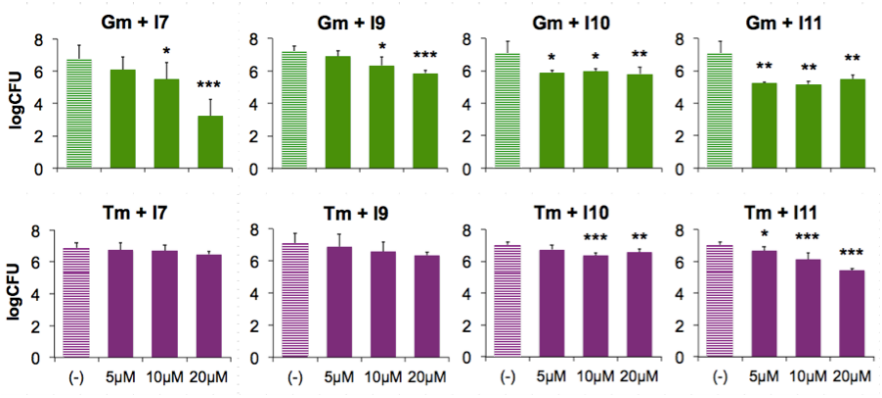

Figure 4.4. Antibiofilm compounds increase killing in PA14 biofilms when used in combination with aminoglycoside antibiotics.

Biofilms grown in the presence of the selected antibiofilm/antivirulence compounds were challenged with sub-eradication concentrations of Gm (3.2 μg/ml) or Tm (0.5 μg/ml) antibiotics. VCC were determined by CFU/peg over detached cells on treated biofilms. Values shown are the mean of triplicate samples and the standard deviation, n=2. Statistical significance between populations was determined by paired two-tailed Student's t-test and significant differences in VCC from untreated (-) controls are indicated: * ($p<0.05$), ** ($p<0.01$) and *** ($p<0.001$).

4.4 Discussion

Biofilm formation is both a protective and a virulence strategy adopted by bacteria to survive within hostile environments and promote long-lasting infections. [20] Therefore we investigated the ability of the identified antibiofilm compounds in reducing *P. aeruginosa* virulence *in vivo* and to promote biofilm killing when associated with antibiotics.

The *C. elegans* infection model has been widely used for the study of host-microbe interactions, especially due to the presence of components in the innate immune system that are conserved with mammalian organisms. [112] Irazoqui *et al.* [105] performed an extensive study looking at the pathogenicity of *P. aeruginosa* in *C. elegans* infections, highlighting the use of common virulence mechanisms involved in human disease to infect and kill nematodes. The observation that *P. aeruginosa* can be found colonizing the nematode's gut in aggregates surrounded by an electron-dense extracellular matrix as early as 8 hours post-infection, [105] indicates the possible presence of biofilms being formed in its GI lumen.

Moreover, it has been shown that *P. aeruginosa* virulence to *C. elegans* depends on active bacterial proliferation within the gut. [113] Similarly, mutations in the *gacA* regulator, which reduce EPS secretion, severally reduce PA14 accumulation within nematodes and attenuate its virulence. [113] In accordance to these findings, previous results also show that mutations in EPS-encoding genes are able to reduce PA14 fitness to colonize the gastrointestinal tract of mice. [114] Taken together, all these indications suggest that EPS molecules are directly involved in *P. aeruginosa* virulence, and led us to investigate the roles of both Pel and Psl molecules in pathogenicity using the *C. elegans* infection model. While numerous high throughput nematode virulence screens have been performed in PA14, a rapid killing strain of *P. aeruginosa*, this is the first report to identify EPS as virulence factors in *C. elegans.*

Initially, we demonstrated that the EPS-deficient *pel/Δpsl* mutant was a preferred food source in the nematode feeding preference assay, when given as a food source option to PAO1 wild type (Fig 4.1.A). As this preferential feeding behaviour has previously identified mutants in genes that encode for virulence factors, [87] this was a strong indication that both Pel and Psl are involved in PAO1 virulence. In the slow killing assay, we showed that mutations in either or both EPS operons reduced bacterial virulence, promoting nematode survival (Fig 4.1.B). Interestingly, the hyperbiofilm producing *retS::lux* demonstrated faster nematode killing and increased virulence *in vivo* (Fig 4.1.B), which could be associated with the increased secretion of EPS molecules. As this mutation in the RetS regulatory protein alters several other virulence factors besides EPS secretion, [42] further testing needs to be done with an EPS-deficient *retS* mutant strain to confirm our interpretation.

Importantly, we identified 4 compounds that reduce the *P. aeruginosa* virulence in the nematode infection model (Fig 4.2). Although these compounds appear to be specific for *P. aeruginosa*, as they did not promote any positive effect in nematode survival when fed their *E. coli* OP50 food source (absence of infection) (Fig S3, Appendix A), further work is needed to confirm this antivirulence activity in other strains and in other infection models, which show biofilm formation as a hallmark for pathogenicity.

Colvin *et al.* [20] suggested that targeting *pel* and *psl* expression could facilitate antimicrobial therapies. In our antimicrobial combination experiments, we determined the ability of our *pel/psl*-repressor compounds to reduce biofilm tolerance to current antibiotic treatment. Similar to previous reports that show that enzymatic degradation of Pel and Psl molecules promote *P. aeruginosa* sensitivity to sub-inhibitory concentration of colistin, [73] the EPS-inhibitor antivirulence compounds identified in the slow killing nematode infection model also

decrease biofilm resistance to antimicrobials. Sub-inhibitory concentrations of aminoglycosides (Gm and Tm), polymixins (PB and Col) and fluoroquinolone (Ci) antimicrobials were more effective in combination with our antibiofilm compounds, reducing the number of CFUs recovered from peg adhered biofilms between 1 and 5 logs (Fig 4.3 and 4.4). We believe this phenotype can be even greater using flow conditions for biofilm cultivation, as non-adhered cells are washed away. Future experiments will be performed to determine susceptibility of biofilms to these compound-antibiotic combinations when cultivated under flow conditions, using live/dead (Syto-9/propidium iodide) staining and biofilm imaging, such as described by de la Fuente-Núñes *et al.* [57] to determine the antibiofilm effects of AMP against *P. aeruginosa* and *B. cenocepacia* biofilms.

The ability of these *pel/psl*-repressor compounds to increased antimicrobial susceptibility can possibly be associated by either or both effects of EPS inhibition over the biofilm lifestyle. The biofilm ECM can act as a physical barrier and prevent to some extend antimicrobial diffusion through the biofilm structure. [115] Consequently, by inhibiting EPS secretion and reducing biofilm formation, we may be reducing this physical barrier and making cells more accessible to the antibiotics. Additionally, both Pel and Psl molecules have been shown to promote resistance to multiple classes of antibiotics, [20, 21, 28] which may be due to specific ionic interactions, and therefore our antibiofilm compounds may be increasing antibiotic diffusion by reducing this charge-related obstacle.

Novel antimicrobial approaches have identified compounds with antivirulence properties against a wide variety of pathogens. These antivirulence strategies have been shown to reduce the deleterious effects of toxins, impair bacterial secretory systems, repress specific virulence genes, especially QS signalling, among others. [116-119] All antivirulence approaches aim to

reduce bacteria colonization and/or the consequent deleterious effects of infection. They may also have the benefit of reducing the selective pressure for resistance, as is commonly observed for antimicrobial growth inhibitors. [116] The EPS-repressor compounds identified in this project are attractive candidates for further testing as new antivirulence therapies, as they reduce the secretion of polymers essential for biofilm formation and persistence of infection, which ultimately reduce *P. aeruginosa* virulence *in vivo* and increase biofilm sensitivity to conventional antimicrobials.

Our 4 lead compounds have both antibiofilm and antivirulence activities, which are excellent properties for new antimicrobials. From a structural comparison, these 4 compounds share some structural similarities with other bioactive antimicrobial compounds. Compound I7 has a benzimidazol backbone and this structural class has been previously shown to have antimicrobial activity against fungi, parasites and bacteria. [120, 121] Compound I9 (brazilin) is a natural product that possesses antimicrobial activity against *Propionibacterium acnes.* [122] Compound I10 (acetylcholine) was recently reported to have antibiofilm and antivirulence activity against *Candida albicans,* [92] and several choline analogs were reported to reduce biofilm activity in *P. aeruginosa* without inhibiting growth. [91] Few bioactivities have been reported for compound I11 (bithionate sodium), although bithionol has very efficient antihelmintic properties against *Anoplocephala perfoliata.* [123]

4.5 Conclusions from Chapter 4

i. EPS-deficient strains of *P. aeruginosa* show reduced virulence in *C. elegans* infection models, suggesting a possible role for EPS secretion in PAO1 virulence.

ii. Four of the identified Pel/Psl-repressor compounds are able to reduce PAO1 virulence and promote nematode survival in the slow killing *C. elegans* assay.

iii. Pel and Psl inhibition promote biofilm killing, reducing VCC upon treatment with sub-inhibitory concentration of antibiotics.

iv. These molecules are effective antivirulence strategies and therefore are attractive molecules for further study as a new therapeutic approach against chronic *P. aeruginosa* infections.

Chapter Five: Transcriptomic studies in antibiofilm-treated *P. aeruginosa*

5.1 Introduction

In previous chapters we discussed the discovery of small molecule EPS repressors able to reduce biofilm formation and additionally reduce virulence of *P. aeruginosa in vivo.* Table 5.1 summarizes the phenotypes and effects of treating *P. aeruginosa* PAO1. EPS repressors were classified as antibiofilm compounds if they were capable of reducing biofilms in at least 2 out of the 3 aerobic biofilm phenotypes, which included EPS/ECM production, microplate biofilm formation, and flow chamber biofilms (Table 5.1). Among the seven antibiofilm compounds identified (I2, I7, I9, I10, I11, I12, I13), only four compounds were also found to have antivirulence activity in the *C. elegans* slow killing assay (Table 5.1, Fig 4.2). This summary also illustrates that some compounds can block EPS gene expression but do not have antibiofilm properties against aerobic biofilms (I1, I4, I5, I6 and I8). However, I1, I5 and I6 were able to reduce biofilms formed under anaerobic conditions. Compound I3, although showing modest effects on biofilm formation was not included in the antibiofilm group due to its non-specific effects on reporter expression (Table 5.1).

Although many studies have identified small molecules with significant antibiofilm properties, the huge majority of them lack a characterized mechanism of action, which delays their possible clinical use for the treatment of persistent bacterial infections. [62] An editorial in *Nature Medicine* [124] has pointed out the necessity of a characterized mechanism of action before a drug progresses to clinical trials, emphasizing that mechanistic studies may facilitate drug development and ultimately, patient therapies. [124]

Table 5.1: Summary of results for PAO1 treated with the antibiofilm small molecules.

Phenotype*	Antibiofilm°/Antivirulence				Antibiofilm°			Pel/Psl repressors					NSR
	I7	**I9**	**I10**	**I11**	**I2**	**I12**	**I13**	**I1**	**I4**	**I5**	**I6**	**I8**	**I3**
pelB expression	+++	++	+++	++	++	+++	++	+++	+++	+++	++	+++	+++
pslA expression	+++	–	–	++	++	–	+++	+++	++	+++	+++	+++	+++
CR assay (EPS/ECM)	++	+	+++	+	+++	++	++	–	–	–	+	–	+
CV assay (biofilm)	++	++	++	++	++	++	–	–	–	–	–	+	+
Flow biofilm (depth)	++	–	++	++	+	++	+++	ND	ND	–	ND	ND	–
Antivirulence	+	+	+	+	–	–	–	–	–	–	–	–	–
Anaerobic biofilm	–	++	–	ND	–	++	–	++	–	+	++	–	++

* Statistically significant repression effects were scored as mild + (>15%), moderate ++ (>30%), strong +++ (>50%) or – (no effect).

° Compounds were grouped as “antibiofilm” molecules if they reduced 2 out of 3 biofilm phenotypes (CR, CV, flow biofilm assays).

ND, not determined, NSR, non-specific repressor.

Therefore, in this chapter we are focusing on performing a more extensive investigation of the antibiofilm small molecules in order to identify a possible mechanism of action of our lead compounds. Because our lead antibiofilm compounds reduce *pel* and *psl* expression, as well as reducing EPS secretion and biofilm formation, we hypothesize that our compounds are acting on the Gac/Rsm pathway or any of the regulatory satellite systems that coordinate Pel and Psl synthesis (Fig 1.2). We used an RNA-seq transcriptome approach to characterize the differentially regulated genes in *P. aeruginosa* treated with our four lead antibiofilm/antivirulence compounds, in order to gain further insight into their possible targets and to provide a systems biology perspective of their effects on cells.

5.2 Specific methods

5.2.1 Strains and growth conditions

Transcriptomics studies were performed in a double mutant *ΔpelFΔpslD* (kindly provided by Dr. Joe Harrison) cultured in BM2 20 μM Mg^{2+} containing 10 μM of our identified antibiofilm/antivirulence compounds or 1% DMSO.

5.2.2 RNA-seq for the investigation of global effects of treatments over gene expression

We performed a next generation RNA-sequencing workflow to produce a transcriptional profile for compound-treated *P. aeruginosa* harvested cells. [125] For RNA-seq experiments, we utilized a mutant lacking the production of both *pel* and *psl* (*ΔpelFΔpslD)*, in order to limit any indirect gene expression effects that may result as a consequence of EPS-mediated aggregation. [33] Cultures were incubated overnight in BM2 20 μM Mg^{2+} containing 1% DMSO (control) or one of the four selected antibiofilm/antivirulence molecules, I7, I9, I10 and I11.

Overnight cultures were subcultured in the same conditions and allowed to grow to an OD_{600} = 0.5. The RNA-seq workflow included an in house-RNA extraction protocol (adapted from Chugani *et al*. [126] , in which total RNA was mobilized with 2:1 volume of RNAprotect bacteria reagent (QIAGEN) and extracted with QIAzol/chloroform reagents, a ribosomal RNA (rRNA) depletion using the Ribo-Zero kit (Epicentre), and a cDNA library preparation using the ScriptSeq v2 kit (Epicentre). A complete experimental workflow can be found in Appendix B. Libraries were sequenced in house on a MiSeq Illumina system to verify quality, then were sent to the Genome Quebec (GQ) core facility, in Montreal, to be loaded and sequenced in one lane of a flow cell of the HiSeq Illumina 2500. Sequencing data received from GQ in FASTQ files were aligned to the PAO1 reference genome using Xpression (Appendix C). Transcriptomic analysis in R was performed using DeSeq2 (Appendix D) and EdgeR (Appendix E) with the customized scripts for the determination of fold-changes and the statistical significance of the expression patterns.

5.2.3 Statistical analysis

In this chapter, EdgeR statistical model was used to determine the significance from differentially expressed transcripts analyzed in R. Also, paired two-tailed Student's t-test was used to determine significance between reporters expression under varying Mg^{2+} conditions. Data considered significant at level of $p<0.05$.

5.3 Results

5.3.1 Growth optimization and RNA-seq workflow

All previous gene expression experiments were performed in small volume cultures (microplate). Therefore, we initially optimized the growth conditions for bacteria grown in larger volume culture tubes, to determine the best time point for harvesting the cells for the RNA-seq approach. We grew the *pelB::lux* reporter in tubes containing 3 ml of BM2 20 μM Mg^{2+} + 1% DMSO (control) or I7, and determined the CPS and OD_{600} values hourly throughout growth. We observed that *pelB* repression by means of I7 was stable throughout incubation, showing an approximate 2-fold repression in gene expression relative to the untreated control at every time point, similar to previous results (Fig 2.4). We therefore decided on harvesting the cells at OD = 0.5, where cells were still in mid-log phase and showed *pelB::lux* repression.

Cells were treated with the RNAprotect reagent, and total RNA was extracted with QIAzol/chloroform. [126] Total RNA samples were treated for rRNA depletion and final mRNA purification, before the RNA-seq libraries were prepared by reverse transcription of the fragmented mRNA molecules, insertion of barcodes, and subsequent amplification (Fig 5.1).

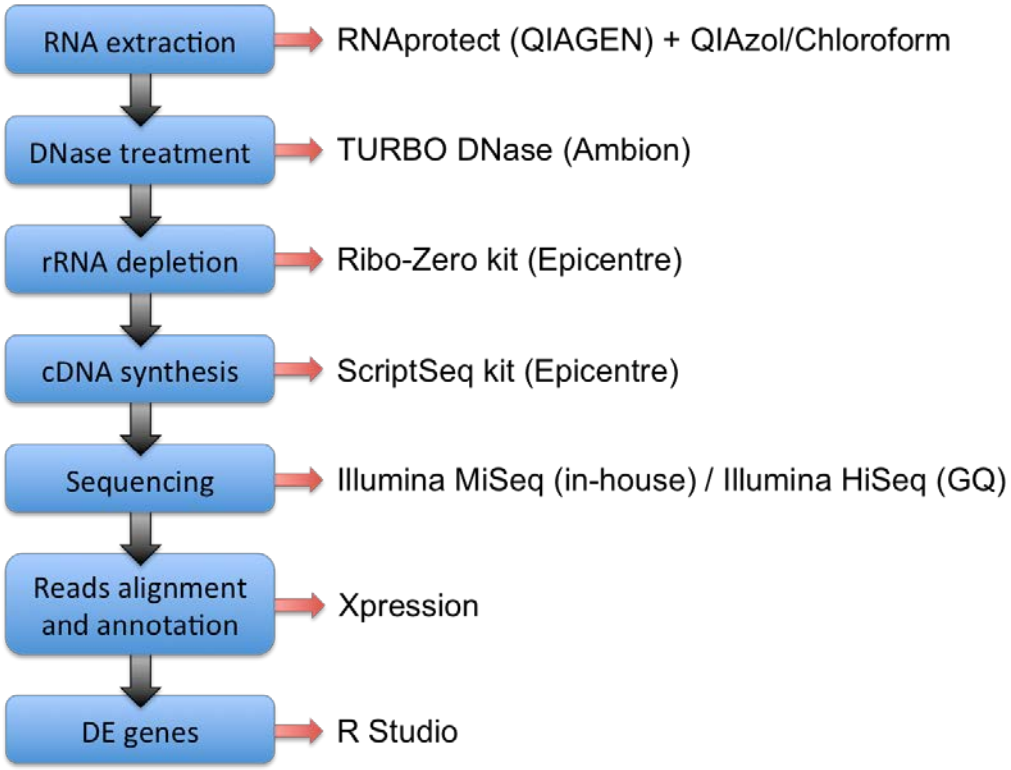

Figure 5.1: RNA-seq workflow summary.

The steps for RNA-seq are summarized. Total RNA of compound-treated cells was extracted with an in-house isolation protocol and followed all steps of RNA purification. Purified mRNA samples were fragmented and reverse-transcribed following Epicentre/Illumina procedures. Ready to sequence libraries were sequenced in-house on the MiSeq to verify quality and then sent to Genome Quebec (GC) core facility to be sequenced in a flow cell of the Illumina HiSeq system. The reads received in FASTQ files were aligned to PAO1 annotated reference genome, using Xpression, and followed transcriptomic analysis in R, using DESeq2 and EdgeR platforms for the identification of differentially expressed (DE) genes.

5.3.2 Reads alignment and biological reproducibility analysis

FastQ files received from the GQ core facility were initially aligned to PAO1 reference annotated genome, and Xpression software analyzed the sequencing reads for their general quality and alignment properties (Fig 5.1). We obtained between 30-47 million reads per treatment, with approximately 85% of high quality reads (Table 5.2). Other general parameters of the sequencing statistics are listed in Table 5.2. We obtained at least 8 million uniquely mapped high-quality reads for each treatment, which were used for the bioinformatics workflows.

Additionally, after reads were aligned to the reference genome, we were able to count the number of raw reads per genome location and plot them in order to determine the biological reproducibility among samples. When comparing replicates between any given treatment conditions, the correlation coefficients (r^2) were all above 0.91 (Table 5.3), indicating high reproducibility between the reads of each biological replicate, which was another indicator of high quality NGS data.

Table 5.2. Sequence read statistics for RNA-seq data generated from *P. aeruginosa ΔpelFΔpslD* upon treatment with the antibiofilm small molecules.

	DMSO control		I7 treatment		I9 treatment		I10 treatment		I11 treatment	
Total reads	41,146,598	100%	30,751,847	100%	35,501,367	100%	34,507,092	100%	47,253,668	100%
High-quality reads	35,230,303	86%	26,308,645	86%	30,120,963	85%	29,321,165	85%	39,479,829	84%
Low-quality reads	5,916,295	14%	4,443,202	14%	5,380,404	15%	5,185,927	15%	7,773,839	16%
Total high-quality reads	35,230,303	100%	26,308,645	100%	30,120,963	100%	29,321,165	100%	39,479,829	100%
Mapped reads	22,620,875	64%	15,143,751	58%	12,045,845	40%	12,136,254	41%	9,975,730	25%
Unmapped reads	12,609,434	36%	11,164,900	42%	18,075,124	60%	17,184,917	59%	29,504,105	75%
Total mapped reads	22,620,875	100%	15,143,751	100%	12,045,845	100%	12,136,254	100%	9,975,730	100%
Uniquely-mapped reads	19,010,108	84%	11,902,907	79%	9,888,768	82%	10,364,408	85%	8,406,130	84%
Partially-mapped reads	1,489,742	7%	1,020,691	7%	803,135	7%	684,054	6%	447,712	5%
Non-uniquely-mapped reads	2,121,019	9%	2,220,147	14%	1,353,936	11%	1,087,786	9%	1,121,882	11%

Table 5.3. Correlation coefficients between samples indicate high reproducibility of the RNA-seq approach.

Treatment	Parallel comparison	r^2
Control (DMSO)	C (1) vs. C (2)	0.9658
	C (2) vs. C (3)	0.9816
	C (3) vs. C (1)	0.9678
I7	I7 (1) vs. I7 (2)	0.9643
	I7 (2) vs. I7 (3)	0.9342
	I7 (3) vs. I7 (1)	0.9162
I9	I9 (1) vs. I9 (2)	0.9301
	I9 (2) vs. I9 (3)	0.9978
	I9 (3) vs. I9 (1)	0.9193
I10	I10 (1) vs. I10 (2)	0.9962
	I10 (2) vs. I10 (3)	0.9884
	I10 (3) vs. I10 (1)	0.9859
I11	I11 (1) vs. I11 (2)	0.9929
	I11 (2) vs. I11 (3)	0.9739
	I11 (3) vs. I11 (1)	0.9700

It is noteworthy to acknowledge that we initially prepared 4 replicates for each condition, leaving one extra replicate in case of any operational error during the RNA purification steps that could compromise the quality of the final data. Nevertheless, all samples yielded very high quality RNA, so we selected the three samples from each treatment with the highest concentrations for subsequent messenger RNA (mRNA) enrichment. rRNA depletion is an essential step in transcriptomic studies, as rRNA is the majority of the total cellular RNA, while mRNA accounts for a very small fraction of all RNA molecules within the cell. [127] The purified mRNAs were then reverse transcribed to generate the cDNA libraries to be sequenced. Ready to sequence libraries were sent to the GQ core facility and loaded to one lane of the HiSeq ultra-high-throughput sequencing system.

5.3.3 Whole genome RNA-seq for global analysis of gene expression

Sequencing reads received from GQ in Fastq files were aligned to the PAO1 reference genome using Xpression and later differential expression analysis in the annotated transcripts was performed in R Studio (Fig 5.1). The initial analysis of differentially expressed genes using DESeq2 resulted in zero significant hits for the majority of treatments, which rather agrees with previous reports that show the DESeq software to be very conservative and to detect a low number of differentially expressed genes. [128] Therefore, we performed a subsequent analysis for differentially expressed genes using the EdgeR software.

After the transcriptome analysis of our samples, in which EdgeR counted the number of high quality sequence reads that were mapped to the PAO1 reference genome, we obtained a list of differentially expressed genes for each antibiofilm treatment. Roughly, the number of reads aligned to the reference genome reflects the relative level of expression for each gene. [125]

Therefore, a simple comparison of the aligned reads in untreated and treated conditions is a good indication of differential expression.

The lists of all differentially expressed genes for each antibiofilm treatment are displayed in Tables S1-S4, in Appendix F. Previous reports have shown that EdgeR, although using similar statistical model to DeSeq, tends to be more wide-ranging in assigning differentially expression genes. [128] For a more in-depth analysis of the hit genes, we included all the significant calls ($p<0.05$), which include the small subset of genes that were determined to be differentially expressed and adjusted for the false discovery rate (p_{adj}). Nevertheless, we are cautious while analyzing this data, being aware that further confirmatory assays need to be performed for more reliable conclusions.

We observed that many genes are commonly regulated by the distinct antibiofilm treatments, with a small core number of genes (14) being commonly regulated by the four different treatments (Fig 5.2). The numbers of overlapping genes that are commonly affected by the individual antibiofilm treatments are shown in Figure 5.2. Our main interest is the differentially expressed genes shared between all four treatments, which include the two neighbouring clusters of F and R-type pyocins (PA0612-PA0648), a third S-type pyocin gene (PA0985) and the anaerobically induced outer membrane porin OprE (PA0291) (Fig 5.3).

We expected to find the *pel* and/or *psl* gene clusters among the differentially regulated genes, given our analysis of *pel/psl* expression using transcriptional *lux* fusions. In the final RNA-seq analysis, we did not observe significant differences in expression on the *pel* and *psl* operons. However, these EPS biosynthetic clusters showed repression trends with decreases in expression between 1.2 and 4.0 fold after all treatments. It is known that the statistical methods for identifying differentially regulated genes can be very stringent, and have a tendency to

overlook some differentially regulated genes, including low level expression genes such as the *pel* and *psl* operons. [129]

Our initial hypothesis was that repressors of *pel/psl* expression could target one of the components of the Gac/Rsm regulatory complex controlling biofilm formation (Fig S4.A, Appendix A). Under limiting magnesium, there is increased biofilm formation, and increased expression of *pel* and *psl* genes, leading to increased EPS production and robust biofilm formation (Fig 3.1, Fig 3.2.A, Fig 3.3.B, Fig 5.4). [17] To confirm an effect of reduced magnesium on the translation of the EPS genes, we showed that translation is also increased from *pslA::lacZ*, a translational β-galactosidase fusion (Fig 5.4). [41] Biofilm formation is generally associated with increases in the intracellular signalling molecule c-di-GMP. We also observed a slight increase in expression of the c-di-GMP biosensor, *cdrA-lux* (Fig 5.4). The *cdrA* gene encodes an adhesin that is transcriptionally regulated by increasing amounts of the intracellular signalling molecule, c-di-GMP, and was previously shown to act as a simple and indirect measure of c-di-GMP levels within the cell. [86, 131]

Our lab has shown that PhoPQ, the TCS that responds to limiting magnesium, can repress the expression of *retS*, which leads to increased biofilm formation (Fig 1.2). [17] It is therefore possible that antibiofilm compounds might target this pathway by i) inhibiting/repressing PhoPQ, LadS or GacAS activity, or ii) by activating/inducing RetS activity, which would shift the pathway out of the biofilm mode of growth (Fig S4.A, Appendix A).

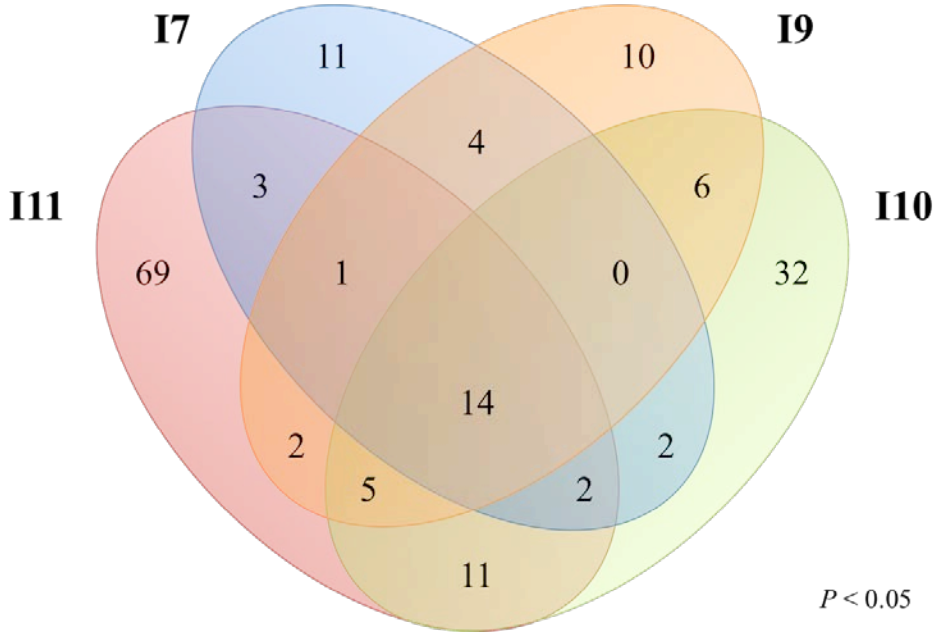

Figure 5.2: Analysis of differentially expressed genes show overlapping effects on overall gene expression after compound treatments.

Venn diagram constructed with 4 ellipses, demonstrating the number of commonly differentially expressed genes between treatments. The diagram includes all genes that were differentially expressed according to EdgeR analysis, $p < 0.05$, n = 3.

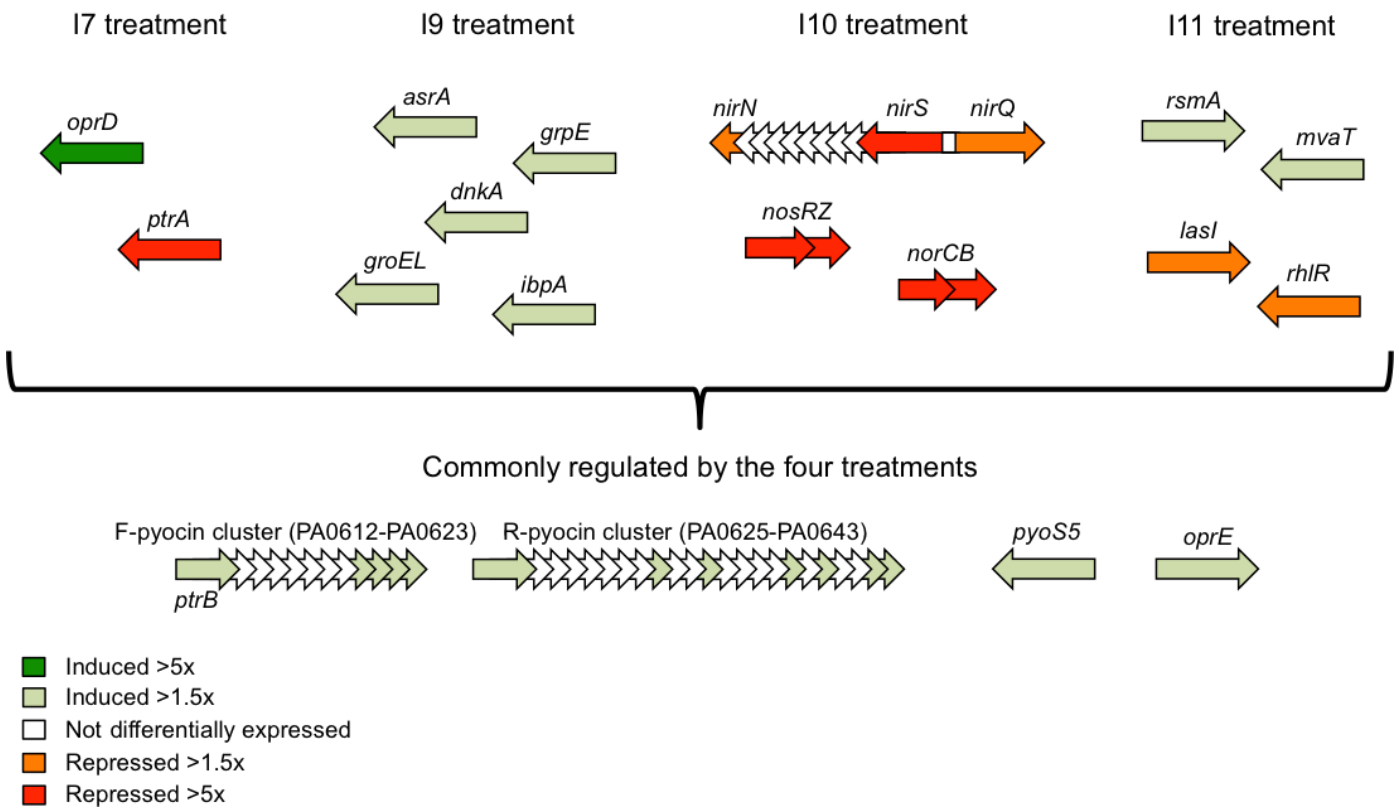

Figure 5.3: Summary of the common and unique differentially regulated genes after antibiofilm treatment.

The RNA-seq study has identified many interesting gene expression changes that have provided further insights into their effect on *P. aeruginosa*. Expression analysis was performed using EdgeR and differential expression was considered significant if $p < 0.05$.

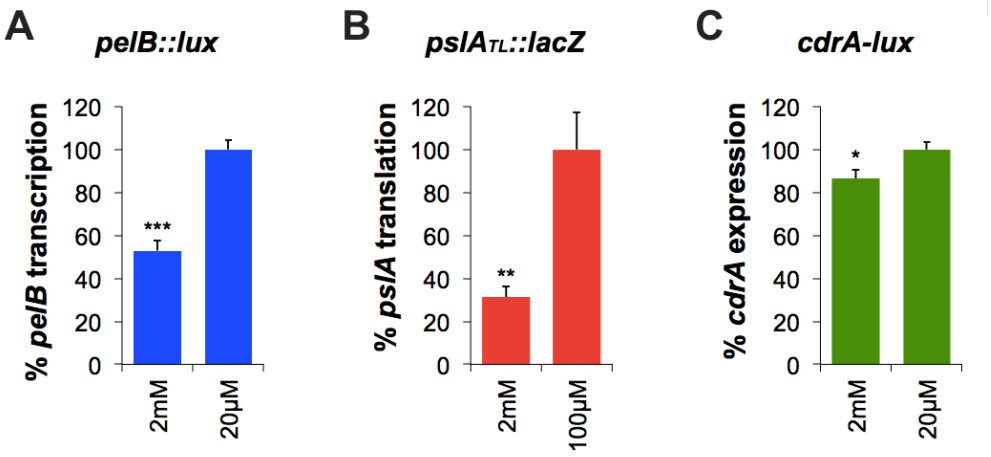

Figure 5.4: Conditions with limiting magnesium concentrations promote EPS-gene transcription, translation and ultimately increased c-di-GMP detection.

Control expression for the **(A)** *pelB::lux* transcriptional reporter, **(B)** *pslA::lacZ* translational reporter and **(C)** *cdrA-lux*, c-di-GMP biosensor in BM2 media containing high and low Mg^{2+} concentration. *PelB* and *cdrA* expression were determined in 96-well microplate format in gene expression assays as previously described. Translational *pslA::lacZ* reporter was incubated in 2 ml cultures for 18 hours with shaking (150 rpm) and 1 ml of grown culture was used to assess β-galactosidase activity using the Galacto-Light Plus kit. Values shown for *pelB* and *cdrA* are the average area under the curve for triplicate samples and the standard deviation, as an indication of total gene expression throughout incubation time. Values for the translational *pslA* reporter are the average normalized CPS value (CPD/OD_{600}) and standard deviation of triplicate samples, in single read after incubation, n=3. Statistical significance between populations was determined by paired two-tailed Student's t-test and significant differences in gene expression are indicates: * ($p<0.05$), ** ($p<0.01$) and *** ($p<0.001$).

In order to test this concept, we measured gene expression from the T3SS system effector ExoT during treatment with our antibiofilm compounds and showed an increased *exoT-lux* expression (Fig S4.B, Appendix A). We also showed that our lead antibiofilm compounds induced *retS* expression (Fig S4.B, Appendix A), and both observations suggest that these compounds may somehow reverse the biofilm switch pathway. Although we were not able to confirm the gene expression patterns of *exoT*, *retS* or *pel/psl* in the RNA-seq transcriptome, this hypothesis will need further testing to possibly confirm the action of these compounds on the PhoPQ/RetS/Gac/Rsm pathway, given that this is an important pathway for biofilm regulation. Future experiments will aim to confirm expression patterns of many genes within this pathway, using techniques such as reverse transcription quantitative polymerase chain reaction (RT-qPCR), which has been previously show to have better sensitivity for low abundance transcripts. [132]

The transcriptome analysis has identified other possible mechanisms of action of these antibiofilm compounds, as other genes outside of the main biofilm regulatory cascade were commonly regulated by all four antibiofilm compounds (Fig 5.3). There are also unique genes regulated by each antibiofilm compound indicating that these molecules have other activities and effects on gene expression (Fig 5.3). The fact that treatment with these compounds affects a diverse subset of bacterial genes is not surprising, and is in fact expected of many transcriptome studies with conventional antibiotics. [133] This is likely due to the fact that biologic active molecules can act as diverse microbial signalling molecules when present at sub-lethal concentrations, in addition to their antimicrobial killing activity. [133]

5.4 Discussion

In this chapter we identify the transcriptome profiles of *P. aeruginosa* exposed to antibiofilm compounds in order to help understand their global effects on bacteria gene expression. Although we were unable to confirm transcriptional repression of the *pel* and *psl* operons using RNA-seq, the transcriptome analysis revealed many other interesting genes for future study (Fig 5.3). The most interesting effect in common to all antibiofilm treatments was the induction of many genes within three clusters of R, F and S-type bacteriocins (Fig 5.3). Both F and R-type pyocins remarkably resemble phage tail structures, which are proteins known to produce a lytic activity in virtue of disrupting the bacterial cell membrane. [134] The S5 pyocin is similar to colicin-type antimicrobial proteins that also have membrane-disrupting activity. [135] Recently, an endolysin within the F pyocin cluster was shown to promote an explosive cell lysis phenotype within a subpopulation of cells, releasing eDNA and outer membrane vesicles and promoting biofilm matrix production in *P. aeruginosa*. [136] We are not exactly sure of the role of pyocins in blocking biofilms, but induction of multiple pyocins by these compounds may have a lytic or membrane-damaging effect within a subpoplation of cells and thus contribute to reducing attachment and/or promoting biofilm dispersal. [137, 138] Interestingly, transcript levels for the DNA-damage responsive recombinase *recA*, which is known to regulate all three types of pyocins, [134, 136] are induced for treatments I10 and I11 (Tables S3 and S4, Appendix F).

To further explore the possibility that treatment with the antibiofilm compounds induce pyocins, we measured the membrane destabilizing effects after treatment. Cells that are lysed by bacteriocins, or whose membranes have lost integrity will stain with the cell-impermeable DNA stain propidium iodide (PI). We performed flow cytometry of antibiofilm treated cultures that

were stained with the DNA stains Syto 9 (stains all cells) and PI (stains dead or membrane-compromised cells). [49] PAO1 was incubated to mid-log phase in 2 ml cultures with 10 μM of the four antibiofilm/antivirulence compounds, washed and diluted 10x in 1x phosphate buffered saline (PBS) (~$1x10^6$ CFU/ml), immediately stained with Syto 9/PI and followed to analysis in the LSR II Flow Cytometer (BD). We found that compounds I9 and I11 did result in an increase in PI staining, where the effect of I11 was much greater than I9 (Fig S5, Appendix A). This reinforces the possibility that there is an increased production of pyocins, and despite the usual presence of immunity proteins, there does appear to be a negative impact on the PAO1 membrane. Future experiments could be performed to confirm the production of pyocins in the supernatants, [101] and to test if these antibiofilm compounds can cause the explosive lysis phenotype, recently reported. [136]

Lastly, all antibiofilm compounds also induced the expression of OprE (Fig 5.3), an outer membrane porin that is highly induced under anaerobic conditions. [139] Porins are diffusion channels for nutrients to cross the outer membrane, and in *P. aeruginosa*, porins are often specifically induced by their substrate, or under specific growth conditions. [139] While porins play roles in acquiring nutrients, uptake of antibiotics, and possibly virulence by binding to host proteins, [139, 140] the possible roles of porins in limiting biofilm formation are unknown. OprE is induced in *P. aeruginosa* biofilms, which also have anaerobic zones, but its specific contribution to biofilms is not known. [36]

In order to expand our analysis of the RNA-seq data, we examined other significantly regulated genes with the uncorrected $p < 0.05$ value. *P. aeruginosa* treated with compound I7 showed increased expression of another outer membrane porin *oprD* (Fig 5.3). OprD is a porin that allows uptake of basic amino acids, and antibiotics imipenem and carbapenem. [141]

Previous work from Skurnik *et al*. [142] showed that a transposon mutation in the *oprD* gene increased transcript levels of *pelA*, other adhesins (*lecA, lecB*), lipopolysaccharide synthesis genes (*wbpL*) and a T3SS export protein (*pscD*), together with increased PA14 fitness in GI colonization and dissemination in an antibiotic-treated mice infectious model. Therefore, we hypothesize that overexpression of such outer membrane protein by means of I7 treatment can potentially revert such a phenotype, reducing EPS and adhesins synthesis, which would be predicted to reduce biofilm formation. Interesting, I7 treatment also promoted a 6-fold reduction in expression of the transcriptional regulator PtrA (Fig 5.3). PtrA is a global transcription regulator in *P. chlororaphis*, which has been recently shown to indirectly regulate the Gac/Rsm pathway in strain PA23. [143] The interaction link between GacS and PtrA is unknown, still *gacS* expression is affected in *ptrA* mutant, and introduction of a plasmid constitutively expressing *gacS* is able to partially restore fungal suppression, protease activity and QS production phenotypes in the *ptrA* mutant. [143] Besides, PtrA also negatively impacts the T3SS in *P. aeruginosa* strain PAK by direct interaction with the DNA-binding protein ExsA, [144] although its effect in other factors underneath the biofilm regulatory pathway were not investigated.

After treatment with compound I9, we observed an increase in expression of the *asrA* gene, which increases the heat shock response in *P. aeruginosa* (Fig 5.3). [145] We also noticed an increased expression of other heat-shock associated genes, such as *grpE, groEL, ibpA* and *dnaK*, indicating the possible activation of the heat shock cascade. Induction of the heat shock cascade interferes with assembly of the type IV pilus [146] and therefore I9 may induce an indirect dispersal by impairing assembly of the pilus, a major adhesin that is essential for *P. aeruginosa* biofilm formation.

Treatment with compound I10 promotes a drastic reduction in expression levels for genes involved in nitric oxide (NO) metabolism, reducing transcript levels from NO reductase (*norB, norC*) and nitrite reductase (*nirS, nirQ*) genes (Fig 5.3). Interestingly, a previous report from Barraud *et al.* [147] has revealed that *ΔnorCB* biofilms show increased dispersal compared to wild type biofilms. Moreover, addition of exogenous NO promotes biofilm dispersal and increases planktonic biomass. [147] Additionally, the expression level of the transcription regulator NosR was also majorly reduced, and it has been shown that a *nosR* transposon mutant show severe deficit in biofilm formation. [148] Compound I10 may therefore increase the levels of NO, which is a known biofilm dispersant for *P. aeruginosa.*

Finally, the transcriptome changes in I11-treated *P. aeruginosa* were marked by altered levels of expression for QS and other transcriptional regulatory proteins (Fig 5.3). The most interesting effect with treatment of compound I11 is the increased expression of the *rsmA* gene (Fig 5.3). As described briefly in Chapter 1, RsmA is a post-transcriptional regulator of the *pel* and *psl* genes that can destabilize the mRNA levels and therefore reduce EPS production and biofilm formation. [25] Additionally, RsmA has also been shown to modulate QS expression. [44] Treatment with I11 also caused increased expression of the *mvaT* QS regulatory gene (Fig 5.3), which is suggested to reduce expression of QS genes and globally affect virulence genes in *Pseudomonas* species. [149] Therefore, it is not surprising that by activation of both RsmA and MvaT, we also observed reduced expression of genes encoding the acylhomoserine lactone (AHL) QS LasI and RhlR regulators (Fig 5.3). Impairing these central QS regulators may reduce biofilm formation, as they were shown to regulate transcription of EPS genes and contribute to biofilm integrity and biocide resistance. [150]

To conclude, mechanistic studies are difficult, time consuming and a major hurdle to new antimicrobial discovery. [124] The initial investigation of our compounds mechanism of action using transcriptional *lux* reporters suggested their ability to interfere with the PhoPQ/RetS/Gac/Rsm pathway, potentially by repressing the PhoPQ system, or activating the RetS sensor in *P. aeruginosa* (Fig S4, Appendix A). In support to this hypothesis, we also observed similar effects in genes regulated by the ortholog PhoPQ TCS in *Salmonella enterica* serovar Typhimurium. [2] The PhoPQ TCS is a very attractive target for new antivirulence compounds, as it is important for biofilm formation, [17] antimicrobial resistance [47, 48, 50] and virulence [2, 4] of *P. aeruginosa* and other Gram-negative bacteria.

Although this initial hypothesis was not supported by the RNA-seq data, the NGS approach has also highlighted many other significant processes that are associated with biofilm formation. This data has given us further insights into other pathways affected by our compounds, such as pyocin production, porin induction, heat shock responses, NO metabolism and QS signalling, all of which are associated with defective biofilm phenotypes in different studies. Future studies could be directed towards exploring and validating these pathways and their contribution to the antibiofilm activity of the lead compounds identified in this thesis.

5.5 Conclusions from Chapter 5

i. An RNA-seq pipeline was used to determine the genome-wide transcription effects of our antibiofilm compound treatments.

ii. Although not supported by the RNA-seq data, we still propose potential effects of these compounds on the PhoPQ/RetS/Gac/Rsm central pathway involved in *pel/psl* transcription, translation and biofilm formation.

iii. RNA-seq has highlighted many interesting differentially expressed genes after antibiofilm treatment.

iv. Among the differentially expressed genes are listed many that have been associated with biofilm formation/maintenance in *P. aeruginosa*, giving us further insights in how they are acting in promoting the reported phenotypes.

v. Like many active molecules, we propose that these compounds have multiple effects on *P. aeruginosa*, interfering with EPS expression and additional effects that may contribute to limiting biofilm formation.

vi. Further effort is needed to confirm these gene expression profiles for a better understanding of the antibiofilm mechanism of action.

5.6 Final considerations

The conserved process of biofilm formation is an attractive target for new antivirulence approaches, given the many advantages of sessile communities of cells enmeshed in a protective extracellular matrix. [1, 3, 15] The Pel and Psl EPS are essential components of the *P. aeruginosa* biofilm matrix, being involved in biofilm formation, maintenance and protection. [16, 20, 22, 24, 25, 28] Therefore, in this project, we reported the EPS biosynthesis genes as a new target for the identification of antibiofilm compounds, and described the characterization of small molecule EPS-repressors that prevent biofilm formation and also reduce virulence of *P. aeruginosa.*

We have developed a high-throughput gene expression screen for small molecules that repress expression of the *pel* and *psl* EPS-genes. We screened 31,096 compounds within the CCBN and have identified 14 molecules that significantly reduced reporters' gene expression,

from which 13 could be purchased and further characterized to determine their effects on biofilm formation (Fig 2.3, Table 2.3). Using different *in vitro* assays, we have shown that ECM secretion (via CR assay, Fig 3.1) and biofilm formation (CV assay, Fig 3.2) are reduced when bacteria is cultured in the presence of 10 μM of the repressor compounds. The antibiofilm effects are observed throughout strains that differ in their ability to produce the EPS molecules, including PA14 ($Pel^{+}Psl^{-}$), PAO1 ($Pel^{+}Psl^{+}$) and a *retS::lux* mutant ($Pel^{++}Psl^{++}$), therefore we believe these effects originate from the active repression of the *pel* and *psl* genes and, consequently, EPS inhibition. We made use of the CR dye for determining the effects of the compounds on ECM secretion, [93] though for confirmation of anti-EPS effects it would be beneficial to subsequently use Pel/Psl specific lectins or antibodies, as previously described [16, 20, 73, 104] for a more accurate detection of these polymers within the matrix.

Interestingly, the EPS-repressor compounds reduced biofilm formation in different settings, inhibiting biofilms in both aerobic (Fig 3.2.B) and anaerobic (Fig 3.4.B) environments, reducing detected adhered biomass in the flow-system biofilm device (Fig 3.3.B), and many even promoting modest decrease in biofilms formed by a mucoid variant of PAO1 strains (PDO300) (Fig 3.4.A), all of them mimicking different conditions that *P. aeruginosa* encounters while infecting CF patients.

We have also illustrated that EPS production is required for *P. aeruginosa* virulence *in vivo* (Fig 4.1), and further testing of these compounds revealed that 4/13 fostered antivirulence activities in the *C. elegans* slow killing infection model, significantly promoting nematode survival when PAO1 was treated with I7, I9, I10 and I11 (Fig 4.2). While numerous high throughput nematode virulence screens have been performed in PA14, a rapid killing strain of *P. aeruginosa*, to our knowledge this is the first report to identify the EPS molecules as virulence

factors in *C. elegans*. Additionally, these antivirulence molecules also promoted biofilm killing when associated with antimicrobials, represented by a reduced recovery of viable cells when biofilms were challenged with sub-eradication concentrations of antibiotics (Fig 4.3, Fig 4.4). These classes of antibiotics tested are known to have reduced effectiveness because of the production of Pel or Psl EPS. [20, 21, 28] At this point we believe these antivirulence activities are due to direct repression of EPS secretion, although further studies are needed to confirm these findings.

Lastly, we used the RNA-seq transcriptome approach to characterize the global effects of the compounds in bacterial gene expression and, possibly, determine their antibiofilm mechanism of action. The RNA-seq workflow has characterized many differentially expressed genes in *P. aeruginosa* upon treatment with the antibiofilm/antivirulence molecules. To have a broader view of all differentially expressed genes in treated bacteria, we have performed a less stringent analysis, including all transcripts assigned from the analysis using the EdgeR package with $p < 0.05$ (Fig 5.2). Additionally, we recognise that as we did not limit our analysis to the calls corrected for false discovery rate (p_{adj}), we need to perform further assays to confirm any hypothesis drawn from this initial investigation.

The RNA-seq analysis in EdgeR has not confirmed the transcriptional repression of the *pel* and *psl* genes, although it has highlighted many other biofilm associated genes that are potentially affected by the antibiofilm molecules (Fig 5.3). Interestingly, all four antibiofilm treatments have induced many genes within three clusters of pyocins (Fig 5.3), which lead us to believe that induction of pyocins can potentially induce a lytic effect within biofilms and promote colony dispersal. Flow cytometry analysis has revealed increase membrane disturbance

in I9 and I11-treated cells, as indicated by increased PI staining (Fig S5, Appendix A), further supporting this hypothesis.

The different treatments have also affected transcript levels in other genes/pathways previously shown to be involved in biofilm formation or dispersal (Fig 5.3), although such speculative analysis need further experiments to confirm their effect, such as qRT-PCR or even alternative gene reporters. Future studies could be directed towards exploring and validating these pathways and their contribution to the antibiofilm activity of the lead compounds identified in this study.

In conclusion, the small molecules identified in this project are examples of a new strategy for treating *P. aeruginosa* biofilm infections, as they do not inhibit bacterial growth but reduce the expression of virulence mechanisms used to promote chronic infections. Here we reported that the *pel* and *psl* EPS biosynthesis genes provide a new target for antivirulence drug development, as the identified molecules effectively inhibit biofilm formation, reduce PAO1 virulence *in vivo* and additionally promote biofilm killing by antibiotics. Further work is needed to understand their mechanism of action, their effectiveness in other infection models, and to assess their potential for therapeutic use to treat chronic, biofilm infections by *P. aeruginosa*.

References

1. **Davies JC, Bilton D.** (2009) Bugs, biofilms, and resistance in cystic fibrosis. Respir Care **54(2):**628-640.

2. **Gooderham WJ, Hancock RE.** (2009) Regulation of virulence and antibiotic resistance by two-component regulatory systems in *Pseudomonas aeruginosa*. FEMS Microbiol Rev **33(2):**279-294.

3. **Wagner VE, Iglewski BH.** (2008) *P. aeruginosa* biofilms in CF infection. Clin Rev Allergy Immunol **35(3):**124-134.

4. **Gooderham WJ, Gellatly SL, Sanschagrin F, McPhee JB, Bains M, Cosseau C, Levesque RC, Hancock RE** (2009) The sensor kinase PhoQ mediates virulence in *Pseudomonas aeruginosa*. Microbiology **155(Pt 3)**:699-711.

5. **Barrow K, Kwon DH.** (2009) Alterations in two-component regulatory systems of PhoPQ and PmrAB are associated with polymyxin B resistance in clinical isolates of *Pseudomonas aeruginosa*. Antimicrob Agents Chemother **53(12):**5150-5154.

6. **Sall KM, Casabona MG, Bordi C, Huber P, de Bentzmann S, Attrée I, Elsen S.** (2014) A *gacS* deletion in *Pseudomonas aeruginosa* cystic fibrosis isolate CHA shapes its virulence. PLoS One **9(4):**e95936.

7. **Driscoll JA, Brody SL, Kollef MH.** (2007) The epidemiology, pathogenesis and treatment of *Pseudomonas aeruginosa* infections. Drugs **67(3)**:351-368.

8. **Rowntree RK, Harris A.** (2003) The phenotypic consequences of CFTR mutations. Ann Hum Genet **67(Pt 5):**471-485.

9. **Quinton PM.** (1990) Cystic fibrosis: A disease in electrolyte transport. FASEB J **4(10):**2709-2717.

10. **Cystic Fibrosis Canada [internet].** What is Cystic Fibrosis? CF Canada. **2016.** Available from: http://www.cysticfibrosis.ca/about-cf/what-is-cystic-fibrosis/.

11. **Høiby N.** (2006) *P. aeruginosa* in cystic fibrosis patients resists host defenses, antibiotics. Microbe **1:**571-577.

12. **Lynch SV, Bruce KD.** (2013) The cystic fibrosis airway microbiome. Cold Spring Harb Perspect Med **3(3):**a009738.

13. **Cox MJ, Allgaier M, Taylor B, Baek MS, Huang YJ, Daly RA, Karaoz U, Andersen GL, Brown R, Fujimura KE, Wu B, Tran D, Koff J, Kleinhenz ME, Nielson D, Brodie EL, Lynch SV.** (2010) Airway microbiota and pathogen abundance in age-stratified cystic fibrosis patients. PLoS One **5(6):** e11044.

14. **Aaron SD, Vandemheen KL, Ramotar K, Giesbrecht-Lewis T, Tullis E, Freitag A, Paterson N, Jackson M, Lougheed MD, Dowson C, Kumar V, Ferris W, Chan F, Doucette S, Fergusson D.** (2010) Infection with transmissible strains of *Pseudomonas aeruginosa* and clinical outcomes in adults with cystic fibrosis. JAMA **304(19):** 2145-2153.

15. **Kirisits MJ, Prost L, Starkey M, Parsek MR.** (2005) Characterization of colony morphology variants isolated from *Pseudomonas aeruginosa* biofilms. Appl Environ Microbiol **71(8):**4809-4821.

16. **Colvin KM, Irie Y, Tart CS, Urbano R, Whitney JC, Ryder C, Howell PL, Wozniak DJ, Parsek MR.** (2012) The Pel and Psl polysaccharides provide *Pseudomonas aeruginosa* structural redundancy within the biofilm matrix. Environ Microbiol **14:**1913-1928.

17. **Mulcahy H, Lewenza S.** (2011) Magnesium limitation is an environmental trigger of the *Pseudomonas aeruginosa* biofilm lifestyle. PLoS One **6(8):**e23307.

18. **Mikkelsen H, Sivaneson M, Filloux A.** (2011) Key two-component regulatory systems that control biofilm formation in *Pseudomonas aeruginosa*. Environ Microbiol **13(7):**1666-1681.

19. **Stoodley P, Sauer K, Davies DG, Costerton JW.** (2002) Biofilms as complex differentiated communities. Annu Rev Microbiol **56:**187-209.

20. **Colvin KM, Gordon VD, Murakami K, Borlee BR, Wozniak DJ, Wong GC, Parsek MR.** (2011) The Pel polysaccharide can serve a structural and protective role in the biofilm matrix of *Pseudomonas aeruginosa*. PLoS Pathog **7(1):**e1001264.

21. **Yang L, Hu Y, Liu Y, Zhang J, Ulstrup J, Molin S.** (2011) Distinct roles of extracellular polymeric substances in *Pseudomonas aeruginosa* biofilm development. Environ Microbiol **13(7):**1705-1717.

22. **Ma L, Conover M, Lu H, Parsek MR, Bayles K, Wozniak DJ.** (2009) Assembly and development of the *Pseudomonas aeruginosa* biofilm matrix. PLoS Pathog **5(3):**e1000354.

23. **Qin Z, Yang L, Qu D, Molin S, Tolker-Nielsen T.** (2009) *Pseudomonas aeruginosa* extracellular products inhibit staphylococcal growth, and disrupt established biofilms produced by *Staphylococcus epidermidis*. Microbiology **155(Pt 7):**2148-2156.

24. **Franklin MJ, Nivens DE, Weadge JT, Howell PL.** (2011) Biosynthesis of the *Pseudomonas aeruginosa* extracellular polysaccharides, alginate, Pel, and Psl. Front Microbiol **2:**167.

25. **Ryder C, Byrd M, Wozniak DJ.** (2007) Role of polysaccharides in *Pseudomonas aeruginosa* biofilm development. Curr Opin Microbiol **10(6):**644-648.

26. **Jennings LK, Storek KM, Ledvina HE, Coulon C, Marmont LS, Sadovskaya I, Secor PR, Tseng BS, Scian M, Filloux A, Wozniak DJ, Howell PL, Parsek MR**. (2015) Pel is a cationic exopolysaccharide that cross-links extracellular DNA in the *Pseudomonas aeruginosa* biofilm matrix. Proc Natl Acad Sci U S A **112(36):** 11353-11358.

27. **Mulcahy H, Sibley CD, Surette MG, Lewenza S.** (2011) *Drosophila melanogaster* as an animal model for the study of *Pseudomonas aeruginosa* biofilm infections in vivo. PLoS Pathog **7(10):**e1002299.

28. **Billings N, Millan M, Caldara M, Rusconi R, Tarasova Y, Stocker R, Ribbeck K**. (2013) The extracellular matrix component Psl provides fast-acting antibiotic defense in *Pseudomonas aeruginosa* biofilms. PLoS Pathog **9(8):**e1003526.

29. **Mishra M, Byrd MS, Sergeant S, Azad AK, Parsek MR, McPhail L, Schlesinger LS, Wozniak DJ.** (2011) *Pseudomonas aeruginosa* Psl polysaccharide reduces neutrophil phagocytosis and the oxidative response by limiting complement-mediated opsonization. Cell Microbiol **14(1):**95-106.

30. **Friedman L, Kolter R.** (2004) Two genetic loci produce distinct carbohydrate-rich structural components of the *Pseudomonas aeruginosa* biofilm matrix. J Bacteriol **186(14):**4457-4465.

31. **Wozniak DJ, Wyckoff TJ, Starkey M, Keyser R, Azadi P, O'Toole GA, Parsek MR.** (2003) Alginate is not a significant component of the extracellular polysaccharide matrix of PA14 and PAO1 *Pseudomonas aeruginosa* biofilms. Proc Natl Acad Sci U S A **100(13):**7907-7912.

32. **Govan JR, Deretic V.** (1996) Microbial pathogenesis in cystic fibrosis: mucoid *Pseudomonas aeruginosa* and *Burkholderia cepacia*. Microbiol Rev **60(3):**539-574.

33. **Starkey M, Hickman JH, Ma L, Zhang N, De Long S, Hinz A, Palacios S, Manoil C, Kirisits MJ, Starner TD, Wozniak DJ, Harwood CS, Parsek MR.** (2009) *Pseudomonas aeruginosa* rugose small colony variants have adaptations likely to promote persistence in the cystic fibrosis lung. J Bacteriol **191(11):**3492-503..

34. **Worlitzsch D, Tarran R, Ulrich M, Schwab U, Cekici A, Meyer KC, Birrer P, Bellon G, Berger J, Weiss T, Botzenhart K, Yankaskas JR, Randell S, Boucher RC, Döring G.** (2002)

Effects of reduced mucus oxygen concentration in airway *Pseudomonas* infections of cystic fibrosis patients. J Clin Invest **109(3):**317-325.

35. **Waite RD, Papakonstantinopoulou A, Littler E, Curtis MA.** (2005) Transcriptome analysis of *Pseudomonas aeruginosa* growth: comparison of gene expression in planktonic cultures and developing and mature biofilms. J Bacteriol **187(18):**6571-6576.

36. **Sauer K, Camper AK, Ehrlich GD, Costerton JW, Davies DG.** (2002) *Pseudomonas aeruginosa* displays multiple phenotypes during development as a biofilm. J Bacteriol **184(4):**1140-1154.

37. **Moscoso JA, Jaeger T, Valentini M, Hui K, Jenal U, Filloux A.** (2014) The diguanylate cyclase SadC is a central player in Gac/Rsm-mediated biofilm formation in *Pseudomonas aeruginosa*. J Bacteriol **196(23):**4081-4088.

38. **Davies DG, Parsek MR, Pearson JP, Iglewski BH, Costerton JW, Greenberg EP.** (1998) The involvement of cell-to-cell signals in the development of a bacterial biofilm. Science **280(5361):**295-298.

39. **Lee J, Zhang L.** (2015) The hierarchy quorum sensing network in *Pseudomonas aeruginosa*. Protein Cell **6(1):** 26-41.

40. **Hickman JW, Tifrea DF, Harwood CS.** (2005) A chemosensory system that regulates biofilm formation through modulation of cyclic diguanylate levels. Proc Natl Acad Sci U S A **102(40):**14422-14427.

41. **Irie Y, Starkey M, Edwards AN, Wozniak DJ, Romeo T, Parsek MR.** (2010) *Pseudomonas aeruginosa* biofilm matrix polysaccharide Psl is regulated transcriptionally by RpoS and post-transcriptionally by RsmA. Mol Microbiol **78(1):**158-72.

42. **Goodman AL, Kulasekara B, Rietsch A, Boyd D, Smith RS, Lory S.** (2004) A signaling network reciprocally regulates genes associated with acute infection and chronic persistence in *Pseudomonas aeruginosa*. Dev Cell **7(5):**745-754.

43. **Heurlier K, Williams F, Heeb S, Dormond C, Pessi G, Singer D, Cámara M, Williams P, Haas D.** (2004) Positive control of swarming, rhamnolipid synthesis, and lipase production by the posttranscriptional RsmA/RsmZ system in *Pseudomonas aeruginosa* PAO1. J Bacteriol **186(10):** 2936-2945.

44. **Pessi G, Williams F, Hindle Z, Heurlier K, Holden MT, Cámara M, Haas D, Williams P.** (2001) The global posttranscriptional regulator RsmA modulates production of virulence determinants and N-acylhomoserine lactones in *Pseudomonas aeruginosa*. J Bacteriol **183(22):**6676-6683.

45. **Burrowes E, Baysse C, Adams C, O'Gara F.** (2006) Influence of the regulatory protein RsmA on cellular functions in *Pseudomonas aeruginosa* PAO1, as revealed by transcriptome analysis. Microbiology **152(Pt 2):**405-418.

46. **Ventre I, Goodman AL, Vallet-Gely I, Vasseur P, Soscia C, Molin S, Bleves S, Lazdunski A, Lory S, Filloux A.** (2006) Multiple sensors control reciprocal expression of

Pseudomonas aeruginosa regulatory RNA and virulence genes. Proc Natl Acad Sci U S A **103(1):**171-176.

47. **Wilton M, Charron-Mazenod L, Moore R, Lewenza S.** (2015) Extracellular DNA acidifies biofilms and induces aminoglycoside resistance in *Pseudomonas aeruginosa*. Antimicrob Agents Chemother **60(1):**544-553.

48. **Lewenza S.** (2013) Extracellular DNA-induced antimicrobial peptide resistance mechanisms in *Pseudomonas aeruginosa*. Front Microbiol **4:**21.

49. **Halverson TW, Wilton M, Poon KK, Petri B, Lewenza S.** (2015) DNA is an antimicrobial component of neutrophil extracellular traps. PLoS Pathog **11(1):**e1004593.

50. **Mulcahy H, Charron-Mazenod L, Lewenza S.** (2008) Extracellular DNA chelates cations and induces antibiotic resistance in *Pseudomonas aeruginosa* biofilms. PLoS Pathog **4(11):**e1000213.

51. **Moscoso JA, Mikkelsen H, Heeb S, Williams P, Filloux A.** (2011) The *Pseudomonas aeruginosa* sensor RetS switches type III and type VI secretion via c-di-GMP signalling. Environ Microbiol **13(12):** 3128-3138.

52. **Baraquet C, Murakami K, Parsek MR, Harwood CS.** (2012) The FleQ protein from *Pseudomonas aeruginosa* functions as both a repressor and an activator to control gene expression from the *pel* operon promoter in response to c-di-GMP. Nucleic Acids Res **40(15):**7207-7218.

53. **Merritt JH, Brothers KM, Kuchma SL, O'toole GA.** (2007) SadC reciprocally influences biofilm formation and swarming motility via modulation of exopolysaccharide production and flagellar function. J Bacteriol **189(22):**8154-64.

54. **Kong W, Chen L, Zhao J, Shen T, Surette MG, Shen L, Duan K.** (2013) Hybrid sensor kinase PA1611 in *Pseudomonas aeruginosa* regulates transitions between acute and chronic infection through direct interaction with RetS. Mol Microbiol **88(4):**784-797.

55. **Miquel S, Lagrafeuille R, Souweine B, Forestier C.** (2016) Anti-biofilm activity as a health issue. Front Microbiol **7:**592.

56. **Wu H, Moser C, Wang HZ, Hoiby N, Song ZJ.** (2015) Strategies for combating bacterial biofilm infections. Int J Oral Sci **7(1):**1-7.

57. **de la Fuente-Núñez C, Mansour SC, Wang Z, Jiang L, Breidenstein EB, Elliott M, Reffuveille F, Speert DP, Reckseidler-Zenteno SL, Shen Y, Haapasalo M, Hancock RE.** (2014) Anti-biofilm and immunomodulatory activities of peptides that inhibit biofilms formed by pathogens isolated from cystic fibrosis patients. Antibiotics (Basel) **3(4):**509-526.

58. **Bernardes EVT, Lewenza S, Reckseidler-Zenteno SL.** (2015) Current research approaches to target biofilm infections. PostDoc Journal **3(6):**36-49.

59. **Junker LM, Clardy J.** (2007) High-throughput screens for small-molecule inhibitors of *Pseudomonas aeruginosa* biofilm development. Antimicrob Agents Chemother **51(10):**3582-3590.

60. **Wenderska IB, Chong M, McNulty J, Wright GD, Burrows LL.** (2011) Palmitoyl-$_{DL}$-carnitine is a multitarget inhibitor of *Pseudomonas aeruginosa* biofilm development. Chembiochem **12(18):**2759-2766.

61. **Nguyen UT, Wenderska IB, Chong MA, Koteva K, Wright GD, Burrows LL.** (2012) Small-molecule modulators of *Listeria monocytogenes* biofilm development. Appl Environ Microbiol **78(5):**1454-1465.

62. **Kiedrowski MR, Horswill AR.** (2011) New approaches for treating staphylococcal biofilm infections. Ann N Y Acad Sci **1241:**104-121.

63. **Melo WC, Perussi JR.** (2013) Strategies to overcome biofilm resistance. In: Méndez-Vilas A, editor. Microbial pathogens and strategies for combating them: science, technology and education. Badajoz, Spain: **FORMATEX**. pp. 179-187.

64. **Lewis K.** (2001) Riddle of biofilm resistance. Antimicrob Agents Chemother **45(4):**999-1007.

65. **Pierce CG, Saville SP, Lopez-Ribot JL.** (2014) High-content phenotypic screenings to identify inhibitors of *Candida albicans* biofilm formation and filamentation. Pathog Dis **70(3):**423-431.

66. **Panmanee W, Taylor D, Shea CJ, Tang H, Nelson S, Seibel W, Papoian R, Kramer R, Hassett DJ, Lamkin TJ.** (2013) High-throughput screening for small-molecule inhibitors of *Staphylococcus epidermidis* RP62a biofilms. J Biomol Screen **18(7):**820-829.

67. **Navarro G, Cheng AT, Peach KC, Bray WM, Bernan VS, Yildiz FH, Linington RG.** (2014) Image-based 384-well high-throughput screening method for the discovery of skyllamycins A to C as biofilm inhibitors and inducers of biofilm detachment in *Pseudomonas aeruginosa*. Antimicrob Agents Chemother **58(2):**1092-1099.

68. **Zeng Z, Qian L, Cao L, Tan H, Huang Y, Xue X, Shen Y, Zhou S.** (2008) Virtual screening for novel quorum sensing inhibitors to eradicate biofilm formation of *Pseudomonas aeruginosa*. Appl Microbiol Biotechnol **79(1):**119-126.

69. **Yang L, Rybtke MT, Jakobsen TH, Hentzer M, Bjarnsholt T, Givskov M, Tolker-Nielsen T.** (2009) Computer-aided identification of recognized drugs as *Pseudomonas aeruginosa* quorum-sensing inhibitors. Antimicrob Agents Chemother **53(6):**2432-2443.

70. **Sambanthamoorthy K, Gokhale AA, Lao W, Parashar V, Neiditch MB, Semmelhack MF, Lee I, Waters CM.** (2011) Identification of a novel benzimidazole that inhibits bacterial biofilm formation in a broad-spectrum manner. Antimicrob Agents Chemother **55(9):**4369-4378.

71. **Sambanthamoorthy K, Luo C, Pattabiraman N, Feng X, Koestler B, Waters CM, Palys TJ.** (2014) Identification of small molecules inhibiting diguanylate cyclases to control bacterial biofilm development. Biofouling **30(1):**17-28.

72. **Boyd A, Chakrabarty AM.** (1994) Role of alginate lyase in cell detachment of *Pseudomonas aeruginosa*. Appl Environ Microbiol **60(7):**2355-2359.

73. **Baker P, Hill PJ, Snarr BD, Alnabelseya N, Pestrak MJ, Lee MJ, Jennings LK, Tam J, Melnyk RA, Parsek MR, Sheppard DC, Wozniak DJ, Howell PL.** (2016) Exopolysaccharide

biosynthetic glycoside hydrolases can be utilized to disrupt and prevent *Pseudomonas aeruginosa* biofilms. Sci Adv **2(5):**e1501632.

74. **Kaplan JB, Ragunath C, Ramasubbu N, Fine DH.** (2003) Detachment of *Actinobacillus actinomycetemcomitans* biofilm cells by an endogenous beta-hexosaminidase activity. J Bacteriol **185(16):**4693-4698.

75. **Itoh Y, Wang X, Hinnebusch BJ, Preston JF,3rd, Romeo T.** (2005) Depolymerization of beta-1,6-N-acetyl-D-glucosamine disrupts the integrity of diverse bacterial biofilms. J Bacteriol **187(1):**382-387.

76. **Hughes KA, Sutherland IW, Clark J, Jones MV.** (1998) Bacteriophage and associated polysaccharide depolymerases--novel tools for study of bacterial biofilms. J Appl Microbiol **85(3):**583-590.

77. **Lu TK, Collins JJ.** (2007) Dispersing biofilms with engineered enzymatic bacteriophage. Proc Natl Acad Sci U S A **104(27):**11197-11202.

78. **Koch B, Jensen LE, Nybroe O.** (2001) A panel of Tn7-based vectors for insertion of the *gfp* marker gene or for delivery of cloned DNA into gram-negative bacteria at a neutral chromosomal site. J Microbiol Methods **45(3)**:187-195.

79. **Riedel CU, Casey PG, Mulcahy H, O'Gara F, Gahan CG, Hill C.** (2007) Construction of *p16Slux*, a novel vector for improved bioluminescent labeling of gram-negative bacteria. Appl Environ Microbiol **73(21):**7092-7095.

80. **Lewenza S, Falsafi RK, Winsor G, Gooderham WJ, McPhee JB, Brinkman FS, Hancock RE.** (2005) Construction of a mini-Tn5-luxCDABE mutant library in *Pseudomonas aeruginosa* PAO1: a tool for identifying differentially regulated genes. Genome Res **15(4):**583-589.

81. **Sibley CD, Duan K, Fischer C, Parkins MD, Storey DG, Rabin HR, Surette MG.** (2008) Discerning the complexity of community interactions using a *Drosophila* model of polymicrobial infections. PLoS Pathog **4(10):**e1000184.

82. **Ma L, Jackson KD, Landry RM, Parsek MR, Wozniak DJ.** (2006) Analysis of *Pseudomonas aeruginosa* conditional *psl* variants reveals roles for the Psl polysaccharide in adhesion and maintaining biofilm structure postattachment. J Bacteriol **188(23):**8213-8221.

83. **Mathee K, Ciofu O, Sternberg C, Lindum PW, Campbell JI, Jensen P, Johnsen AH, Givskov M, Ohman DE, Molin S, Høiby N, Kharazmi A.** (1999) Mucoid conversion of *Pseudomonas aeruginosa* by hydrogen peroxide: a mechanism for virulence activation in the cystic fibrosis lung. Microbiology **145(Pt 6):**1349-1357.

84. **Choi KH, Schweizer HP.** (2006) Mini-Tn7 insertion in bacteria with single attTn7 sites: axample *Pseudomonas aeruginosa*. Nat Protoc **1(1):**153-161.

85. **Duan K, Dammel C, Stein J, Rabin H, Surette MG.** (2003) Modulation of *Pseudomonas aeruginosa* gene expression by host microflora through interspecies communication. Mol Microbiol **50(5):** 1477-1491.

86. **Pawar SV, Messina M, Rinaldo S, Cutruzzola F, Kaever V, Rampioni G, Leoni L.** (2016) Novel genetic tools to tackle c-di-GMP-dependent signalling in *Pseudomonas aeruginosa*. J Appl Microbiol **120(1):**205-217.

87. **Lewenza S, Charron-Mazenod L, Giroux L, Zamponi AD.** (2014) Feeding behaviour of *Caenorhabditis elegans* is an indicator of *Pseudomonas aeruginosa* PAO1 virulence. PeerJ **2:**e521.

88. **Zhang JH, Chung TD, Oldenburg KR.** (1999) A simple statistical parameter for use in evaluation and validation of high throughput screening assays. J Biomol Screen **4(2):**67-73.

89. **Selin C, Stietz MS, Blanchard JE, Gehrke SS, Bernard S, Hall DG, Brown ED, Cardona ST.** (2015) A pipeline for screening small molecules with growth inhibitory activity against *Burkholderia cenocepacia*. PLoS One **10(6):**e0128587.

90. **Amundsen SK, Spicer T, Karabulut AC, Londono LM, Eberhart C, Fernandez Vega V, Bannister TD, Hodder P, Smith GR.** (2012) Small-molecule inhibitors of bacterial AddAB and RecBCD helicase-nuclease DNA repair enzymes. ACS Chem Biol **7(5):**879-891.

91. **Mi L, Licina GA, Jiang S. (**2014) Nonantibiotic-based *Pseudomonas aeruginosa* biofilm inhibition with osmoprotectant analogues. ACS Sustainable Chem Eng **2:**2448-2453.

92. **Rajendran R, Borghi E, Falleni M, Perdoni F, Tosi D, Lappin DF, O'Donnell L, Greetham D, Ramage G, Nile C.** (2015) Acetylcholine protects against *Candida albicans* Infection by inhibiting biofilm formation and promoting hemocyte function in a *Galleria mellonella* Infection model. Eukaryot Cell **14(8):**834–844.

93. **Madsen JS, Lin YC, Squyres GR, Price-Whelan A, de Santiago Torio A, Song A, Cornell WC, Sørensen SJ, Xavier JB, Dietrich LE.** (2015) Facultative control of matrix production optimizes competitive fitness in *Pseudomonas aeruginosa* PA14 biofilm models. Appl Environ Microbiol **81(24):**8414-8426.

94. **O'Toole GA, Kolter R**. (1998) Flagellar and twitching motility are necessary for *Pseudomonas aeruginosa* biofilm development. Mol Microbiol **30(2):**295-304.

95. **Benoit MR, Conant CG, Ionescu-Zanetti C, Schwartz M, Matin A.** (2010) New device for high-throughput viability screening of flow biofilms. Appl Environ Microbiol **76(13):**4136-4142.

96. **Lam J, Chan R, Lam K, Costerton JW.** (1980) Production of mucoid microcolonies by *Pseudomonas aeruginosa* within infected lungs in cystic fibrosis. Infect Immun **28(2):**546-556.

97. **Rodriguez-Rojas A, Oliver A, Blazquez J.** (2012) Intrinsic and environmental mutagenesis drive diversification and persistence of *Pseudomonas aeruginosa* in chronic lung infections. J Infect Dis **205(1):**121-127.

98. **Yang L, Hengzhuang W, Wu H, Damkiaer S, Jochumsen N, Song Z, Givskov M, Høiby N, Molin S.** (2012) Polysaccharides serve as scaffold of biofilms formed by mucoid *Pseudomonas aeruginosa*. FEMS Immunol Med Microbiol **65(2):**366-376.

99. **Li X, Yan Z, Xu J.** (2003) Quantitative variation of biofilms among strains in natural populations of *Candida albicans*. Microbiology **149(Pt 2):**353-362.

100. **Yoon SS, Hennigan RF, Hilliard GM, Ochsner UA, Parvatiyar K, Kamani MC, Allen HL, DeKievit TR, Gardner PR, Schwab U, Rowe JJ, Iglewski BH, McDermott TR, Mason RP, Wozniak DJ, Hancock RE, Parsek MR, Noah TL, Boucher RC, Hassett DJ.** (2002) *Pseudomonas aeruginosa* anaerobic respiration in biofilms: Relationships to cystic fibrosis pathogenesis. Dev Cell **3(4):**593-603.

101. **Waite RD, Curtis MA.** (2009) *Pseudomonas aeruginosa* PAO1 pyocin production affects population dynamics within mixed-culture biofilms. J Bacteriol **191(4):**1349-1354.

102. **Ma L, Wang J, Wang S, Anderson EM, Lam JS, Parsek MR, Wozniak DJ.** (2012) Synthesis of multiple *Pseudomonas aeruginosa* biofilm matrix exopolysaccharides is post-transcriptionally regulated. Environ Microbiol **14(8):**1995-2005.

103. **Kirisits MJ, Margolis JJ, Purevdorj-Gage BL, Vaughan B, Chopp DL, Stoodley P, Parsek MR.** (2007) Influence of the hydrodynamic environment on quorum sensing in *Pseudomonas aeruginosa* biofilms. J Bacteriol **189(22):**8357-8360.

104. **Byrd MS, Sadovskaya I, Vinogradov E, Lu H, Sprinkle AB, Richardson SH, Ma L, Ralston B, Parsek MR, Anderson EM, Lam JS, Wozniak DJ.** (2009) Genetic and biochemical analyses of the *Pseudomonas aeruginosa* Psl exopolysaccharide reveal overlapping roles for polysaccharide synthesis enzymes in Psl and LPS production. Mol Microbiol **73(4):**622-638.

105. **Irazoqui JE, Troemel ER, Feinbaum RL, Luhachack LG, Cezairliyan BO, Ausubel FM.** (2010) Distinct pathogenesis and host responses during infection of *C. elegans* by *P. aeruginosa* and *S. aureus*. PLoS Pathog **6:**e1000982.

106. **Powell JR, Ausubel FM.** (2008) Models of *Caenorhabditis elegans* infection by bacterial and fungal pathogens. Methods Mol Biol **415:**403-427.

107. **Harrison JJ, Turner RJ, Joo DA, Stan MA, Chan CS, Allan ND, Vrionis HA, Olson ME, Ceri H.** (2008) Copper and quaternary ammonium cations exert synergistic bactericidal and antibiofilm activity against *Pseudomonas aeruginosa*. Antimicrob Agents Chemother **52(8):**2870-2881.

108. **Gueroult M, Picot D, Abi-Ghanem J, Hartmann B, Baaden M.** (2010) How cations can assist DNase I in DNA binding and hydrolysis. PLoS Comput Biol **6(11):**e1001000.

109. **Harrison JJ, Stremick CA, Turner RJ, Allan ND, Olson ME, Ceri H.** (2010) Microtiter susceptibility testing of microbes growing on peg lids: a miniaturized biofilm model for high-throughput screening. Nat Protoc **5(7):**1236-1254.

110. **Geller DE, Pitlick WH, Nardella PA, Tracewell WG, Ramsey BW.** (2002) Pharmacokinetics and bioavailability of aerosolized tobramycin in cystic fibrosis. Chest **122(1):**219-226.

111. **Ratjen F, Rietschel E, Kasel D, Schwiertz R, Starke K, Beier H, van Koningsbruggen S, Grasemann H.** (2006) Pharmacokinetics of inhaled colistin in patients with cystic fibrosis. J Antimicrob Chemother **57(2):**306-311.

112. **Irazoqui JE, Urbach JM, Ausubel FM.** (2010) Evolution of host innate defence: insights from *Caenorhabditis elegans* and primitive invertebrates. Nat Rev Immunol **10(1)**:47-58.

113. **Tan MW, Mahajan-Miklos S, Ausubel FM.** (1999) Killing of *Caenorhabditis elegans* by *Pseudomonas aeruginosa* used to model mammalian bacterial pathogenesis. Proc Natl Acad Sci U S A **96(2)**:715-720.

114. **Skurnik D, Roux D, Aschard H, Cattoir V, Yoder-Himes D, Lory S, Pier GB.** (2013) A comprehensive analysis of *in vitro* and *in vivo* genetic fitness of *Pseudomonas aeruginosa* using high-throughput sequencing of transposon libraries. PLoS Pathog **9(9):**e1003582.

115. **Mah TF, O'Toole GA.** (2001) Mechanisms of biofilm resistance to antimicrobial agents. Trends Microbiol **9(1):**34-39.

116. **Rasko DA, Sperandio V.** (2010) Anti-virulence strategies to combat bacteria-mediated disease. Nat Rev Drug Discov **9(2):**117-128.

117. **Bender KO, Garland M, Ferreyra JA, Hryckowian AJ, Child MA, Puri AW, Solow-Cordero DE, Higginbottom SK, Segal E, Banaei N, Shen A, Sonnenburg JL, Bogyo M.** (2015) A small-molecule antivirulence agent for treating *Clostridium difficile* infection. Sci Transl Med **7(306):**306ra148.

118. **Hung DT, Shakhnovich EA, Pierson E, Mekalanos JJ.** (2005) Small-molecule inhibitor of *Vibrio cholerae* virulence and intestinal colonization. Science **310(5748):**670-674.

119. **Baron C.** (2010) Antivirulence drugs to target bacterial secretion systems. Curr Opin Microbiol **13(1):**100-105.

120. **Mendez-Cuesta CA, Herrera-Rueda MA, Hidalgo-Figueroa S, Tlahuext H, Moo-Puc R, Chale-Dzul JB, Chan-Bacab M, Ortega-Morales BO, Hernández-Núñez E, Méndez-Lucio O, Medina-Franco JL, Navarrete-Vazquez G.** (2016) Synthesis, screening and in silico simulations of anti-parasitic propamidine/benzimidazole derivatives. Med Chem [Epub ahead of print].

121. **Vasantha K, Basavarajaswamy G, Vaishali Rai M, Boja P, Pai VR, Shruthi N, Bhat M.** (2015) Rapid 'one-pot' synthesis of a novel benzimidazole-5-carboxylate and its hydrazone derivatives as potential anti-inflammatory and antimicrobial agents. Bioorg Med Chem Lett **25(7):**1420-1426.

122. **Batubara I, Mitsunaga T, Ohashi HJ.** (2010) Brazilin from *Caesalpinia sappan* wood as an antiacne agent. J Wood Sci. **56:**77-81.

123. **Sanada Y, Senba H, Mochizuki R, Arakaki H, Gotoh T, Fukumoto S, Nagahata H.** (2009) Evaluation of marked rise in fecal egg output after bithionol administration to horse and its application as a diagnostic marker for equine *Anoplocephala perfoliata* infection. J Vet Med Sci **71(5):**617-620.

124. **Mechanism matters.** (2010) Nature Med **16:**347

125. **Wang Z, Gerstein M, Snyder M.** (2009) RNA-seq: a revolutionary tool for transcriptomics. Nat Rev Genet **10(1):**57-63.

126. **Chugani S, Kim BS, Phattarasukol S, Brittnacher MJ, Choi SH, Harwood CS, Greenberg EP.** (2012) Strain-dependent diversity in the *Pseudomonas aeruginosa* quorum-sensing regulon. Proc Natl Acad Sci U S A **109(41):**E2823-31.

127. **Giannoukos G, Ciulla DM, Huang K, Haas BJ, Izard J, Levin JZ, Livny J, Earl AM, Gevers D, Ward DV, Nusbaum C, Birren BW, Gnirke A.** (2012) Efficient and robust RNA-seq process for cultured bacteria and complex community transcriptomes. Genome Biol **13(3):**R23

128. **Seyednasrollah F, Laiho A, Elo LL.** (2015) Comparison of software packages for detecting differential expression in RNA-seq studies. Brief Bioinform **16(1):**59-70.

129. **Tarazona S, Garcia-Alcalde F, Dopazo J, Ferrer A, Conesa A.** (2011) Differential expression in RNA-seq: a matter of depth. Genome Res **21(12):**2213-2223.

130. **Whiteley M, Lee KM, Greenberg EP.** (1999) Identification of genes controlled by quorum sensing in *Pseudomonas aeruginosa*. Proc Natl Acad Sci U S A **96(24):**13904-13909.

131. **Rybtke MT, Borlee BR, Murakami K, Irie Y, Hentzer M, Nielsen TE, Givskov M, Parsek MR, Tolker-Nielsen T.** (2012) Fluorescence-based reporter for gauging cyclic di-GMP levels in *Pseudomonas aeruginosa*. Appl Environ Microbiol **78(15):**5060-5069.

132. **Matsukawa M, Greenberg EP.** (2004) Putative exopolysaccharide synthesis genes influence *Pseudomonas aeruginosa* biofilm development. J Bacteriol **186(14):**4449-4456.

133. **Romero D, Traxler MF, Lopez D, Kolter R.** (2011) Antibiotics as signal molecules. Chem Rev **111(9):**5492-5505.

134. **Nakayama K, Takashima K, Ishihara H, Shinomiya T, Kageyama M, Ohnishi M, Murata T, Mori H, Hayashi T.** (2000) The R-type pyocin of *Pseudomonas aeruginosa* is related to P2 phage, and the F-type is related to lambda phage. Mol Microbiol **38(2):**213-231.

135. **Ling H, Saeidi N, Rasouliha BH, Chang MW.** (2010) A predicted S-type pyocin shows a bactericidal activity against clinical *Pseudomonas aeruginosa* isolates through membrane damage. FEBS Lett **584(15):**3354-3358.

136. **Turnbull L, Toyofuku M, Hynen AL, Kurosawa M, Pessi G, Petty NK, Osvath SR, Cárcamo-Oyarce G, Gloag ES, Shimoni R, Omasits U, Ito S, Yap X, Monahan LG, Cavaliere R, Ahrens CH, Charles IG, Nomura N, Eberl L, Whitchurch CB.** (2016) Explosive cell lysis as a mechanism for the biogenesis of bacterial membrane vesicles and biofilms. Nat Commun **7:**11220.

137. **Nanda AM, Thormann K, Frunzke J.** (2015) Impact of spontaneous prophage induction on the fitness of bacterial populations and host-microbe interactions. J Bacteriol **197(3):**410-419.

138. **Webb JS, Thompson LS, James S, Charlton T, Tolker-Nielsen T, Koch B, Givskov M, Kjelleberg S.** (2003) Cell death in *Pseudomonas aeruginosa* biofilm development. J Bacteriol **185(15):** 4585-4592.

139. **Yamano Y, Nishikawa T, Komatsu Y.** (1993) Cloning and nucleotide sequence of anaerobically induced porin protein E1 (OprE) of *Pseudomonas aeruginosa* PAO1. Mol Microbiol **8(5):**993-1004.

140. **Rebiere-Huet J, Guerillon J, Pimenta AL, Di Martino P, Orange N, Hulen C.** (2002) Porins of *Pseudomonas fluorescens* MFO as fibronectin-binding proteins. FEMS Microbiol Lett **215(1):**121-126.

141. **Tamber S, Hancock RE.** (2006) Involvement of two related porins, OprD and OpdP, in the uptake of arginine by *Pseudomonas aeruginosa*. FEMS Microbiol Lett **260(1):**23-29.

142. **Skurnik D, Roux D, Cattoir V, Danilchanka O, Lu X, Yoder-Himes DR, Han K, Guillard T, Jiang D, Gaultier C, Guerin F, Aschard H, Leclercq R, Mekalanos JJ, Lory S, Pier GB.** (2013) Enhanced *in vivo* fitness of carbapenem-resistant oprD mutants of *Pseudomonas aeruginosa* revealed through high-throughput sequencing. Proc Natl Acad Sci U S A **110(51):**20747-20752.

143. **Shah N, Klaponski N, Selin C, Rudney R, Fernando WG, Belmonte MF, de Kievit TR.** (2016) PtrA is functionally intertwined with GacS in regulating the biocontrol activity of *Pseudomonas chlororaphis* PA23. Front Microbiol **7:**1512.

144. **Ha UH, Kim J, Badrane H, Jia J, Baker HV, Wu D, Jin S.** (2004) An *in vivo* inducible gene of *Pseudomonas aeruginosa* encodes an anti-ExsA to suppress the type III secretion system. Mol Microbiol 54(2): 307-320.

145. **Kindrachuk KN, Fernandez L, Bains M, Hancock RE.** (2011) Involvement of an ATP-dependent protease, PA0779/AsrA, in inducing heat shock in response to tobramycin in *Pseudomonas aeruginosa*. Antimicrob Agents Chemother **55(5):**1874-1882.

146. **Chan KG, Priya K, Chang CY, Abdul Rahman AY, Tee KK, Yin WF.** (2016) Transcriptome analysis of *Pseudomonas aeruginosa* PAO1 grown at both body and elevated temperatures. **PeerJ 4:**e2223.

147. **Barraud N, Hassett DJ, Hwang SH, Rice SA, Kjelleberg S, Webb JS.** (2006) Involvement of nitric oxide in biofilm dispersal of *Pseudomonas aeruginosa*. J Bacteriol **188(21):**7344-7353.

148. **Yeung AT, Torfs EC, Jamshidi F, Bains M, Wiegand I, Hancock RE, Overhage J.** (2009) Swarming of *Pseudomonas aeruginosa* is controlled by a broad spectrum of transcriptional regulators, including MetR. J Bacteriol **191(18):**5592-5602.

149. **Diggle SP, Winzer K, Lazdunski A, Williams P, Camara M.** (2002) Advancing the quorum in *Pseudomonas aeruginosa*: MvaT and the regulation of N-acylhomoserine lactone production and virulence gene expression. J Bacteriol **184(10):**2576-2586.

150. **Sakuragi Y, Kolter R.** (2007) Quorum-sensing regulation of the biofilm matrix genes (*pel*) of *Pseudomonas aeruginosa*. J Bacteriol **189(14):** 5383-5386.

APPENDIX A: SUPPLEMENTARY DATA

The supplementary data, including additional results and some control experiments, discussed throughout the text are shown.

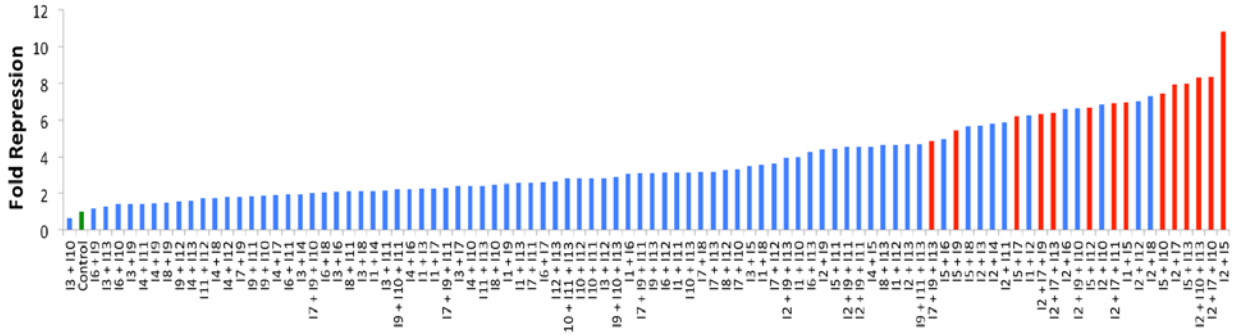

Figure S1: Antibiofilm compounds show additive properties and promote *pelB::lux* repression in combination.

pelB::lux expression is majorly reduced upon treatment with antibiofilm compound mixtures. Average expression from *pelB::lux* reporter was normalized to *16Slux* and the sorted NET fold repression relative to control is shown. Gene reporters (~1x10^7 CFU/ml) were incubated in duplicate in BM2 media containing 20 μM Mg^{2+} with ~10 μM of the compound mixtures in 384-well microplate. The control expression of the gene reporter grown in untreated BM2 media is highlighted in green. We tested all possible 78 combinations of 2 compounds and additionally 17 random 3-compound mixtures. The 14 combinations selected to continue biofilm formation studies in CV assays are highlighted in red, n=2.

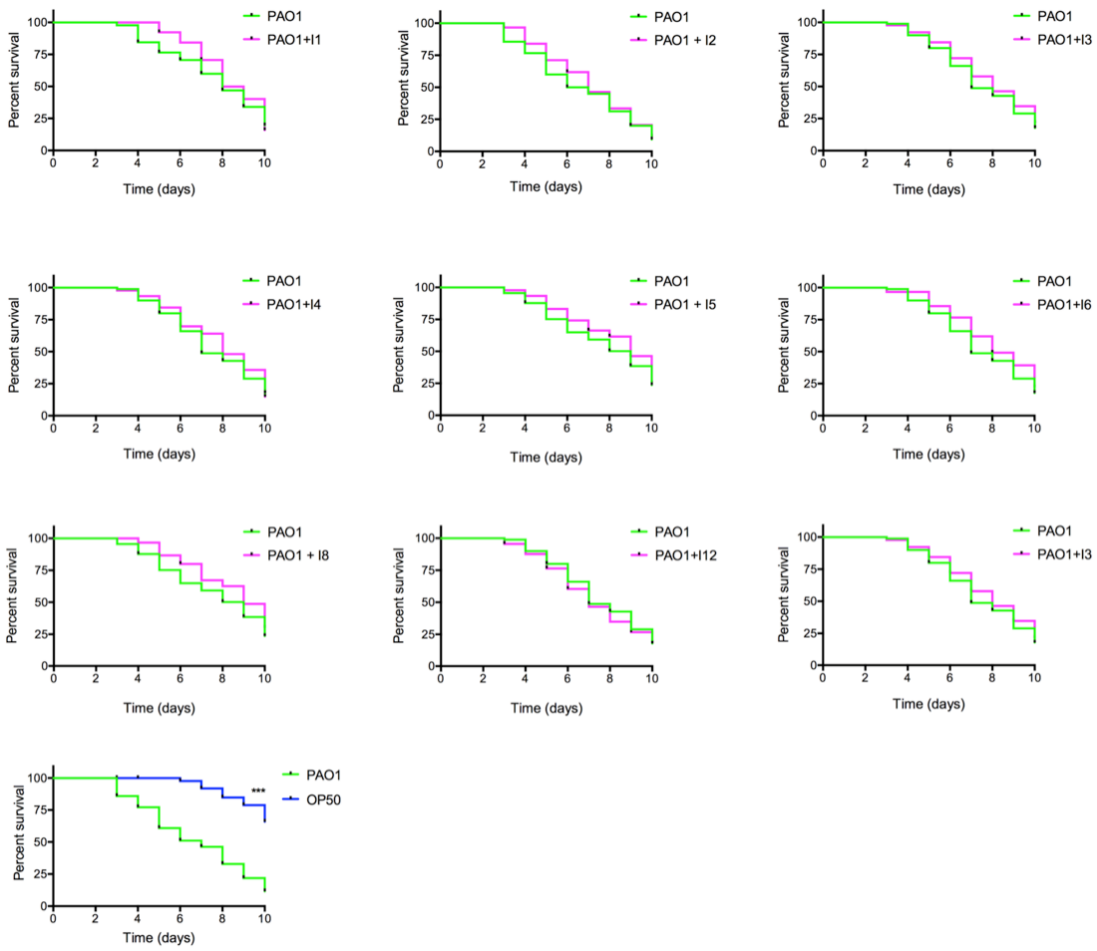

Figure S2: Antibiofilm compounds with no antivirulence activity against PAO1 in the *C. elegans* slow killing virulence assay.

Nine out of the 13 tested small molecules did not promote a significant effect in nematode survival, the other 4 that did are show in Figure 4.2. *E. coli* OP50 was used as a positive control of reduced virulence *in vivo.* Nematodes were fed antibiofilm compound-treated PAO1 and monitored for increased survival. Kaplan-Meyer curves with % survival represent three independent experiments (n=30) where the total number of worms equals 90. Statistical significance was determined with Log-rank test (Graph Pad Prism) and significant difference in nematode survival when fed the non-pathogenic food source is indicated: *** ($p<0.001$).

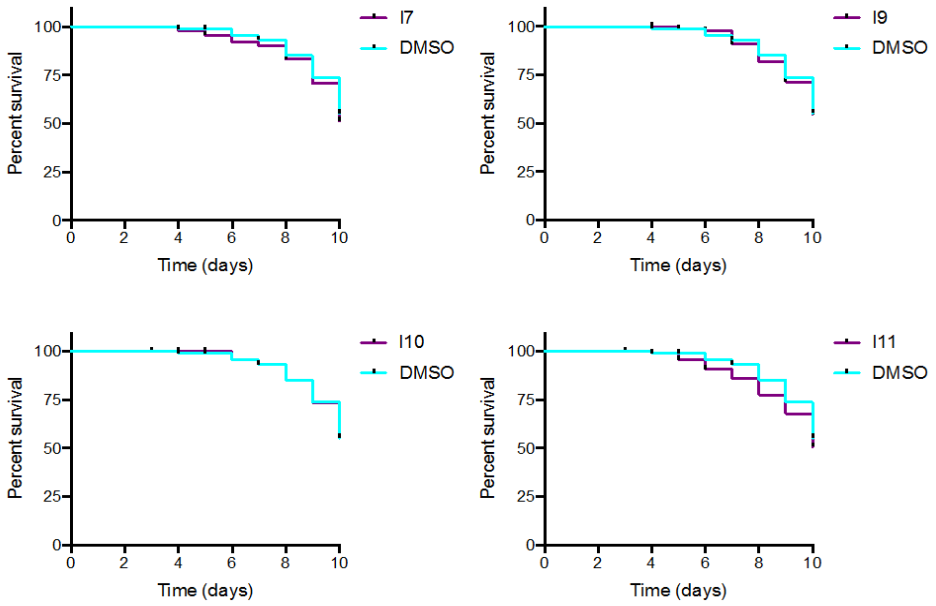

Figure S3: Antivirulence small molecules do not promote nematode survival in absence of infection.

Compound-treated *E. coli* OP50 did not promote any positive or negative effect in nematode survival. We limited our assay to the 4 small molecules that showed antivirulence *in vivo* and demonstrated the effects in viability are exclusive to PAO1 (Fig 4.2). Slow killing assays were performed as previously described, with compounds added to SK media, at a final concentration of 10 μM. Kaplan-Meyer curves with % survival represent three independent experiments (n=30) where the total number of worms equals 90.

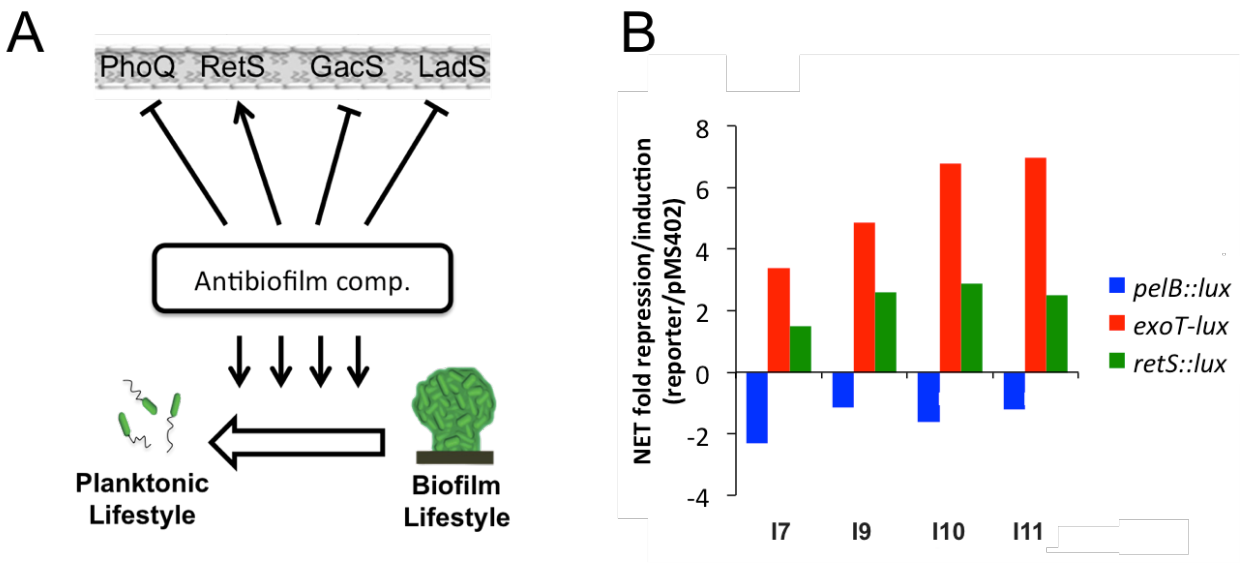

Figure S4: Preliminary investigation of antibiofilm mechanism of action suggests Gac/Rsm pathway as a possible target.

(A) Initial hypothesis of antibiofilm mechanism of action. Pel/Psl repression could be due to targeting of the PhoPQ/RetS/Gac/Rsm regulatory pathway, which coordinates the switch from a planktonic to the biofilm lifestyle (for more details see Fig 1.2). The antibiofilm properties could be instigated by inhibiting PhoPQ, GacAS or LadS, or even activating/inducing RetS, which all could potentially promote the observed phenotypes. **(B)** The small molecules increase the expression of the T3SS effector *exoT* and the orphan sensor *retS* gene reporters while simultaneously repressing *pelB.* Gene expression from *pelB::lux*, *exoT-lux* and *retS::lux* were normalized to *pMS402*. Gene expression assays were performed as previously described, in 96-well microplates. Bars represent the average net fold induction (positive) or repression (negative) from triplicate samples of the target genes relative to the untreated condition, n=2.

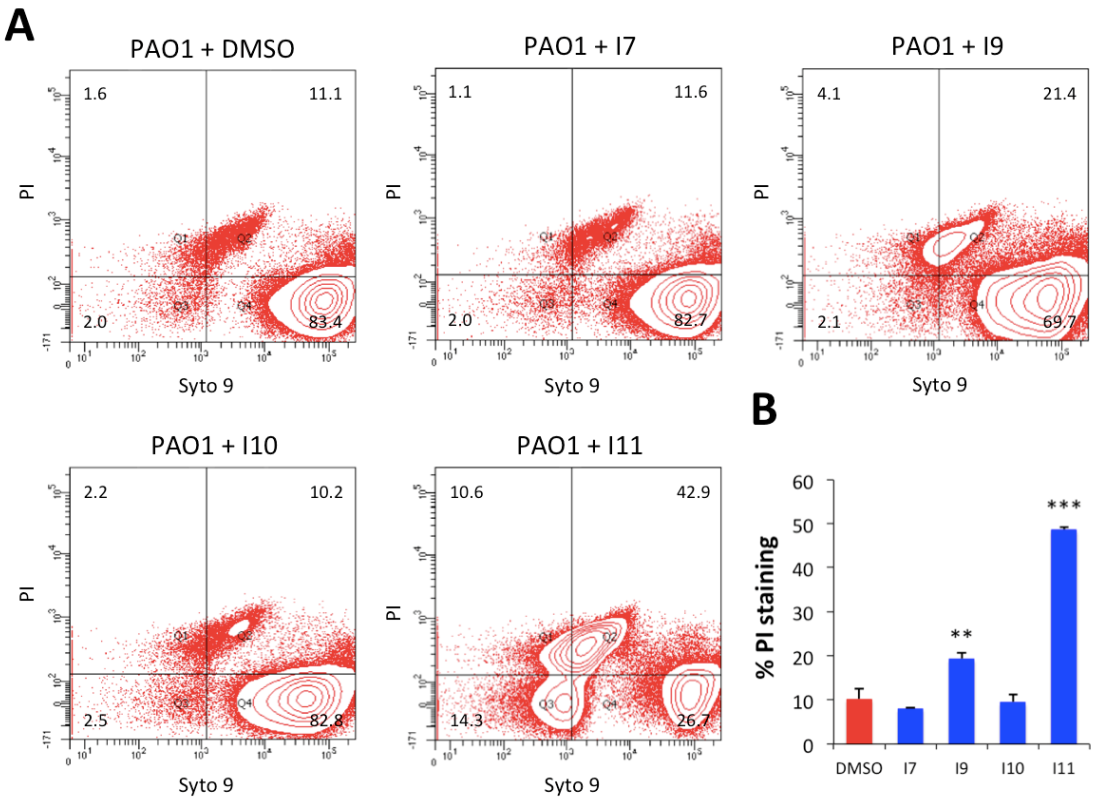

Figure S5: Antibiofilm compound-treated cells show increased membrane damage as determined by altered PI-staining.

(A) Flow cytometry of compound-treated PAO1 using Syto9-PI dual staining was used to determine membrane-damaged bacteria. Numbers in corners represent the % of events that fall into each quadrant gate. Cells were grown in 2 ml cultures to mid-log phase in the presence of 10 µM of the select compounds, diluted in 1x PBS, immediately stained with Syto9/PI and analysed in BD LSRII Flow Cytometer. Approximately 10^5 events were determined for each replicate. **(B)** Quantification of membrane-disturbed, PI-stained PAO1. % of events from the PI-channel are the average of three replicates and the standard deviation, n=3. Statistical significance between populations was determined by paired two-tailed Student's t-test and significant increase in PI staining from control (1% DMSO) are indicated: ** ($p<0.01$) and *** ($p<0.001$).

APPENDIX B: RNA-SEQ WORKFLOW

The molecular workflow for RNA-seq, including the protocols for RNA purification, DNA digestion, rRNA depletion and cDNA synthesis and library preparations are described.

Protocol for total RNA isolation and purification – adapted from Chugani *et al.* [126]

1. Mobilize RNA by transferring 2 volumes of RNAprotect bacteria reagent (QIAGEN) to the tubes containing 1 volume of bacterial subcultures to be harvested;
2. Transfer the whole content of the tube (RNAprotect + subculture) to a clean 15 ml falcon tube, and mix immediately, by vortexing;
3. Incubate the mobilized cultures for 15 min at room temperature, and spin samples for 10 min at 5,000 g;
4. Decant supernatant carefully and let tubes dry;
5. Store pellets at -80^{o}C, if not proceeding with 'step 6' immediately;
6. Resuspend RNA-protected cell pellets in 1 ml QIAzol and pipet into a 2 ml screw-cap tube containing 0.1 mm glass beads (keep tubes on ice);
7. Beat in beat-beater at maximum rpm for 1 min and chill the tube on ice for 1 min;
8. Repeat 'step 7' two more times, shaking tubes vigorously before each pulse;
9. Place the tubes at room temperature for 5 min;
10. Add 200 µl of chloroform to the sample and shake the tube vigorously for 15 seconds,
11. Place the tubes at room temperature for 3 min;
12. Centrifuge for 15 min at 12,000 g at 4^{o}C;

13. Carefully transfer exactly 500 µl of the aqueous colorless upper phase to a new 1.5 ml tube (be very careful to not disturb the pink organic layer);
14. Centrifuge again for 15 min at 12,000 g at 4^{o}C;
15. Carefully transfer exactly the top 450 µl upper phase to a new 1.5 ml tube,
16. Add 675 µl (1.5 volumes) of 100% ethanol and mix thoroughly by pipetting;
17. Apply 700 µl of the sample to the RNeasy Mini column, centrifuge for 1 min at 14,000 g at room temperature, and discard the flow-through;
18. Repeat ‘step 17’ using the remaining of the sample;
19. Add 700 µl Buffer RWT to the RNeasy Mini column, centrifuge for 1 min at 14,000 g, and discard the flow-through;
20. Transfer the RNeasy mini column into new 2 ml collection tube (optional);
21. Add 500 µl Buffer RPE to the RNeasy Mini column, centrifuge for 1 min at 14,000 g, and discard the flow-through;
22. Add another 500 µl Buffer RPE to the RNeasy Mini column and centrifuge for 2 min at 14,000 g;
23. Transfer the RNeasy Mini column into new 1.5 ml tube and centrifuge for 3 min at 14,000 g;
24. Transfer the RNeasy Mini column into new 1.5 ml tube and leave it open for 2.5 min to remove any residual ethanol;
25. Pipet 30 µl RNase-free water (Invitrogen) directly to the column silica-gel membrane, let the column stand for 1 min, and centrifuge for 1 min at 14,000 g to elute the RNA;
26. Pipet another 30 µl RNase-free water onto the silica-gel membrane, let the column stand for 1 min, and centrifuge for 1 min at 14,000 g,

27. Determine the RNA concentration in nanodrop, store samples at -80ºC if not proceeding with DNA digestion and final RNA purification protocol immediately.

Protocol for DNA digestion and final RNA purification – adapted from Chugani *et al.* [126]

1. Prepare the digest mix, by mixing in 1.5 ml tube the following items:

Item	Volume (µl)
7.5 µg RNA	Calculated by each sample RNA concentration
10x TURBO DNase Buffer (Ambion)	10
TURBO DNase 92 U/µl (Ambion)	2
RNase-free water	Up to 100 µl

2. Incubate the tube in 37ºC water bath for 30 min and short spin (for 5 s);
3. Add another 2 µl of TURBO DNase 92 U/µl, mix gently by pipetting, incubate the tube in 37ºC water bath for another 30 min, and short spin;
4. Pipet 350 µl of freshly prepared Buffer RTL plus β-mercaptoethanol (β-ME) into DNase treated tubes and mix thoroughly by pipetting;

P.S.: Prepare, right before performing the protocol, 100 times dilution of β-ME in Buffer RTL and store at room temperature (25ºC) until needed. Solution needs to be fresh to ensure complete inactivation of RNases during the RNA isolation protocol.

5. Add 675 µl of 100% ethanol to the sample and mix thoroughly by pipetting;
6. Apply 700 µl of the sample to the RNeasy MinElute column, centrifuge for 1 min at 14,000 g (or higher), and discard the flow-through;
7. Repeat ‘step 6’ using the remaining of the sample;

8. Transfer the RNeasy MinElute column to a new 2 ml collection tube;
9. Add 500 µl of Buffer RPE to the RNeasy MinElute column, centrifuge for 1 min at 14,000 g, and discard the flow-through;
10. Add 500 µl of 80% ethanol to the RNeasy MinElute column and centrifuge for 1 min at 14,000 g;
11. Transfer the RNeasy MinElute column to a new 2 ml collection tube, and centrifuge for 6 min at 14,000 g;
12. Transfer the RNeasy MinElute column into a new 1.5 ml RNase-free tube and open the lid of the column for 2.5 min to remove any residual ethanol;
13. Pipet 15 µl RNase-free water (Invitrogen) directly onto the MinElute column membrane, let the column stand for 1 min, and centrifuge for 1 min at 14,000 g,
14. Determine the RNA concentration in nanodrop, store samples at -80^{o}C if not proceeding with rRNA depletion protocol immediately.

Protocol for Ribo-Zero kit in the ScriptSeq Complete kit

rRNA depletion was performed following Epicentre/Illumina's specifications. Initial preparation of magnetic beads (protocol for "Batch Washing Procedure"), treatment of the total RNA sample with rRNA Removal Solution and removal of rRNA were performed as described within the ScriptSeq Complete Kit. Lastly, the purification of rRNA-depleted samples was performed with the modified RNeasy MinElute procedure, using the RNeasy MinElute Cleanup kit, as described.

P.S.: For more details and complete step-by-step on the rRNA depletion protocol, please refer to Section 1 – The RiboZero rRNA removal procedure – in the ScriptSeq Complete Kit Guide. Available online at: http://support.illumina.com/content/dam/illumina-support/documents/documentation/chemistry_documentation/samplepreps_truseq/scriptseq-complete/scriptseq-complete-kit-bacteria-library-prep-guide.pdf.

Protocol for cDNA synthesis and library preparation using the ScriptSeq kit

The remaining of the ScriptSeq protocol was performed following Epicentre/Illumina's specifications. Fragmentation of the purified RNA, primer annealing, cDNA synthesis, barcoding and amplifications were performed according to the ScriptSeq Complete Kit guidelines. Final RNA-seq library purification was obtained with the Mag-Bind RXNPure Plus magnetic bead system (protocol for "AMPure XP Purification").

P.S.: For more details and complete step-by-step on the RNA-seq sample preparation protocol, please refer to Section 2 – The ScriptSeq v2 RNA-Seq Library Preparation Procedure – in the ScriptSeq Complete Kit Guide. Available online at: http://support.illumina.com/content/dam/illumina-support/documents/documentation/chemistry_documentation/samplepreps_truseq/scriptseq-complete/scriptseq-complete-kit-bacteria-library-prep-guide.pdf.

Quality assessment and quantification of RNA/DNA samples

Additional to the quantification in Nanodrop, after each step of RNA preparation, starting after DNase digestion, samples quality and size distribution of fragments was evaluated in the Agilent 2100 Bioanalyzer, using the Agilent RNA 6000 Pico kit.

cDNA concentration within the final RNA-seq libraries was determined using the extremely precise fluorescent-based Qubit quantification assay, following the guidelines in the Qubit dsDNA HS Assay kit protocol. Lastly, quality assessment of cDNA libraries was determined in Agilent 2100 Bioanalyzer, using the High Sensitivity DNA kit.

P.S.[1]: For more details and complete step-by-step on the RNA 6000 Pico protocol, please refer to the RNA 6000 Pico Kit Guide. Available online at: http://www.agilent.com/cs/library/usermanuals/Public/G2938-90049_RNA6000Pico_QSG.pdf.

P.S.[2]: For more details and complete step-by-step on the Qubit quantification protocol, please refer to the Qubit dsDNA HS Assay Kit Guide. Available online at: https://tools.thermofisher.com/content/sfs/manuals/Qubit_dsDNA_HS_Assay_UG.pdf.

P.S.[3]: For more details and complete step-by-step on the High Sensitivity DNA protocol, please refer to the Agilent High Sensitivity DNA Kit Guide. Available online at: http://www.nature.com/protocolexchange/system/uploads/3549/original/Manual_G2938-90322_HighSensitivityDNA_QSG.pdf?1423511847.

APPENDIX C: XPRESSION

The first part of the bioinformatics workflow, consisting in the alignment of the sequencing raw reads obtained from the HiSeq system to the PAO1 reference genome, is described. The expression software additionally filters low quality reads, ensuring high quality of reads to further run differential expression in R studio.

Protocol for reads alignment to the PAO1 annotated reference genome (J Harrison, personal communication)

1. Save files generated from MiSeq run:
    A. Select files from “MiSeq Output” folder;
    B. Copy (.gz) files on a new folder (“Erik-RNA-seq”) on the external hard drive;
    C. GNU zip (.gz) file already separated by barcodes. There is no need of a barcode splitter step.
2. Calculate expression profile on Xpression software:
    D. Upload GenBank file containing PAO1 reference genome (with annotation);
    E. Select sequencing FASTQ file for analysis parameter;
    F. Select options:
        a. Select strand specific library method = ✔;
        b. Select reversing orientation = ✔;
        c. Read start position = 1 (barcodes already trimmed);

d. Imput format = FastQ;

e. Allow mismatches = 2 (base level of errors);

f. CPU processes = 6 (Dr. Harrison's computer has 8);

g. Select output location on same folder.

3. After acquiring the annotated files, run differential expression analysis with DESeq2 and EdgeR (Appendices C and D, respectively).

P.S.: The PAO1 reference genome can be downloaded from the *Pseudomonas Genome Database.* Available online at: http://www.pseudomonas.com/strain/download.

APPENDIX D: DESEQ2 SCRIPT

The following part of the bioinformatics workflow, consisting of the differential expression in R Studio using the DESeq platform, is described.

Running differential expression analysis with DESeq2 (J Harrison, personal communication)

1. Create a data file in Microsoft Excel with the following format:
   A. Use raw count data to populate each cell (DO NOT use RPKM measurements);
   B. No header in first column;
   C. First row of each column has the sample name;
   D. Genomic regions are not named but are kept in order;
   E. Must have same number of columns in every row (other than first row);
   F. Save from Excel in comma separated value (.CSV) format; use TablePad to convert to tab separated table (done through options; do not separate text with “);
   G. NOTE: Default is that row.names is first column (no need to specify when data is imported into RStudio) – Rstudio will automatically number these when imported.

2. Adapt and run the following script in RStudio (NOTE: Change file names and conditions in script below accordingly):

#Text following a hash tag is not read by RStudio and is used to provide comments to the user
source("http://www.bioconductor.org/biocLite.R")

```
biocLite("DESeq")

biocLite("DESeq2")

CountTable = read.csv ("file name.csv", header=TRUE)

CountTable = read.table ("file name.csv", header=TRUE, sep="\t")

head(CountTable)

#If the data import has worked correctly this will display the first 6 rows of data in the data table


tail(CountTable)

#If the data import has worked correctly this will display the last 6 rows of data in the data table


expt_design <- data.frame(row.names = colnames(CountTable), condition =

c("C","C","C","T","T","T"))

expt_design

conditions = expt_design$condition

conditions

library("DESeq")

library("DESeq2")

data <- newCountDataSet(CountTable, conditions)

head(counts(data))

data <- estimateSizeFactors(data)

sizeFactors(data)

data <- estimateDispersions(data)
```

results = nbinomTest(data,"C","T")

write.table(results, file="file name.txt", sep="\t", row.names=rownames(results), col.names=colnames(results), quote=F)

P.S.: The previous instructions and script are adapted from a Tutorial for DEseq available at the following link: http://cgrlucb.wikispaces.com/Spring+2012+DESeq+Tutorial

P.S.: For running the described protocol, download and install the following platforms:

Download and install R: http://www.r-project.org/

Download and install RStudio: http://www.rstudio.com/products/rstudio/download/

Download and install TablePad: http://sourceforge.net/projects/tablepad/

APPENDIX E: EDGER SCRIPT

The subsequent part of the bioinformatics workflow, consisting of the differential expression in R Studio using the EdgeR platform, is described.

Running differential expression analysis with EdgeR (A Ostaszewski, personal communication)

1. Create a data file in Microsoft Excel with the following format:
    A. Use raw count data to populate each cell (DO NOT use RPKM measurements);
    B. Genomic regions are not named but are kept in order;
    C. Must have same number of columns in every row;
    D. Save from Excel in .txt format (Tab delimited text).

2. Adapt and run the following script in RStudio (NOTE: Change file names and conditions in script below accordingly):

```
#Text following a hash tag is not read and is used to provide comments to the user
source("http://www.bioconductor.org/biocLite.R")

biocLite("edgeR")
library("edgeR")
CountTable = read.table (file.choose(file name.csv), header=TRUE, sep="\t")
head(CountTable)
```

```
#If the data import has worked correctly this will display the first 6 rows of data in the data table

tail(CountTable)
#If the data import has worked correctly this will display the last 6 rows of data in the data table

expt_design <- data.frame(row.names = colnames(CountTable), condition = c("C","C","C","T","T","T"))
expt_design
conditions = expt_design$condition
conditions
d<-DGEList(counts=CountTable,group=factor(conditions))
#Filtering data, getting rid of genes that did not occur frequently enough (require at least 100 counts/million to keep)

dim(d)
d.full<-d
head(d$counts)
head(cpm(d))
apply(d$counts, 2, sum) #total gene counts per sample
keep<-rowSums(cpm(d)>100) >=2
d<-d[keep,]
dim(d)
d$samples$lib.size<-colSums(d$counts)
```

```
d$samples

#normalizing data


<-calcNormFactors(d) #normalizes for RNA composition

d

d$samples

d$samples$lib.size*d$samples$norm.factors

d<-estimateCommonDisp(d)

names(d)

d$common.dispersion

d<-estimateTagwiseDisp(d)

names(d)

d<-estimateTagwiseDisp(d, prior.n=10)

de.cmn<-exactTest(d, pair=c("C", "T"))

names(de.cmn)

dd<-topTags(de.cmn, n=2000, sort.by="p.value")

write.csv(dd, "file name.csv")
```

P.S.: For running the described protocol, download and install the following platforms:

Download and install R: http://www.r-project.org/

Download and install RStudio: http://www.rstudio.com/products/rstudio/download/

APPENDIX F: DIFFERENTIALLY EXPRESSED GENES

Tables containing the list of differentially expressed genes in *P. aeruginosa* PAO1 *ΔpelFΔpslD* upon treatment with 10 μM of the four selected antibiofilm/antivirulence small molecules are shown.

Table S1: Genes differentially expressed in PAO1 Δ*pelFpslD* upon I7 treatment

Locus	Gene	Type	Description	Fold-change	p_{val}	p_{adj}
PA0291	oprE	intergenic	Anaerobically-induced outer membrane porin OprE	5.73	0.00001	0.00235
PA0291	oprE	sense	Anaerobically-induced outer membrane porin OprE	8.37	0.00002	0.00520
PA0622		sense	Bacteriophage protein	2.26	0.00030	0.02499
PA0623		sense	Bacteriophage protein	2.48	0.00012	0.01453
PA0625		sense	Hypothetical protein	2.16	0.00104	0.07982
PA0636		sense	Hypothetical protein	2.09	0.00028	0.02499
PA0641		sense	Bacteriophage protein	2.13	0.00022	0.02260
PA0958	oprD	sense	Porin	10.42	>0.00001	0.00235
PA0959		intergenic	Hypothetical protein	7.57	0.00007	0.01014
PA0985	pyoS5	sense	Pyocin S5	3.98	0.00013	0.01453
PA2760	oprQ	sense	Outer membrane protein OprQ	4.72	0.00004	0.00714
PA3690		intergenic	Metal-transporting P-type Probable metal-transporting P-type ATPase	-6.06	0.00002	0.00520
PA0263.1		sense	tRNA-Arg	2.53	0.01065	0.42602
PA0612	ptrB	intergenic	Repressor PtrB	2.17	0.00387	0.22253
PA0620		sense	Bacteriophage protein	2.06	0.00160	0.10519
PA0621		sense	Hypothetical protein	1.92	0.00904	0.39587
PA0625		sense	Hypothetical protein	2.16	0.00104	0.07982

PA0633		sense	Hypothetical protein	1.89	0.00682	0.33117
PA0643		intergenic	Hypothetical protein	2.25	0.00160	0.10519
PA0643		sense	Hypothetical protein	2.02	0.03608	0.91473
PA0646		sense	Hypothetical protein	1.93	0.00684	0.33117
PA0647		sense	Hypothetical protein	1.70	0.01702	0.60210
PA0887	acsA	sense	Acetyl-CoA synthetase	-1.83	0.02026	0.62118
PA1838	cysI	sense	Sulfite reductase	1.70	0.02456	0.68474
PA2523	czcR	intergenic	Two-component response regulator CzcR	-5.12	0.01568	0.58704
PA2664	fhp	sense	Nitric oxide dioxygenase	-4.50	0.01931	0.62118
PA2760	oprQ	intergenic	Outer membrane protein OprQ	3.92	0.00180	0.11012
PA2808	ptrA	intergenic	Repressor PtrA	-6.02	0.03019	0.81691
PA2808	ptrA	sense	Repressor PtrA	-5.98	0.04146	0.95366
PA3038	opdQ	sense	Probable porin	-1.65	0.02355	0.67711
PA3161	himD	intergenic	Integration host factor subunit beta	-1.65	0.03748	0.91473
PA3531	bfrB	sense	Bacterioferritin	-2.38	0.00967	0.40434
PA3981	ybeZ	intergenic	Hypothetical protein	-1.73	0.01991	0.62118
PA4264	rpsJ	intergenic	30S ribosomal protein S10	1.74	0.03778	0.91473
PA4276.1		sense	tRNA-Trp	-2.38	0.00431	0.23331
PA4378	inaA	sense	InaA protein	-1.96	0.02246	0.66645
PA4422	yraL	intergenic	Hypothetical protein	2.21	0.04376	0.98201
PA4443	cysD	sense	Sulfate adenylyltransferase subunit 2	1.87	0.00836	0.38437
PA4541.2		sense	tRNA-Pro	2.07	0.03200	0.84106
PA4673.1		sense	tRNA-Met	2.27	0.01595	0.58704
PA5062		sense	Hypothetical protein	1.99	0.01931	0.62118
PA5446		intergenic	Hypothetical protein	-1.69	0.04088	0.95366

*Differential expression was considered significant if $p < 0.05$. Highlighted in gray the genes with differentially expression counts showing $p_{adj} < 0.05$ (false discovery rate). Analysis was performed using edgeR.

Table S2: Genes differentially expressed in PAO1 Δ*pelFpslD* upon I9 treatment

Locus	Gene	Type	Product	Fold-change	p_{val}	p_{adj}
PA0612	ptrB	intergenic	Repressor PtrB	2.94	0.00010	0.00923
PA0620		sense	Bacteriophage protein	2.61	0.00010	0.00923
PA0621		sense	Hypothetical protein	2.35	0.00077	0.04694
PA0622		sense	Bacteriophage protein	3.16	>0.00001	0.00227
PA0623		sense	Bacteriophage protein	3.14	0.00001	0.00301
PA0625		sense	Hypothetical protein	2.96	0.00004	0.00539
PA0633		sense	Hypothetical protein	2.66	0.00049	0.03465
PA0636		sense	Hypothetical protein	2.84	0.00001	0.00298
PA0641		sense	Bacteriophage protein	2.88	0.00003	0.00532
PA0643		intergenic	Hypothetical protein	2.98	0.00006	0.00680
PA0643		sense	Hypothetical protein	2.59	0.00074	0.04694
PA0646		sense	Hypothetical protein	2.34	0.00034	0.02569
PA0985	pyoS5	sense	Pyocin S5	3.69	0.00030	0.02468
PA2819.1		sense	tRNA-Gly	-2.75	0.00084	0.04833
PA3366.1	amiL	sense	AmiL	2.91	0.00004	0.00539
PA3824.1		sense	tRNA-Leu	-6.48	>0.00001	>0.00001
PA0291	oprE	sense	Anaerobically-induced outer membrane porin OprE	4.15	0.00564	0.24661
PA0336	ygdP	intergenic	Dinucleoside polyphosphate hydrolase	1.61	0.02188	0.55791
PA0633		intergenic	Hypothetical protein	2.53	0.00116	0.06286
PA0644		sense	Hypothetical protein	1.85	0.01685	0.48337
PA0647		sense	Hypothetical protein	1.92	0.00282	0.14402
PA0779	asrA	sense	ATP-dependent protease	1.56	0.02794	0.67495
PA0905.3		intergenic	tRNA-Arg	-1.74	0.02945	0.69323
PA1386		antis	Probable ABC transporter ATP-binding protein	-1.46	0.04292	0.89548
PA2485		sense	Hypothetical protein	-1.85	0.00755	0.31495
PA2493	mexE	sense	Resistance-nodulation-cell division (RND) multidrug efflux membrane fusion protein MexE	-1.79	0.01862	0.50274

PA2494	mexF	sense	Resistance-nodulation-cell division (RND) multidrug efflux transporter MexF	-1.93	0.00971	0.35649
PA2570.1		sense	tRNA-Leu	-2.05	0.01530	0.45762
PA2637	nuoA	intergenic	NADH dehydrogenase subunit A	-1.80	0.01221	0.40026
PA3038	opdQ	sense	Probable porin	-1.67	0.01075	0.36545
PA3126	ibpA	sense	Heat-shock protein IbpA	1.54	0.03560	0.77820
PA3690		intergenic	Metal-transporting P-type Probable metal-transporting P-type ATPase	-2.48	0.01545	0.45762
PA3785		sense	Hypothetical protein	-2.42	0.02427	0.60221
PA3790	oprC	sense	Copper transport outer membrane porin OprC	-1.86	0.03028	0.69501
PA3866		sense	Pyocin S4 protein	1.96	0.00526	0.24140
PA3981	ybeZ	intergenic	Hypothetical protein	-1.79	0.00790	0.31514
PA4276.1		sense	tRNA-Trp	-2.29	0.00411	0.19849
PA4385	groEL	sense	Molecular chaperone GroEL	1.71	0.02079	0.54520
PA4541.2		sense	tRNA-Pro	2.16	0.01447	0.45762
PA4742	truB	intergenic	tRNA pseudouridine synthase B	-1.83	0.01021	0.36046
PA4761	dnaK	sense	Molecular chaperone DnaK	1.71	0.01796	0.49971
PA4762	grpE	sense	Heat shock protein GrpE	1.69	0.00887	0.33936
PA5149.1		intergenic	tRNA-Phe	-1.67	0.03979	0.84937
PA5349	rubB	intergenic	Rubredoxin reductase	-1.74	0.03292	0.73707

*Differential expression was considered significant if $p < 0.05$. Highlighted in gray the genes with differentially expression counts showing $p_{adj} < 0.05$ (false discovery rate). Analysis was performed using edgeR.

Table S3: Genes differentially expressed in PAO1 Δ*pelFpslD* upon I10 treatment.

Locus	Gene	Type	Description	Fold-change	p_{val}	p_{adj}
PA0519	nirS	sense	Nitrite reductase	-7.52	0.00004	0.00287
PA0520	nirQ	intergenic	Regulatory protein NirQ	-3.68	0.00006	0.00295
PA0520	nirQ	intergenic	Regulatory protein NirQ	-5.68	0.00024	0.00996
PA0523	norC	intergenic	Nitric-oxide reductase subunit C	-28.39	>0.00001	0.00025
PA0523	norC	sense	Nitric-oxide reductase subunit C	-26.35	>0.00001	0.00045
PA0524	norB	sense	Nitric-oxide reductase subunit B	-15.87	>0.00001	0.00012
PA0612	ptrB	intergenic	Repressor PtrB	2.11	0.00066	0.02507
PA0620		sense	Bacteriophage protein	2.52	0.00005	0.00295
PA0621		sense	Hypothetical protein	2.26	0.00027	0.01082
PA0622		sense	Bacteriophage protein	3.12	>0.00001	0.00016
PA0623		sense	Bacteriophage protein	3.11	>0.00001	0.00025
PA0625		sense	Hypothetical protein	2.74	0.00001	0.00075
PA0633		sense	Hypothetical protein	2.93	>0.00001	0.00022
PA0633		intergenic	Hypothetical protein	3.01	0.00004	0.00287
PA0636		sense	Hypothetical protein	3.09	>0.00001	>0.00001
PA0640		sense	Bacteriophage protein	2.65	0.00019	0.00819
PA0641		sense	Bacteriophage protein	2.94	>0.00001	0.00012
PA0643		intergenic	Hypothetical protein	2.83	>0.00001	0.00005
PA0643		sense	Hypothetical protein	2.44	0.00011	0.00505
PA0646		sense	Hypothetical protein	2.33	0.00002	0.00168
PA0647		sense	Hypothetical protein	2.09	0.00008	0.00422
PA0922.1		intergenic	tRNA-Met	2.75	0.00091	0.03178
PA3366.1	amiL	sense	AmiL	2.41	0.00149	0.04510
PA3391	nosR	intergenic	Regulatory protein NosR	-9.22	0.00004	0.00288
PA3391	nosR	sense	Regulatory protein NosR	-8.70	0.00005	0.00295
PA3392	nosZ	sense	Nitrous-oxide reductase	-6.61	0.00070	0.02553
PA3743	trmD	intergenic	tRNA (guanine-N(1)-)-methyltransferase	1.82	0.00014	0.00646

PA4825	mgtA	sense	Mg(2+) transport ATPase	-7.57	0.00127	0.04143
PA5149.1		intergenic	tRNA-Phe	-1.85	0.00095	0.03220
PA5227.1	ssrS	intergenic	6S RNA	-1.89	0.00146	0.04510
PA0041a		intergenic	Transposase	-1.58	0.04985	0.54539
PA0291	oprE	sense	Anaerobically-induced outer membrane porin OprE	4.36	0.00403	0.11484
PA0336	ygdP	intergenic	Dinucleoside polyphosphate hydrolase	1.50	0.01712	0.28886
PA0509	nirN	sense	Cytochrome C	-2.39	0.00852	0.19913
PA0644		sense	Hypothetical protein	1.83	0.00480	0.13253
PA0729		intergenic	Hypothetical protein	1.54	0.03013	0.42714
PA0806		intergenic	Hypothetical protein	1.60	0.02503	0.38009
PA0953	helX	intergenic	Thioredoxin	1.86	0.04215	0.51896
PA0985	pyoS5	sense	Pyocin S5	2.90	0.00323	0.09503
PA1132		intergenic	Hypothetical protein	1.72	0.00550	0.14736
PA1386		antisense	ABC transporter ATP-binding protein	-1.49	0.01288	0.25396
PA1430	lasR	sense	Transcriptional regulator LasR	-1.58	0.01329	0.25396
PA1572		intergenic	Hypothetical protein	-1.44	0.04398	0.52965
PA1800	tig	intergenic	Trigger factor	1.77	0.01232	0.25396
PA1838	cysI	sense	Sulfite reductase	1.51	0.01999	0.31393
PA2493	mexE	sense	Resistance-nodulation-cell division (RND) multidrug efflux membrane fusion protein MexE	-1.61	0.02627	0.39225
PA2571		intergenic	Two-component sensor	-1.55	0.02895	0.42534
PA2819.1		sense	tRNA-Gly	-1.75	0.03550	0.45547
PA3159	wbpA	intergenic	UDP-N-acetyl-d-glucosamine 6-dehydrogenase	1.63	0.03050	0.42714
PA3229		intergenic	Hypothetical protein	-1.57	0.01449	0.26394
PA3229		sense	Hypothetical protein	-1.51	0.03095	0.42714
PA3341		intergenic	Probable transcriptional regulator	-1.86	0.00953	0.21710
PA3477	rhlR	intergenic	Transcriptional regulator RhlR	-1.64	0.04419	0.52965
PA3531	bfrB	sense	Bacterioferritin	-2.04	0.01169	0.25346
PA3558	arnF	sense	Hypothetical protein	-1.59	0.01001	0.22241

PA3617	recA	sense	Recombinase A	1.43	0.03239	0.44042
PA3621.1	rsmZ	sense	Rregulatory RNA RsmZ	-1.75	0.01624	0.28235
PA3743	trmD	sense	tRNA (guanine-N(1)-)-methyltransferase	1.67	0.01365	0.25396
PA3785		sense	Hypothetical protein	-1.81	0.00762	0.19061
PA3866		sense	Pyocin S4 protein	1.68	0.02224	0.34339
PA3997	lipB	sense	Lipoate-protein ligase B	-1.46	0.01887	0.31261
PA4067	oprG	intergenic	Outer membrane protein OprG	1.68	0.01254	0.25396
PA4246	rpsE	sense	30S ribosomal protein S5	1.53	0.03027	0.42714
PA4247	rplR	sense	50S ribosomal protein L18	1.44	0.03732	0.46739
PA4250	rpsN	intergenic	30S ribosomal protein S14	1.69	0.01506	0.26903
PA4264	rpsJ	intergenic	30S ribosomal protein S10	1.48	0.03466	0.45547
PA4272.1	p27	antisense	P27	1.59	0.01923	0.31289
PA4277.3		sense	tRNA-Tyr	1.67	0.01275	0.25396
PA4413	ftsW	sense	Cell division protein FtsW	-1.53	0.00719	0.18722
PA4415	mraY	sense	Phospho-N-acetylmuramoyl-pentapeptide-transferase	-1.42	0.05000	0.54539
PA4420	mraW	sense	S-adenosyl-methyltransferase MraW	-1.59	0.00810	0.19426
PA4421.1	rnpB	intergenic	RNA component of RNaseP RnpB	1.82	0.00774	0.19061
PA4443	cysD	sense	Sulfate adenylyltransferase subunit 2	1.61	0.01643	0.28235
PA4567	rpmA	sense	50S ribosomal protein L27	1.49	0.03530	0.45547
PA4614	mscL	sense	Large-conductance mechanosensitive channel	-1.49	0.01961	0.31342
PA4661	pagL	sense	Lipid A 3-O-deacylase	-1.38	0.04566	0.54019
PA4742	truB	sense	tRNA pseudouridine synthase B	1.56	0.03290	0.44082
PA4826		intergenic	Hypothetical protein	-3.23	0.01366	0.25396
PA5349	rubB	intergenic	Rubredoxin reductase	-1.51	0.03745	0.46739

*Differential expression was considered significant if $p < 0.05$. Highlighted in gray the genes with differentially expression counts showing $p_{adj} < 0.05$ (false discovery rate). Analysis was performed using edgeR.

Table S4: Genes differentially expressed in PAO1 Δ*pelFpslD* upon I11 treatment

Locus	Gene	Type	Description	Fold-change	p_{val}	p_{adj}
PA0612	ptrB	intergenic	Repressor PtrB	2.25	0.00166	0.04744
PA0620		sense	Bacteriophage protein	2.51	0.00076	0.02754
PA0621		sense	Hypothetical protein	2.82	0.00058	0.02532
PA0622		sense	Bacteriophage protein	3.08	0.00001	0.00081
PA0623		sense	Bacteriophage protein	3.11	>0.00001	0.00041
PA0625		sense	Hypothetical protein	4.07	>0.00001	0.00002
PA0628		sense	Hypothetical protein	4.30	>0.00001	0.00041
PA0633		sense	Hypothetical protein	4.14	>0.00001	0.00002
PA0633		intergenic	Hypothetical protein	3.88	0.00001	0.00081
PA0634		sense	Hypothetical protein	4.87	>0.00001	0.00019
PA0636		sense	Hypothetical protein	3.43	>0.00001	0.00002
PA0640		sense	Bacteriophage protein	4.05	0.00001	0.00090
PA0641		sense	Bacteriophage protein	3.44	>0.00001	0.00052
PA0643		intergenic	Hypothetical protein	2.58	0.00017	0.00954
PA0646		sense	Hypothetical protein	2.42	0.00114	0.03900
PA0647		sense	Hypothetical protein	3.02	0.00007	0.00487
PA0664		sense	Hypothetical protein	2.42	0.00060	0.02532
PA0826.2	ssrA	intergenic	tmRNA	2.82	0.00175	0.04857
PA0953	helX	intergenic	Thioredoxin	3.36	0.00078	0.02754
PA0985	pyoS5	sense	Pyocin S5	5.19	0.00009	0.00587
PA1075		intergenic	Hypothetical protein	2.27	0.00127	0.04173
PA1132		intergenic	Hypothetical protein	3.53	0.00011	0.00671
PA2381		sense	Hypothetical protein	-2.87	0.00033	0.01629
PA2381		intergenic	Hypothetical protein	-2.18	0.00162	0.04744
PA3366.1	amiL	sense	AmiL	3.14	0.00145	0.04585
PA3690		intergenic	Probable metal-transporting P-type ATPase	-7.90	>0.00001	0.00003
PA4490	magC	sense	MagC protein	2.63	0.00035	0.01629

PA4723	dksA	intergenic	Suppressor protein DksA	2.26	0.00070	0.02710
PA4825	mgtA	sense	Mg(2+) transport ATPase	-13.98	0.00011	0.00671
PA4826		intergenic	Hypothetical protein	-4.22	0.00158	0.04744
PA4937.1		sense	tRNA-Leu	3.18	0.00027	0.01420
PA5446		intergenic	Hypothetical protein	-2.38	0.00070	0.02710
PA0019	def	sense	Peptide deformylase	-1.67	0.02943	0.28374
PA0071	tagR1	sense	TagR1 protein	1.66	0.03658	0.32128
PA0291	oprE	sense	Anaerobically-induced outer membrane porin OprE	3.28	0.00758	0.13175
PA0668	tyrZ	intergenic	Tyrosyl-tRNA synthetase	1.70	0.04389	0.35768
PA0762	algU	intergenic	RNA polymerase sigma factor AlgU	1.91	0.01040	0.16284
PA0905	rsmA	sense	Carbon storage regulator	2.68	0.00294	0.07231
PA0905	rsmA	intergenic	Carbon storage regulator	2.02	0.01985	0.24052
PA0982		intergenic	Hypothetical protein	-1.93	0.03135	0.29514
PA1070	braG	sense	Branched-chain amino acid ABC transporter	1.87	0.03780	0.32277
PA1092	fliC	intergenic	Flagellin type B	-1.67	0.04538	0.35962
PA1095	fliS	sense	Flagellar protein FliS	1.93	0.01714	0.22353
PA1432	lasI	sense	Autoinducer synthesis protein LasI	-1.88	0.02738	0.27284
PA1533		intergenic	Hypothetical protein	1.98	0.00695	0.12332
PA1775	cmpX	sense	Hypothetical protein	2.18	0.00848	0.14344
PA1804	hupB	intergenic	DNA-binding protein HU	1.98	0.02673	0.26944
PA2101		antisense	Hypothetical protein	2.22	0.00257	0.06695
PA2222		sense	Hypothetical protein	-1.93	0.01864	0.23623
PA2461		intergenic	Hypothetical protein	1.75	0.01969	0.24052
PA2485		sense	Hypothetical protein	-1.98	0.00523	0.10534
PA2604	yccA	sense	Hypothetical protein	-1.90	0.03784	0.32277
PA2637	nuoA	intergenic	NADH dehydrogenase subunit A	-2.46	0.00310	0.07231
PA2709	cysK	intergenic	Cysteine synthase A	2.19	0.00201	0.05405
PA2730		intergenic	Hypothetical protein	-2.06	0.04118	0.34140
PA2736.1		intergenic	tRNA-Pro	1.88	0.01322	0.18615

PA2743	infC	intergenic	Translation initiation factor IF-3	2.16	0.01061	0.16284
PA2760	oprQ	sense	Outer membrane protein OprQ	2.94	0.02007	0.24052
PA2760	oprQ	intergenic	Outer membrane protein OprQ	2.54	0.04877	0.37523
PA2819.1		sense	tRNA-Gly	-2.27	0.01224	0.17792
PA2853	oprI	intergenic	Outer membrane lipoprotein OprI	-2.14	0.01124	0.16619
PA2856	tesA	antisense	Acyl-CoA thioesterase	2.25	0.03228	0.29514
PA2943		intergenic	Phospho-2-dehydro-3-deoxyheptonate aldolase	-2.04	0.02816	0.27448
PA2967	fabG	intergenic	3-ketoacyl-ACP reductase	2.10	0.02559	0.26765
PA2970	rpmF	sense	50S ribosomal protein L32	-1.92	0.03012	0.28732
PA3031		intergenic	Hypothetical protein	-1.68	0.04603	0.35962
PA3092	fadH1	intergenic	2,4-dienoyl-CoA reductase FadH1	1.83	0.02308	0.25603
PA3151	hisF2	intergenic	Imidazole glycerol phosphate synthase subunit HisF	1.84	0.02496	0.26765
PA3309	uspK	intergenic	Hypothetical protein	-2.93	0.00490	0.10106
PA3441	ssuF	sense	Molybdopterin-binding protein	1.81	0.04996	0.37876
PA3442	ssuB	intergenic	Aliphatic sulfonates transport ATP-binding subunit	2.20	0.00665	0.12042
PA3477	rhlR	intergenic	Transcriptional regulator RhlR	-2.25	0.01534	0.20611
PA3477	rhlR	sense	Transcriptional regulator RhlR	-1.65	0.02796	0.27448
PA3531	bfrB	intergenic	Bacterioferritin	1.90	0.02168	0.24654
PA3531	bfrB	sense	Bacterioferritin	1.95	0.02589	0.26765
PA3536		intergenic	Hypothetical protein	2.68	0.00477	0.10106
PA3558	arnF	sense	Hypothetical protein	1.74	0.01568	0.20763
PA3602	yerD	intergenic	Hypothetical protein	1.71	0.04622	0.35962
PA3617	recA	sense	Recombinase A	1.62	0.03743	0.32277
PA3623		intergenic	Hypothetical protein	1.70	0.04395	0.35768
PA3639	accA	sense	Acetyl-CoA carboxylase carboxyltransferase subunit alpha	2.31	0.00571	0.11265
PA3653	frr	sense	Ribosome recycling factor	2.09	0.02625	0.26765
PA3662		intergenic	Hypothetical protein	-1.93	0.00928	0.15235
PA3743	trmD	sense	tRNA (guanine-N(1)-)-methyltransferase	1.92	0.02333	0.25603
PA3785		sense	Hypothetical protein	-2.76	0.01778	0.22857

PA3865a		antisense	Hypothetical protein	2.82	0.00486	0.10106
PA3866		sense	Pyocin S4 protein	2.40	0.00663	0.12042
PA3982		sense	Metalloprotease	2.13	0.01256	0.17975
PA4000	rlpA	intergenic	Hypothetical protein	2.19	0.01068	0.16284
PA4034	aqpZ	intergenic	Aquaporin Z	-1.96	0.02157	0.24654
PA4115		intergenic	Hypothetical protein	-1.80	0.02625	0.26765
PA4259	rpsS	sense	30S ribosomal protein S19	2.32	0.02062	0.24383
PA4264	rpsJ	sense	30S ribosomal protein S10	-1.83	0.03532	0.31641
PA4272.1	p27	antisense	P27	1.67	0.03886	0.32830
PA4277	tufB	sense	Elongation factor Tu	-1.91	0.01001	0.16145
PA4277.2		sense	tRNA-Gly	1.89	0.01982	0.24052
PA4291		sense	Hypothetical protein	1.82	0.01426	0.19750
PA4315	mvaT	intergenic	Transcriptional regulator MvaT	2.36	0.00641	0.12042
PA4315	mvaT	sense	Transcriptional regulator MvaT	2.10	0.01447	0.19750
PA4387	fxsA	intergenic	FxsA protein	1.78	0.02338	0.25603
PA4421.1	rnpB	intergenic	RNA component of RNaseP	1.82	0.03225	0.29514
PA4541.3		sense	tRNA-Asn	2.07	0.02104	0.24562
PA4542	clpB	intergenic	ClpB protein	2.75	0.00857	0.14344
PA4587	ccpR	intergenic	Cytochrome C551 peroxidase	-1.97	0.03440	0.31135
PA4723	dksA	sense	Suppressor protein DksA	1.73	0.04907	0.37523
PA4726.11	crcZ	intergenic	CrcZ	3.28	0.00275	0.06958
PA4742	truB	sense	tRNA pseudouridine synthase B	1.82	0.04010	0.33559
PA4746.2		sense	tRNA-Leu	-3.15	0.00305	0.07231
PA4765	omlA	sense	Outer membrane lipoprotein OmlA	1.79	0.01083	0.16284
PA4937.2		intergenic	tRNA-Leu	1.87	0.03201	0.29514
PA5042	pilO	sense	Type 4 fimbrial biogenesis protein PilO	2.21	0.00403	0.08934
PA5062		sense	Hypothetical protein	2.98	0.00398	0.08934
PA5169	dctM	sense	C4-dicarboxylate transporter	-1.82	0.02581	0.26765
PA5285	sutA	sense	Hypothetical protein	2.03	0.00596	0.11489

PA5446		intergenic	Hypothetical protein	1.76	0.03569	0.31661
PA5493	polA	intergenic	DNA polymerase I	-1.93	0.04609	0.35962
PA5559	atpE	sense	ATP synthase F0F1 subunit C	-1.68	0.04502	0.35962

*Differential expression was considered significant if $p < 0.05$. Highlighted in gray the genes with differentially expression counts showing $p_{adj} < 0.05$ (false discovery rate). Analysis was performed using edgeR.

APPENDIX G: COPYRIGHT PERMISSION

The panels used for assembling Figure 1.1 (The coordinated process of biofilm formation) were adapted from previously published papers. Information on the copyright permission, granted by the Copyright Clearance Center, are shown:

The first panel, adapted from Wagner and Igleski (2008), comes from an open access article and therefore allows any non-commercial use of their content providing appropriated credits to the original authors.

Copyright Clearance Center RightsLink®

Home | Create Account | Help

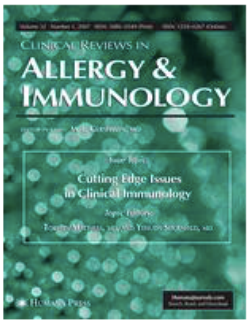

Title: P. aeruginosa Biofilms in CF Infection
Author: Victoria E. Wagner
Publication: Clinical Reviews in Allergy and Immunology
Publisher: Springer
Date: Jan 1, 2008
Copyright © 2008, 2008

LOGIN
If you're a copyright.com user, you can login to RightsLink using your copyright.com credentials. Already **a RightsLink user** or want to learn more?

Permissions Request

This is an open access article distributed under the terms of the Creative Commons Attribution Noncommercial License, which permits any noncommercial use, distribution, and reproduction in any medium, provided the original author(s) and source are credited.

BACK | CLOSE WINDOW

On the other hand, the second panel, from Mikkelsen *et al*. (2011), was adapted from a copyrighted protected figure. Permission to use this material in this thesis was granted and license details are shown.

JOHN WILEY AND SONS LICENSE TERMS AND CONDITIONS

Dec 19, 2016

This Agreement between Erik Bernardes ("You") and John Wiley and Sons ("John Wiley and Sons") consists of your license details and the terms and conditions provided by John Wiley and Sons and Copyright Clearance Center.

License Number	4010370702343
License date	Dec 15, 2016
Licensed Content Publisher	John Wiley and Sons
Licensed Content Publication	Environmental Microbiology
Licensed Content Title	Key two-component regulatory systems that control biofilm formation in Pseudomonas aeruginosa
Licensed Content Author	Helga Mikkelsen,Melissa Sivaneson,Alain Filloux
Licensed Content Date	May 9, 2011
Licensed Content Pages	16
Type of use	Dissertation/Thesis
Requestor type	University/Academic
Format	Print and electronic
Portion	Figure/table
Number of figures/tables	1
Original Wiley figure/table number(s)	Figure 4
Will you be translating?	No
Title of your thesis / dissertation	Small molecule biofilm inhibitors with antivirulence properties against Pseudomonas aeruginosa
Publisher Tax ID	EU826007151
Billing Type	Invoice
Total	0.00 CAD